SKI Report 98:2

RICK ___
KEITH ___
MAKE SURE COVER IS AWARE OF THIS

Pitting Corrosion of Copper in Nuclear Waste Disposal Environments

Sture Eriksson
Hans-Peter Hermansson

December 1997

ISSN 1104-1374
ISRN SKI-R--98/2--SE

SKI
STATENS KÄRNKRAFTINSPEKTION
Swedish Nuclear Power Inspectorate

SKI Report 98:2

Pitting Corrosion of Copper in Nuclear Waste Disposal Environments

Sture Eriksson
Hans-Peter Hermansson

Studsvik Material AB, SE-611 82 Nyköping, Sweden

December 1997

SKI Project Number 95217

Norstedts Tryckeri AB
Stockholm 1998

STUDSVIK MATERIAL AB STUDSVIK/M-97/101

97-10-30 M-7764

Sture Eriksson
H-P Hermansson

Pitting corrosion of copper in nuclear waste disposal environments

Abstract

A frequently asked question is if pitting corrosion could penetrate the walls of the copper canister in the final repository for spent nuclear fuel. Theoretical calculations indicates that a penetration of the copper canister through uniform corrosion is very unlikely within the time scale where the nuclear waste is dangerous. A first step in trying to answer the question of pitting corrosion is to find environments where pitting will take place. For this purpose, a literature survey on pitting corrosion of copper and polarisation experiments was performed. From the literature survey it was found that chloride, sulphate, carbonate and nitrate ions together with dissolved oxygen will be likely to promote the pitting corrosion of copper in groundwaters. Other components that can be expected to have some effect are Ca^{2+}, Fe^{3+} and HS^- ions, and H_2O_2 from radiolysis. The pH of the water also seems to be important while the temperature only is of minor importance. From these literature findings an experimental matrix was derived for experiments to possibly verify environments that could cause pitting corrosion. As the experiments have continued, some alterations have been made to the matrix as a feed-back from the current experimental results.

Basically it was found that the corrosion of copper in the synthetic groundwater is dominated by the high salt concentration (mainly NaCl). A high salt content gives an environment that inhibits the formation of a passive layer on the surface. Only in a few cases is there a clear evidence for a passive layer formation in such an environment. With no passive layer on the surface, general corrosion dominates and pitting is less likely to occur. Two species were found that are more likely to cause pitting corrosion of the copper surface under repository conditions, namely sulphide and carbonate ions (HS^- and HCO_3^-). Groundwater with HCO_3^- was forming a passive layer at pH 8.5 that was penetrated locally during the polarisation scan and thereby opened the surface to pitting corrosion. With HS^-, a surface film was formed immediately after immersion, and the corrosion potential moved to very low values. During the polarisation scan there was an extensive formation of whiskers (dendrites formed through reactions between copper ions and sulphide) on the copper surface at high anodic potentials.

Reviewed by Approved by

Gropfrätning på koppar i slutförvarsmiljö

Sammanfattning

En viktig fråga är om kopparkapselns väggar i slutförvaret för utbränt kärnbränsle kan penetreras genom gropfrätning. Teoretiska beräkningar visar att penetrering av kopparkapseln genom allmän korrosion är högst osannolikt inom den tidsram som avfallet kan anses farligt. Ett första steg i att besvara frågan om gropfrätning på kopparkapseln är att finna de grundvattenmiljöer där gropfrätning kan ske. Av den anledningen gjordes dels en litteraturstudie om gropfrätning på koppar och dels polarisationsmätningar på koppar i syntetiska grundvatten. Från litteraturstudien framkom att klorid-, sulfat-, karbonat- och nitratjoner tillsammans med syre löst i grundvattnet kan förväntas påskynda gropfrätning av koppar i kontakt med grundvatten. Andra komponenter som kan förväntas ha viss effekt är Ca^{2+}, Fe^{3+} och HS^- -joner, och H_2O_2 från radiolys. Vattnets pH verkar också vara av vikt medan temperaturen är av mindre betydelse. Från det som framkommit vid litteraturstudien sammanställdes en experimentmatris för att om möjligt fastställa grundvattenmiljöer som kan orsaka gropfrätning. Under försökens gång gjordes en del förändringar på matrisen som en följd av de erhållna experimentella resultaten.

I första hand kunde konstateras att korrosionen på koppar i det syntetiska grundvattnet domineras av den höga saltkoncentrationen (främst NaCl). En hög saltkoncentration ger en miljö där bildningen av en passiv oxidfilm på kopparytan motverkas. Endast i några få fall finns klara belägg för bildning av en passiv film på kopparytan. Utan passiv film på ytan dominerar den allmänna korrosionen och gropfrätning blir mindre sannolik. Två specier befanns vara mera sannolika som orsak till gropfrätning på koppar under slutförvarsbetingelser, nämligen sulfid- och karbonatjoner (HS^- och HCO_3^-). Grundvatten med HCO_3^- bildade vid pH 8.5 ett passivt skikt som penetrerades lokalt under polarisationsmätningen och därmed öppnade ytan för lokal korrosion. Med HS^- bildas en ej passiverande ytfilm på koppar direkt vid kontakt med vattnet och korrosionspotentialen förskjuts till mycket låga värden. Under polarisationsmätningen bildas vid höga anodiska potentialer en mängd s.k. 'whiskers' (dendritisk utväxt bildad genom reaktion mellan kopparjoner och sulfid) på kopparytan.

Contents

1 Introduction

Copper is a material that has good resistance to corrosion in most water environments. This is the main reason for the common use of copper in hot and cold water distribution systems in buildings. It is for similar reasons that copper is suggested as canister material for the final disposal of spent nuclear fuel from our nuclear power plants. Under certain conditions copper may however corrode, and one form of corrosion that can occur is pitting corrosion. If the right conditions are at hand, the pitting can be rather fast and eventually result in a breakthrough of the copper wall. This is sometimes seen in water systems in buildings.

The question is if serious pitting can occur in the copper canister in the deep rock repository, i.e. is there a risk for the copper canister to be damaged by pitting corrosion at some stage of repository life-time. The long time period involved, thousands of years, makes direct measurements of very slow but in the long run important corrosion reactions impossible. One way to address the question is to make accelerated tests, i.e. tests where the reactions are forced to go much quicker, but in an environment that resembles what can be expected around the copper canister in the deep storage. One such accelerated test method is anodic polarisation, where the resulting current through the specimen under test is measured as the potential is slowly scanned towards an increasingly anodic potential.

The aim of this work is to find environments where there is an increased risk for pitting corrosion of the copper canister. The work has been carried out in two steps. Step one is a literature survey to see what species could pose an increased risk for pitting corrosion. Step two comprises polarisation tests which were performed on copper in a synthetic groundwater to further establish the environments where there could be an increased risk for pitting corrosion.

2 Literature survey

Databases used to find literature on local corrosion on copper were METADEX, NTIS, Chemical Abstracts (CA) and Uncover, complemented with material from earlier literature surveys on copper corrosion performed at Studsvik Material AB [1-4].

The literature survey has focused on articles dealing with pitting corrosion on copper in environments that have relevance for the nuclear waste disposal. A special attention has been given to information that could help in planning the anodic polarisation test matrix, by pointing out species in the groundwater that can be expected to cause pitting corrosion on the copper canister.

2.1 Background

Copper and copper alloys are considered among the most promising materials for the waste fuel canister, as copper has a very good corrosion resistance in many environments.

Presently pure copper is used as reference material for testing, manufacturing and sealing of the canister, with the following levels of additions and impurities [5]:

P: 40-60 ppm, O: <10 ppm, S: <6 ppm, H: <2 ppm

The desired size of the largest grains are ≈250 μm.

There are rather large variations in the composition of groundwater depending on where and how deep down the water is fetched. With this in mind a rather broad approach was taken in the literature survey to cover the variations in the species present in the water and their concentrations.

2.2 Pitting corrosion on copper

Several cases of pitting corrosion on copper, with different causes, are reported in the literature. In a reported case, copper piping in a house was broken through and leaked as a result of pitting corrosion. The water had high levels of dissolved gases [6]. The concentration of O_2 was 5.9 ppm, of CO_2 19.2 ppm, pH was 6.1. The water was also heavily chlorinated. Analysis of the corrosion products around the pits showed copper oxide (Cu_2O), hydrated copper carbonate and copper phosphate.

In a series of experiments oxygen free copper (99.98 % Cu, 0.02 % P) was exposed to tap-water in Kuwait, a water that is a mixture of desalinated sea-water and 7 % brackish water [7]. The water had the following composition (Table 1):

Table 1
Composition of tap-water in Kuwait.

pH	8.1
conductivity (μS/cm)	350.0
total hardness ($CaCO_3$, mg/*l*)	93.0
HCO_3^- (mg/*l*)	15.0
Cl^-(mg/*l*)	51.8
SO_4^{2-} (mg/*l*)	75.0
SiO_2 (mg/*l*)	4.0

The *critical pitting corrosion potential* (definition see Appendix A) was found to be around 240 mV_{SHE} and the initiation is said to depend on a local breakdown of the protective film on the corroded spot. The presence of chloride ions was found to be an important factor for the initiation of pitting corrosion in this case. The process is explained by an exchange of oxide ions by chloride ions in the copper oxide film on the surface, followed by an increase of the number of cation vacancies to maintain electroneutrality in the film. This eventually leads to a detachment of the film from the metal surface, and the surface is open to corrosive attack. The pitting corrosion is usually initiated in the grain boundaries.

Cohen and Myers [8-10] report on cases of pitting corrosion on copper caused by small amounts of hydrogen sulphide in cold water.

Pitting corrosion in cold water is usually dependent on the concentration of free carbon dioxide in the water. This is in turn directly dependent on the pH of the water and the amount of free carbon dioxide is negligibly small at pH-values above 8.5. An increased pH-value is therefore an effective inhibition of this pit propagation mechanism [9].

In warm water the pitting corrosion usually takes place in combination with microdeposition of cathodic material such as magnesiumdioxide, hydrated hematite and aluminium hydroxide if such materials are present [9].

As a summary of the factors influencing the pitting corrosion of copper according to Cohen [9] the following conclusions can be given:

pH	a low pH accelerates dissolution of copper
Dissolved oxygen	Cu is usually not corroding in the absence of oxygen
Free carbon dioxide	accelerates pitting corrosion of copper in cold water
Calcium	reduces corrosion if a protective film is formed
Silicon	reduces corrosion if a protective film is formed
Metal ions	iron, magnesium, aluminium above a certain concentration accelerates pitting corrosion in warm water
Chloride	may initiate pitting corrosion of copper in cold water
Sulphate	may initiate pitting corrosion of copper in cold water
Sulphide	accelerates pitting corrosion of copper

According to Royuela and Otero [11] pitting corrosion of copper can only take place when the electrochemical potential is above a threshold value (the *critical pitting corrosion potential*, definition see Appendix A), usually between 340 and 410 mV_{SHE}. Pitting corrosion can be rapid in very soft waters rich in O_2 and CO_2. Natural inhibitors can inhibit the pitting corrosion (i.e.>100 mg/l HCO_3^-).

Oxygenated solutions of bicarbonate (HCO_3^-), chloride (Cl^-), nitrate (NO_3^-), perchlorate (ClO_4^-), or sulphate (SO_4^{2-}) in natural water at pH 5.5, 7.0, 8.5 and 10.0 was used in one investigation of pitting corrosion on copper [12]. It was found that chloride ions gave an increased tendency for pitting corrosion in short terms, but in a longer perspective contributed to the formation of a passive film. Sulphate and nitrate on the other hand gave pitting corrosion that did not slow down with time. In the investigated water compositions it was rather sulphate and nitrate that was mainly responsible, even for the initiation of pitting corrosion of the copper surface.

The following maximum pitting corrosion speeds were measured at 75 °C in the Ontario groundwater (Table 2) with and without 10 mg/l sulphide added to the water [13]:

oxygen free	0.014	mm/year
with oxygen	0.087	mm/year
oxygen free with sulphide	0.57	mm/year
with oxygen and sulphide	1.2	mm/year

It is obvious that 10 mg/l sulphide strongly enhances the pitting corrosion rate in both oxygenated and oxygen free groundwater. The increase in corrosion rate is actually larger in oxygen free water (about 40 times) then in oxygenated water (about 10 times). Oxygen is thus not necessary to give a considerable corrosion rate in sulphide containing water.

Table 2
Composition of Ontario groundwater (1 ppm = 1 mg/l) [13].

Na^+	83	mM	1910	ppm
K^+	0.36	mM	14	ppm
Mg^{2+}	2.5	mM	61	ppm
Ca^{2+}	53	mM	2120	ppm
Sr^{2+}	0.01	mM	1	ppm
Fe	0.28	mM	16	ppm
HCO_3^-	1.1	mM	67	ppm
Cl^-	180	mM	6380	ppm
SO_4^{2-}	11	mM	1060	ppm
NO_3^-	0.53	mM	33	ppm

In a Finnish study [14] the equilibrium between groundwater, bentonite and copper was investigated, by measuring pH and the equilibrium relation between Fe^{3+} and Fe^{2+} during 36 months. The groundwater was synthetic and had three different compositions, according to Table 3 and the bentonite had the elementary composition given in Table 4.

Table 3
Groundwaters in the Finnish long time test. ("MS"= Simulated Groundwater).

	----------SPECIES (mg/l)----------					
WATER	SO_4^{2-}	Cl^-	HCO_3^-	Cu^+	κ (μS/cm)	pH
"MS"	59	60	570	0.00	1	8.4
"MS"+Cl^-	62	7600	600	0.00	19.7	7.9
"MS"+SO_4^{2-}	6200	62	590	0.00	9.2	8.2

The most important results from this investigation are to demonstrate the buffer capacity of the bentonite clay and to show how the redox potential depends on the Fe^{2+}/Fe^{3+}-equilibrium. At the end of the 36 month period the measured redox potential was -360 mV_{SHE} in "MS" water, -340 mV_{SHE} in "MS" +Cl^- water and -350 mV_{SHE} in the "MS" + SO_4^{2-} water. The buffer capacity of the bentonite will make the pH relatively high (in this case 9.5-10), which is of importance for the corrosion of copper. Iron is considered as the species that almost totally decides the redox potential, also an important parameter for the corrosion of copper.

Table 4
Elementary composition of the bentonite (Volclay MX-80, batch 3) [14].

Element	w %
Na	0.53--2.2
Mg	0.82--2.9
Al	~ 20
Si	> 40
P	0.014--0.074
S	0.033--0.29
Cl	0.021--0.20
K	0.31--1.3
Ca	0.69--3.2
Ti	0.12--1.1
Mn	0.014--0.040
Fe	3.4--13
Zn	0.019--0.086
Sr	0.066--0.85
Ba	0.046--0.84
Nb	0.0061--0.029
As, Pb, Zr, Rb, Ga, Y	traces

Sridhar and Cragnolino [15] have investigated the effect of bicarbonate (HCO_3^-), chloride (Cl^-) and sulphate (SO_4^{2-}) on the corrosion of copper at 30 and 95 °C and a pH around 9. A low and a high concentration was chosen for each species and the possible combinations where examined by polarisation measurements followed by examination under a light microscope. In addition to the sodium salts of the investigated ions the water contained 10 ppm nitrate and 2 ppm fluoride. The solutions where held free from oxygen through bubbling with argon gas. The concentrations of bicarbonate, chloride and sulphate were varied in the following manner:

HCO_3^-	85 ppm / 8500 ppm
Cl^-	6 ppm / 1000 ppm
SO_4^{2-}	20 ppm / 1000 ppm

At low temperature (30 °C) the pitting corrosion took place only at the high level of carbonate (8500 ppm). At the higher temperature (95 °C) pitting corrosion was observed only in a single case, being when all the species above had their lower concentration value. The *breakthrough potential* (pitting potential, definition see Appendix A) was slightly higher then 300 mV_{SCE} at the higher temperature and at the lower temperature when the amount of sulphate was high. At the low level of sulphate more then 800 mV_{SCE} was needed to cause breakthrough of the oxide film. In this study both chloride and sulphate were found to give an increase of the pitting corrosion.

A survey of different corrosion mechanisms for different metals, including copper was done by Farmer et al. [16, 17], with a large number of references to the literature. Ions pointed out as important for pitting corrosion of copper include S^{2-}, HS^-, HCO_3^-, SO_4^{2-}, Cl^-, Fe^{3+} and H^+. In addition the concentration of dissolved oxygen (O_2) is important. Three types of pitting corrosion on copper are described and two different mechanisms are given as explanation for the pitting.

The three types of pitting and the mechanism behind is also reviewed in [1] and [4]. The review in [4] gives a different picture in some cases. This is due to the uncertainty that still exists about the pitting mechanisms.

Type 1 pitting takes place at low temperature (< 60°C) in hard or medium hard water (high pH) and typically consists of relatively large, well defined areas of attack. The copper material has to be annealed or medium hard (i.e. the copper has to be heat treated).

The type 1 mechanism described gives pitting corrosion on a small anodic surface and oxygen reduction on a large cathodic area on the copper surface around the pit [16, 17]. One explanation given in the literature is a carbon containing surface film that forms the cathodic area. This explanation is now questioned [4].

Type 2 pitting only takes place in certain soft waters at low pH (< 7) and temperatures above 60°C and is characterised by narrow and deep attacks [16, 17]. Hydrogen carbonate is present but at concentrations less then 100 mg/l and usually at less then 50 mg/l. The sulphate concentration is between 1 and 70 mg/l. The hydrogen carbonate to sulphate ratio is less then one ($HCO_3^- / SO_4^{2-} < 1$) [4]. Type 2 pitting occurs on hard-drawn copper pipes (i.e. the copper is cold worked without heat treatment).

In the type 2 mechanism the oxygen reduction takes place locally above the pit and not on the copper surface. A porous, electrically conducting membrane is formed, that separates cathode from anode. Pitting corrosion is initiated where CuCl is formed under the membrane [16, 17].

Type 3 pitting takes place on both soft heated and hard materials in cold water at high pH and low salt concentration [16, 17]. Hydrogen carbonate concentrations are less then 1 mg/l and sulphate concentrations are between 10 and 70 mg/l. The pH is in the span 5 - 5.5 [4].

In type 2 and type 3 pitting there is a local acidification and breakthrough of the passive film. A support for this idea is that an increase in pH and carbonate concentration usually inhibits the pitting [4].

In a series of experiments performed by Thompson et al. [18, 19] a number of different species and environments as well as pH and temperatures were tested for their influence on pitting corrosion on copper. As the number of experimental parameters was so large the effect of every individual parameter could not be seen directly from the experiments, but after a statistical analysis (F function) based on an 80 % (or 90 %, coefficients marked with an asterisk) confidence level, a

statistical coefficient was obtained for each parameter. These coefficients indicate the size and direction of the influence a certain parameter has on *corrosion potential*, *corrosion current*, *break through potential* (pitting potential) and *repassivation potential* (definitions see Appendix A) according to the following equation:

$$Y = a_0 + \Sigma(a \cdot x)$$

where Y is the corrosion parameter (*corrosion potential*, *corrosion current*, *break through potential* or *repassivation potential*), a_0 is the intercept, a is the statistical coefficient (see Table 5) and x is the solution variable in mg/l (or volume % for oxygen, °C for temperature, pH units for pH). The given coefficient must be multiplied by the range of the solution variable (see Table 6) to determine the magnitude of the effect on the corrosion parameter. It is obvious that the ranges of oxygen, temperature and pH are much smaller then the ranges of the other variables and thus their coefficients has to be larger to give the same effect on the corrosion. The results are summarised in Table 5. The limits between which the parameters have been varied are given in Table 6.

Table 5
Coefficients of influence on pitting corrosion of copper.

	COEFFICIENTS FOR THE OBSERVED EFFECT			
Parameter	E_{corr}	I_{corr}	E_b	E_{rp}
SiO_2	0.141	~	0.384	0.136
HCO_3^-	-0.036*	$-8.3 \cdot 10^{-4}$	0.092*	~
F^-	~	~	0.338	0.180*
Cl^-	-0.028	~	-0.078	-0.069*
NO_3^-	0.030	~	~	~
NO_2^-	~	~	~	0.190*
H_2O_2	0.411*	0.014*	~	~
Ca^{2+}	~	~	~	-38.621
Mg^{2+}	~	~	~	-42.454
Al^{3+}	-35.453	~	~	~
PO_4^{3-}	-23.376*	~	~	~
Oxalic acid	~	0.022*	~	~
O_2	1.640*	0.079*	~	~
Temp.	-1.975*	~	~	~
pH	-6.553	-0.414*	34.305*	~
Intercept	140	2.672	-155	84.924

~ indicates no detected influence (i.e. the effect of a change in the parameter is neglible)
* indicates a 90 % confidence level

Table 6
The upper and the lower limit between which corrosion parameters were varied.

PARAMETER	LOWER LIMIT	UPPER LIMIT	
SiO_2	2.2	215	ppm
HCO_3^-	0.4	2000	ppm
F^-	0.04	200	ppm
Cl^-	0.2	1000	ppm
NO_3^-	0.2	1000	ppm
NO_2^-	0	200	ppm
H_2O_2	0	200	ppm
Ca^{2+}	0.004	0.8	ppm
Mg^{2+}	0.004	0.8	ppm
Al^{3+}	0.0004	0.8	ppm
PO_4^{3-}	0.01	2.0	ppm
Oxalic acid	0	172	ppm
O_2	5	30	vol. %
Temp.	50	90	°C
pH	5	10	

To summarise these data it can be said that the chloride concentration is the parameter that has the most obvious influence on the pitting corrosion , as chloride lowers both the *breakthrough (pitting) potential* and the *repassivation potential.* Also a lowering of pH gives a noticeable lowering of the breakthrough potential and thus an increased risk for pitting corrosion. Magnesium and calcium lower the repassivation potential but not the breakthrough potential, and are therefore mainly affecting the growth of pits already formed.

Taxén [20, 21] has performed theoretical calculations on the rate of pitting corrosion of copper with sulphide as the reaction determining reactant and under mildly oxidising conditions. The results are dependent on the accuracy of values given to parameters in the calculations (concentrations, diffusion coefficients etc.). The results give very low pitting rates, and a penetration time of approx. 50 000 years is calculated for a pit one cm deep. The calculations does not take into account the possibility of whisker formation, which would give a higher pitting rate. It is thus difficult to judge how significant these results are for the real situation. As a complement to the experimental data the theoretical calculations are still valuable.

Microbiologically induced pitting corrosion is believed to depend mainly on the biofilm that can be formed on the copper surface under certain conditions [22]. The film results in a different chemical composition of the water in contact with the copper surface, but the actual pitting is still caused by the anions and pH at the

copper surface. The same type of attack can be caused by a polysilicate film that is of non-biological origin.

Maiya [23] has looked at local corrosion on several materials, including pure copper. One factor among others that he discusses, is pitting corrosion caused by hydrogen sulphide, produced by bacterial reduction of sulphate. This reaction is favoured by a low redox value in the water (< -200 mV_{SHE}). As the Finnish study indicates [14] the redox value is likely to be below this potential after some time, thus favouring the bacterial sulphate reduction to sulphide. It would therefore be possible that sulphide corrosion replaces other types of corrosion in the long run.

Sequeira has done a very extensive literature study on corrosion of copper (368 references) [24]. One chapter deals with pitting corrosion. The specific factors he emphasise as important for the pitting corrosion of copper are by large the same as already mentioned in this work. A species he points out as important for the initiation of pitting corrosion is Fe^{3+}.

The bicarbonate ion has been found to stabilise the oxide on the copper surface and thus inhibit pitting corrosion [25, 26]. At a bicarbonate concentration above 61 mg/l or a high bicarbonate/chloride ratio the copper surface remained intact, but with a bicarbonate concentration below 31 mg/l pitting corrosion of the surface was observed.

As can be seen from the description of type 2 and type 3 pitting the HCO_3^- / SO_4^{2-} ratio is also very important for pitting corrosion [1, 4, 16, 17]. So if the water contains chloride or sulphate the carbonate concentration is of vital importance for the pitting corrosion. Pitting is inhibited if there is enough carbonate but a low carbonate concentration will increase the risk for pitting. On the other hand free CO_2 will increase the corrosion of copper and thus may carbonate increase the corrosion through the '$H_2CO_3 \leftrightarrow H_2O + CO_2$' equilibrium.

2.3 Conclusions from the literature study

From information in the reviewed literature the following conclusions can be drawn about pitting corrosion of copper in environments that are of interest for the deep rock repository:

- Chloride is by many authors believed to be necessary for the initiation of corrosion pits on the copper surface. It is also considered to be important for pit propagation.
- Sulphate and nitrate has also shown to be active in pitting of copper.
- Hydrogen carbonate can both enhance and inhibit pitting of copper depending on the environment.

- Oxygen or hydrogen peroxide is believed necessary for the cathodic reaction during copper corrosion under oxidising conditions.
- Sulphide is found to cause pitting under reducing conditions.
- The Fe^{3+}/Fe^{2+} redox couple is important for the redox potential in the groundwater. Fe^{3+} can function as an electron acceptor during corrosion under reducing conditions.
- Free carbon dioxide and high levels of metal ions accelerate pitting corrosion.
- The pH has a large influence on the pitting corrosion, a high pH usually gives less corrosion.
- Temperature seems to be of minor importance for the pitting under final repository conditions, and corrosion rates are lower at higher temperature.

Based on the above conclusions an experimental matrix was formulated for polarisation measurements in synthetic groundwater, with a composition according to what is typically expected in crystalline bedrock. To this basic groundwater are added species, as pointed out in literature to be active in pitting corrosion of copper, in concentrations that resembles worst case scenarios.

3 Experimental

3.1 Disposal environment

Large variations can be found in the composition of the groundwater depending on where and at what depth the water is sampled. Since the site for the final disposal of the nuclear waste still is not decided, a synthetic groundwater with a composition that is "typical" for a site 500 meters down in the rock was used (Tables 7 and 8) [27]. The concentration of one or more of the components in the synthetic groundwater was then increased or species that can be formed by radiolysis was added to find the influence of that specific species on the copper corrosion. These variations are based on the variations found in natural waters and the findings in the literature study. An experimental matrix (Table 9) was set up to study species that possibly could cause pitting corrosion of copper.

Table 7
The basic synthetic groundwater was made from ultrapure water and the following compounds. The desired composition was achieved by dissolving the given amounts (ppm = mg/l) of the compounds to have the listed ion concentrations:

COMPOUND ADDED /ppm		CATION /ppm		ANION /ppm	
$CaCl_2$	2769	Ca^+	1000	Cl^-	1769
NaCl	2235	Na^+	893	Cl^-	1342
Na_2SO_4	296	Na^+	96	SO_4^{2-}	200
$MgCl_2*6H_2O$	167	Mg^{2+}	20	Cl^-	57
$SrCl_2*6H_2O$	30.4	Sr^{2+}	10	Cl^-	8.1
NaBr	25.8	Na^+	5.8	Br^-	20
KCl	15.4	K^+	8.1	Cl^-	7.3
$NaHCO_3$	13.8	Na^+	3.8	HCO_3^-	10
SiO_2	8.8	(Si	4.1)*)		
LiCl	6.1	Li^+	1.0	Cl^-	5.1
NaF	3.3	Na^+	1.8	F^-	1.5
$FeSO_4*7H_2O$	1.0	Fe^+	0.2	SO_4^{2-}	0.35

*) SiO_2 is only slightly soluble in water in the form of H_2SiO_3 and thus Si is not really a cation, but calculated on Si the concentration is 4.1 ppm.

Based on the literature [27] the following table (Table 8) could be set up with the approximate concentrations (in ppm = mg/l) found in natural groundwaters and at the canister surface (in equilibrium with the bentonite). The concentrations in the used synthetic groundwater are also given and the maximum concentrations used for the species which were specifically tested in the polarisation measurements. These concentrations were set high to reflect a worst case situation and to have a clear effect on the polarisation behaviour from that species.

Table 8
Concentrations (in ppm = mg/l) found in natural deep rock groundwaters [13, 17, 27], expected concentrations at the canister surrounded by bentonit [13] and concentrations in the used synthetic groundwaters.

Species	Min.conc. in natural groundwater	Max. conc.	Conc. at canister	Conc. in synth. groundwater	Max. conc. in polaris. meas.
HCO_3^-	2	500	180	10	sat. at pH 8.5
SO_4^{2-}	40	500	3000	200	2000
HS^-/S^{2-}	0.1	100	—[1]	—[2]	1000
HPO_4^{2-}	0.1	0.2	—[1]	—[2]	—[2]
PO_4^{3-}	0.01	1	—[1]	—[2]	—[2]
NO_3^-	0.01	1	—[1]	—[2]	200
NO_2^-	0.01	0.1	—[1]	—[2]	—[2]
Cl^-	1	20000	1-20000	3189	5 %
F^-	0.2	10	—[1]	1.5	—[3]
Br^-	5	50	—[1]	20	—[3]
Ca^{2+}	5	3200	370	1000	1 %
Mg^{2+}	1	80	15	20	1000
Fe^{2+}	0.1	3	—[1]	0.2	—[3]
Fe^{3+}		< 0.1	—[1]	—[2]	sat. at pH 8.5
Mn^{2+}	0.2	0.5	—[1]	0.3	—[3]
K^+	1	25	—[1]	8.1	—[3]
Na^+	10	10000	10-10000	1000	5 %
Li^+		5?	—[1]	1.0	—[3]
Al^{3+}	0.01	0.2	—[1]	—[2]	—[2]
Sr^{2+}	5	50	—[1]	—[2]	—[2]
Si (SiO_2)	2	20	—[1]	4.1	—[3]
H_2O_2		0	5	—[2]	100
O_2	0	1	—[1]	—[2]	8
TOC	1	20	—[1]	—[2]	—[2]
pH	6.5	9	~9-10	8.5	7-11

[1] Concentrations were not found in the literature
[2] These species are not included in the basic synthetic groundwater
[3] These species are not specifically tested in the polarisation tests

The polarisation measurements have been made according to an experimental matrix (Table 9) that tells what was added to the environment beside the basic synthetic groundwater. The added negative ions were balanced with Na^+ ions, as they are not believed to affect the corrosion behaviour and they are also present in rather high amounts in natural groundwaters. Positive ions were balanced with Cl^- ions that already are present in a relatively large amount in the deep rock groundwater. The strongly pH dependent species, HCO_3^- and Fe^{3+} were added to or close to saturation at the given pH. Beside the different species, pH was also varied and adjusted by additions of small amounts of NaOH or HCl (conc. ~0.1 M).

The total experimental matrix is shown in Table 9. It is based on data on pitting corrosion of copper from the literature and discussions on what species may possibly be found in the final repository environment. The species under investigation are added to higher concentrations than what is normally found in natural waters and represents an imagined worst case. This high concentration could be the result from ion exchange in the bentonite, water evaporating at the canister surface, or some other mechanism that increases the concentration.

Table 9
Experimental matrix: The concentrations of the added species are given in mg/l = ppm where not stated otherwise, - means nothing extra is added and thus the concentration of this species equals that of the used synthetic groundwater. The materials are from two sources, samples Cu01-Cu18 are from a rod provided by Outokumpu Copper and samples Cu101-Cu106 are from a test manufactured canister (see section 3.2).

No.	Sample	Cl^-	HCO_3^-	SO_4^{2-}	NO_3^-	Fe^{3+}	HS^-	O_2	H_2O_2	pH
1	Cu01/ Cu02	-	-	-	-	-	-	-	-	8,5
2	Cu03	*Natural ambient air formed surface oxide*								8,5
3	Cu07	-	-	-	-	-	-	8	-	8,5
4	Cu04	1 %	-	-	-	-	-	-	-	8,5
5	Cu05	5 %	-	-	-	-	-	-	-	8,5
6	Cu06	1 %	-	-	-	-	-	8	-	8,5
7	Cu15	1 %	-	-	-	-	-	-	100	8,5
8	Cu12	1 %	-	-	-	-	330	-		8,5
9	Cu17/ Cu105	1 %	-	-	-	sat'd	-	-	-	8,5
10	Cu14	1 %	*No synthetic groundwater, only NaCl added*							8,5
11	Cu08	-	sat'd	-	-	-	-	-	-	8,5
12	Cu09	-	sat'd	-	-	-	-	8	-	8,5
13	Cu104	-	sat'd	-	-	-	-	-	-	7,1
14	Cu10	-	-	1 %	-	-	-	-	-	8,5
15	Cu11	-	-	1 %	-	-	-	8	-	8,5
16	Cu101	*Long resting time in synthetic groundwater without additions before measurements*								8,5
17	Cu16	-	-	-	200	-	-	-	-	8,5
18	Cu102	-	-	-	-	-	-	-	-	8,5
19	Cu103	-	-	-	-	-	330	-	-	8,5
20	Cu106	1 %	-	-	-	-	-	-	-	7,0
21	Cu18	1 %	-	-	-	-	-	-	-	10

3.2 Materials and preparations

Disks for the polarisation tests were cut from a ∅ = 16 mm rod of copper from Outokumpu Copper OY for use as test specimens. The material is of the same composition as the present reference material for the copper canister (see below). The heat treatment may not be exactly the same as proposed for the copper canister, but the grainsize is of the same order (grains usually between 100-200 μm within the same sample, see pictures in Appendix B). The microhardness of this material is $H_{v\ 0,2\ kp/30\ s} \approx 95\ kp/mm^2$.

The composition of the present reference copper material is [5]:

P: 40-60 ppm, O: <10 ppm, S: <6 ppm, H: <2 ppm.
Desired largest grainsize ≈250 μm.

A few samples of a piece of material cut out from a test manufactured copper canister are also included in the polarisation tests. This material has a grainsize that is much larger than the desired largest grainsize (the average grainsize within the sample used for characterisation was around 400 μm, see pictures in Appendix B). The microhardness of this material is $H_{v\ 0,2\ kp/30\ s} \approx 82\ kp/mm^2$.

The polarisation test samples were made with diameter ∅ = 16 mm and a thickness of about 4 mm (Figure 1). They were placed in a special holder that exposes the middle parts of one side in a way that the active surface area (area of surface in contact with the solution during polarisation measurements) was very close to 1 cm^2. This area will give currents in a suitable range and will make calculations easy. In addition the way the samples were prepared and mounted in the holder will ensure good reproducibility.

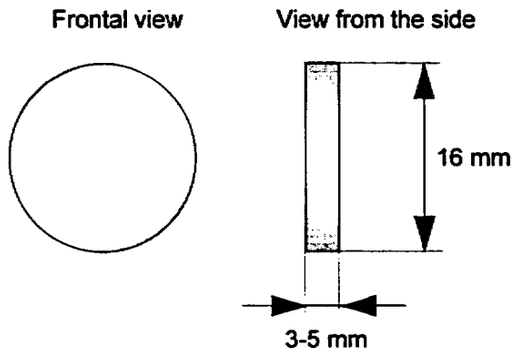

Figure 1
Shape and size of the specimens used for polarisation measurements.

The state of the canister surface in the repository is hard to predict in detail and will most probably vary across the canister surface, depending on the manufacturing methods used, handling procedures, etc. For the polarisation tests a reproducible surface is considered important and the following preparation procedure has been followed:

Wet polishing on gradually finer paper with 600-mesh paper in the final stage was used to remove scratches and other defects on the surface. This was followed by ultrasonic washing in deionised water, acetone and ethanol, 5 min. each. Finally the specimen was dried with warm air and stored in desiccator until used in the experiments.

To have a reproducible surface oxide in every experiment, a pre-treatment of the specimen was carried out, consisting of an electrochemical reduction followed by a cyclic oxidation in 20 mM KOH [28, 29]. Reduction is for 20 min. at -0.8 V_{SHE} and the cyclic oxidation is up to +0.7 V_{SHE} with a scan speed of 10 mV/s. After the oxidation the specimen is rinsed carefully in deionised water and directly moved into the testing solution where it is applied as the working electrode.

3.3 Equipment

The polarisation curves were recorded with an EG&G PARC Model 263 Potentiostat/Galvanostat connected to a personal computer running the EG&G PARC Model 352/252 SoftCorr II software for corrosion measurements and analysis.

The measurements were made in an electrochemical cell made according to ASTM G-05 standards, with a saturated calomel electrode (SCE) as reference, separated from the cell with a salt bridge. As counter electrodes two symmetrically placed carbon rod electrodes were used. The electrochemical cell and the arrangement of the electrodes is shown schematically in Figure 2.

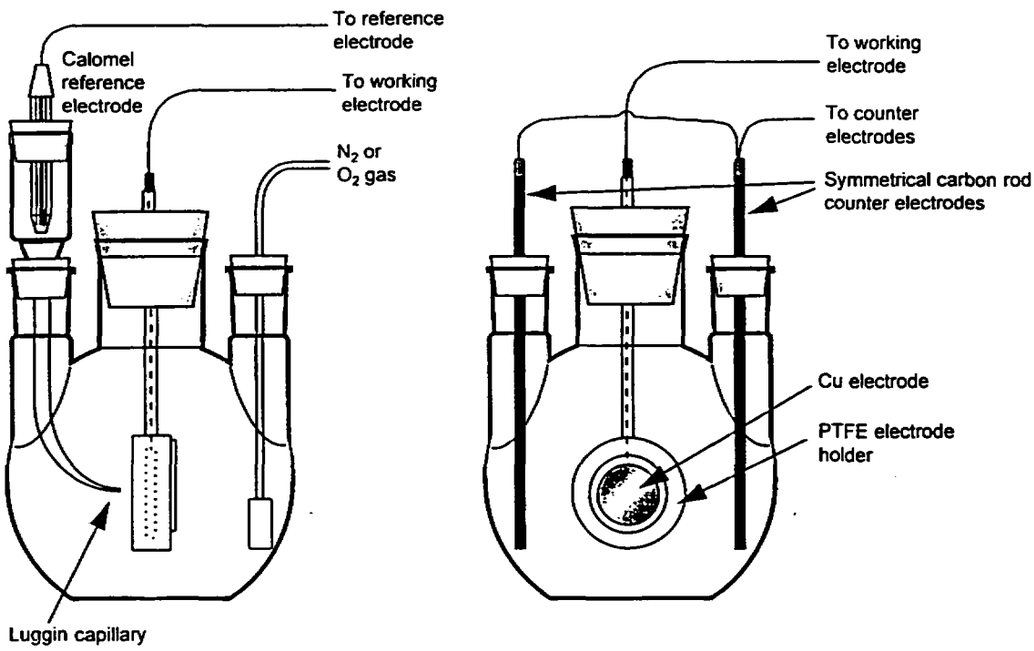

Figure 2
The electrochemical cell for polarisation measurements viewed from two perpendicular angles. Electrodes outside the plane of the paper have been removed from the picture for the sake of clarity.

3.4 Polarisation measurements

All solutions were prepared from ultrapure water and oxygen was removed from the solutions through purging with nitrogen. The oxygenated solutions where bubbled with air to get approximately 8 ppm of oxygen. The spontaneous potential (the *corrosion potential*, see appendix F) of the samples at open circuit (no current going through the system) was monitored from the moment the sample was brought in contact with the measuring solution until the actual polarisation measurement was started (see examples in Appendix C).

From this monitoring it was decided when stable conditions were reached and the sample and the solution had reached a quasi-equilibrium. As a criterion, the rate of change of the corrosion potential was used, and a change of less then a few mV per hour was taken as being slow enough for the polarisation measurement to be started. The open circuit potential was also used to decide the starting potential of the polarisation scan, as the polarisation scans were started approx. 150 mV cathodic (negative) of the open circuit (*corrosion*) potential.

The polarisation scans were first run in the anodic (positive) direction from the starting potential up to a potential where the anodic corrosion current density of the copper specimen was above 20 mA/cm^2, which usually happened above +800 mV_{SHE}. There the scan direction was reversed and the potential was scanned in the opposite direction back to the starting potential. During the scan the current through the sample was recorded as a function of applied potential. The scan speed during polarisation measurements was 10 mV/min. For a few of the specimens where there was much noise in the current data, a noise filtering routine was used to get a more readable polarisation curve. The filtering was a seven point sliding average, i.e. three points on each side and the point itself are added together for every point and then divided by seven. This will filter out fast changes (noise) while slower changes (the polarisation curve) is left essentially unchanged.

3.5 Post treatment

After the polarisation measurements, the specimens were washed ultrasonically in deionised water and in ethanol (~ 5 min. each), and dried with warm air. This treatment removed loosely attached corrosion products from the surface. Finally the specimens were placed in a desiccator.

After the mild cleaning procedure, the specimens where examined visually and pictures were taken in a Scanning Electron Microscope (SEM) to document the changes of the sample surface as a result of the polarisation measurements. (The SEM pictures are found in Appendix E).

4 Results

4.1 Corrosion potential

The spontaneous potential (the *corrosion potential*, see appendix A) of the samples at open circuit can indicate when stable conditions are reached and the sample and the solution have reached a quasi-equilibrium (see examples in Appendix C). The corrosion potential also gives indications on the changes that may take place on the sample surface when in contact with the groundwater. Comparing the corrosion potentials indicates environments in which the corrosion potentials differ noticeably from the others. One environment that differs considerably from the rest is where sulphide is added (see Table 6). Obviously there is a change taking place on the surface in this environment also before the polarisation test starts.

The open circuit corrosion potential can also be used to detect the photoelectrochemical sensitivity of the surface film, but no systematic investigations of photoelectrochemical properties were made. However, in the few tests made with light falling on the surface, very little or no photoelectrochemical sensitivity was observed in most cases, but in one case (with the surface film formed in water containing hydrogen carbonate) a large photoelectrochemical sensitivity was observed (Appendix C). Consequently experiments were performed in a dark-box to avoid any false signals from light falling on the copper surface during measurements.

Another way to measure the corrosion potential is to read the potential when the current passes zero during polarisation measurements. This is observed as a deep minimum in the polarisation (log I vs. E) curve. The two potentials obtained should be close to each other. A large difference indicates that the electrode surface has changed or that the open circuit potential was not yet stabilised. Corrosion potentials at open circuit and extracted from the polarisation curve are given in Table 6 together with the corrosion currents obtained by manual extrapolation and by computer curve fitting.

4.2 Polarisation curves

The polarisation curves were recorded with a scan speed of 10 mV/min. The scan was started at a potential 100-200 mV cathodic from the open circuit corrosion potential and continued up to a potential where the anodic current exceeded 20 mA/cm^2. Thereafter the potential was brought back to the starting potential. The recorded curves are displayed as potential / logarithmic current plots (Appendix D). To show the hysteresis more clearly, some linear potential / current plots are also displayed. The used software (EG&G PARC Model 352/252 SoftCorr II) can perform a number of calculations on the recorded curves. One of these calculations makes a fit to the curve around the corrosion potential to find the best values of the corrosion potential (E_{corr}) and the corrosion current (I_{corr}).

When the potential becomes anodic enough to cause a breakthrough of the protecting oxide film on the surface and the metal is locally corroding actively, there is ideally a sharp increase in current. The potential where this takes place is called the *breakthrough* or the *pitting potential* (see Appendix A). In cases where the increase in current is not so sharp (and to avoid any uncertainty), the breakthrough is said to take place when the current density passes a certain limit. In this work the current density limit is set to 10 $\mu A/cm^2$, a value often used in ASTM standards. A breakthrough potential very close to the corrosion potential indicates that there is no protective film on the surface. Accordingly the surface corrodes as soon as an anodic potential is applied. In Table 6 the corrosion potentials, the corrosion currents and the breakthrough potentials are given for copper in the different environments designed according to Table 5.

Besides *corrosion potential*, *corrosion current*, *breakthrough potential* and *repassivation potential* (for definition, see Appendix A) there is information to extract from the shape of the corrosion curve and the difference in forward (anodic) scan and return (cathodic) scan. A large hysteresis in the anodic current (i.e. the current stays high or even increases when the potential is scanned back in cathodic direction) usually indicates pitting or crevice corrosion (Appendix A). A large change of the potential where the current passes zero (and shifts from anodic to cathodic) between forward scan and return scan indicates changes of the surface or in the surface film.

Table 6

Corrosion potentials measured at open circuit (OC) and calculated from polarisation measurements. Corrosion currents from manual estimation, (MAN) and from computer curve fitting. Breakthrough potentials taken at I = 10 $\mu A/cm^2$.

Sample No.	Environment	$E_{corr,\ OC}$ mV_{SHE}	E_{corr} mV_{SHE}	$I_{corr,\ MAN}$ $\mu A/cm^2$	I_{corr} $\mu A/cm^2$	E_{break} mV_{SHE}
Cu01	SGW	*95*	*)	*)	*)	*220*
Cu02	SGW **)	*155*	*130*	*6.0*	*8.2*	*143*
Cu03	SGW (air oxid.)	38	12	0.14	0.10	151
Cu04	SGW + Cl^- (1 %)	51	43	0.34	0.38	123
Cu05	SGW + Cl^- (5 %)	-34	-59	0.62	0.80	27
Cu06	SGW + Cl^- / O_2	26	26	1.0	1.1	77
Cu07	SGW + O_2	121	122	0.12	0.10	186
Cu08	SGW + HCO_3^-	137	126	0.14	0.25	238
Cu09	SGW + HCO_3^- / O_2	109	103	0.12	0.10	186
Cu10	SGW + SO_4^{2-}	-31	-49	0.26	*0.67*	124
Cu11	SGW + SO_4^{2-} / O_2	53	70	1.1	0.76	133
Cu12	SGW + Cl^- / HS^-	-705	-728	3.3	7.4	-692
Cu13	SGW + Cl^- / HS^-	-38	*)	*)	*)	*)
Cu14	Cl^-, pH 8.5	-52	*-66*	*0.26*	*0.20*	100
Cu15	SGW + Cl^- / H_2O_2	-2	-45	0.65	0.34	58
Cu16	SGW + NO_3^-	-30	-51	0.30	*0.10*	111
Cu17	SGW + Cl^- / Fe^{3+}	-48	-79	0.30	0.33	47
Cu18	SGW + Cl^-, pH 10	-2	-71	0.06	0.11	150
CuX1	20 mM NaOH	47	31	0.30	0.31	860
Large grainsize material						
Cu101	SGW, long time	-30	-83	0.44	*0.30*	109
Cu102	SGW	-65	-85	0.28	0.48	97
Cu103	SGW + HS-	-743	-756	3.4	6.1	-724
Cu104	SGW + HCO_3^-	-6	-20	1.3	3.9	23
Cu105	SGW + Fe^{3+}	-57	-88	0.32	0.35	25
Cu106	SGW + Cl^-, pH 7	-67	-101	0.48	*0.20*	24

SGW = Synthetic Groundwater according to 2.2

*) Data in italics indicates a large degree of uncertainty. In a few cases no data is available due to a computer error. Sometimes computer curve fitting is erroneous or impossible (due to curve shape, noise, lack of data points, etc.).

**) These values were obtained during a second polarisation cycle, when the surface already had some damage. The values are therefore rather uncertain, and the corrosion currents are higher then during the first cycle.

In most environments the polarisation behaviour is very similar. The corrosion potential is close to 0 V_{SHE} (-70 to 70 mV_{SHE}) and the current raises quickly on the anodic side of the corrosion potential. Thus, the breakthrough potential is just anodic of the corrosion potential indicating a very superficial or non-existent passive film. On the scan back in cathodic direction the curve follows essentially the same trace, but passes the potential of zero current 100-200 mV more anodic compared with the anodic scan. The presence of oxygen or addition of large amounts of chloride ions does not change this behaviour significantly (c.f. figures in Appendix D).

A film or a surface layer is usually formed during the scan from interaction between species in the surrounding water and corrosion products. The colour and attachment of the film can vary depending on solution composition, but the surface layer is in most cases not protecting the surface from corrosion.

This can clearly be seen on the electrodes after the polarisation tests. The surface has usually clear signs of corrosion attack and in many cases pitting can be seen. To what extent this pitting is due to pit formation at lower potentials or to what extent it depends on high anodic potentials and currents (often above 1 V_{SHE} and 10-20 mA/cm^2) is presently not clear.

In a couple of cases there are indications of formation of a passive film, i.e. a potential region of low anodic corrosion currents (Appendix D; Cu10, Cu18, Cu101), but the potential region of passivity is very small. Compare with the polarisation curve of copper in 20 mM NaOH, where a large region of passivity can be seen (Appendix D; CuX1). The environments in which some passivity occurred are in groundwater with high concentration of SO_4^{2-}-ions (1%, Cu10), in groundwater with high chloride concentration at a high pH (1% Cl^- and pH10, Cu18) and with a very long resting time in the groundwater prior to the polarisation measurements (~one week, Cu101).

There are also a few cases where the polarisation curves show a hysteresis, possibly an indication of pitting corrosion. (Appendix D; Cu02, Cu08, Cu15, Cu17, Cu18, Cu101, Cu105, Cu106). However, the hysteresis is relatively small and on a limited part of the anodic potential range and at high potentials far from the corrosion potential. Such high anodic potentials are not likely in the real repository environment. An exception is specimen Cu08, (HCO_3^- saturated at pH 8.5) that shows a rather large hysteresis throughout the anodic potential region, indicating a film breakthrough and localised corrosion. This is especially interesting as the carbonate system is expected to be present in rather high concentrations in the repository.

4.3 Optical microscopy and SEM

Prior to the polarisation tests a sample of each batch of the used copper materials was characterised with respect to the size and the shape of the grains. The samples were polished and etched and then examined in an optical microscope. (Appendix B) The hardness of the material was also determined as a part of the characterisation.

The appearance of the copper surfaces after the polarisation tests can give an additional hint to the resistance to pitting corrosion of copper in the used water. The results must however be used with caution as the applied potentials are high and reactions proceeding at high rates due to the applied potentials may be very slow without an applied potential. Also the current passing through the sample at the very anodic potentials and the time spent in that potential region differs between the samples. Thus the amount of visible attack on the surface can differ from that reason alone.

In addition to the direct inspection with the naked eye, the surfaces where inspected in a SEM (Appendix E). Optical microscopy was not used as deep pits are very hard to display, due to the limited depth of focus in the optical microscope. The SEM was only used to look at the appearance of the surface. No analysis of the chemical composition of the surface was made, as the main interest was to look at the amount of damage to the surface and the presence of eventual corrosion pits. Here follows a list of observations on all samples, both with the naked eye and in SEM (SGW = Synthetic Groundwater).

Cu01 SGW

Visible general corrosion, some pitting. The SEM shows a film covering most of the surface. Surface attack visible where the film is not covering the surface.

Cu02 SGW

General and pitting corrosion clearly visible, with many pits. In SEM a number of corrosion pits a few hundred μm in diameter are visible. Some grains and grain boundaries are also visible especially in the pits, where grain boundaries are clearly corroded.

Cu03 SGW, sample oxidised in air

Some visible general corrosion, some pitting. Oxide film consisting of irregular grains a few μm in size are visible in SEM. The film seems to be very thin (some grain boundaries visible), and is not fully covering the surface. A number of pits are also visible.

Cu04 SGW / Cl^-

Strongly corroded surface. In SEM the surface looks very uneven and there is a pronounced attack on grain boundaries in the most corroded areas. The general corrosion dominates and there are no clear pits.

Cu05 SGW / Cl^-

A slight general corrosion, large part of the surface film covered. A well covering film with lots of small cracks is visible in SEM.

Cu06 SGW / Cl^- / O_2

Some general corrosion with a few pits can be seen. There seems to be a thin surface film visible in SEM.

Cu07 SGW / O_2

Some general corrosion with a few pits can be seen. In SEM a surface film with lots of small cracks is visible. The surface seems to cover the surface well, but there are still some pits in the surface.

Cu08 SGW / HCO_3^-

General corrosion, remnants of a surface film and some slight pitting visible. A surface film with small irregular grains is covering parts of the surface, as can be seen in SEM. Grains and grain boundaries are seen in parts not covered by the film. The grain boundaries show signs of corrosion. No clear pitting visible.

Cu09 SGW / HCO_3^- / O_2

General corrosion and some slight pitting. No clear pitting or film formation visible in the SEM pictures. Some grains and grain boundaries are visible, with the grain boundaries slightly corroded.

Cu10 SGW / SO_4^{2-}

Only slight general corrosion visible. No pitting or film formation visible in the SEM pictures. Some grains and grain boundaries are visible, with the grain boundaries slightly corroded. The crystal plans visible in some grains (no or very thin oxide covering the surface of the grains).

Cu11 SGW / SO_4^{2-} / O_2

Some general corrosion visible. No pitting or film formation visible in the SEM pictures but some general corrosion. Grains and grain boundaries are visible, with the grain boundaries corroded. The crystal plans visible in the grains (no or very thin oxide covering the surface).

Cu12 SGW / Cl^- / HS^-

A slight general corrosion and a surface film visible. The surface covered by a film, with darker and lighter regions, as can be seen in SEM. The film appears to be formed of two layers, a covering layer with a large amount of larger grains spread out on top. No pitting or general corrosion visible.

Cu13 SGW / Cl^- / HS^-

Some general corrosion and a few corrosion pits visible. A few pits visible in SEM. The whole surface, including pits, covered with a film.

Cu14 SGW, pH8.5

Some general corrosion visible. No pitting or clear film formation visible in the SEM pictures but some general corrosion. Grains and grain boundaries are clearly visible, with the grain boundaries corroded. Grain surfaces a little rough, but no crystal plans visible.

Cu15 SGW / Cl^- / H_2O_2

Some general corrosion and a clear pitting corrosion visible. Heavily corroded surface visible in SEM, with many pits of variable sizes. Some pits appear to be rather deep.

Cu16 SGW / NO_3^-

General corrosion and a slight pitting visible. No clear pitting or film formation visible in the SEM pictures but some general corrosion. Some grain boundaries are corroded and clearly visible. Grain surfaces a little rough, with lots of very small holes or cracks.

Cu17 SGW / HS^-

Some general corrosion and clear pitting is visible. Heavily corroded surface visible in SEM, with many pits of variable sizes. Some pits appear to be rather deep.

Cu18 Cl^-, pH10

Both general and pitting corrosion visible. A heavily corroded surface with both general and pitting corrosion can be seen in SEM, with many pits of variable sizes. Some pits appear to be rather deep. Some attack on grain boundaries visible. Some parts of the surface covered with a thin film.

Cu101 SGW (long time)

General corrosion and some slight pitting visible. Some general corrosion with a few pits can be seen in SEM. Some grain boundaries are visible. It is hard to tell if the surface is corroded or there is a surface film, but many small cracks are visible on the surface.

Cu102 SGW

Strong general corrosion of the surface. A very clean surface is visible in SEM, with no signs of film formation or pitting corrosion. Some corrosion of grain boundaries. Crystal plans visible on some grains (no or very thin oxide).

Cu103 SGW / HS^-

Most of the surface covered with a film. Some general corrosion visible. Some darker and lighter regions of the film can be seen in SEM. The film regions appears to reflect underlying grains. The film consists of a large number of small grains of similar size. No pitting or general corrosion visible.

Cu104 SGW / HCO_3^-

Clear general corrosion of the surface is visible to the naked eye. A very clean surface is visible in SEM, with no signs of film formation or pitting corrosion, but apparently some general corrosion. Clear corrosion of grain boundaries. Crystal plans visible on the grains (no or very thin oxide).

Cu105 SGW / Fe^{3+}

General corrosion, some slight pitting and a surface film visible. In SEM is some general corrosion visible. The surface is covered with a film with a grainy structure.

Cu106 SGW / Cl^-, pH 7

General corrosion, some slight pitting and remnants of a surface film visible. Some pits and a surface film visible in SEM. Some grains can be seen.

CuX1 NaOH

Some slight general corrosion and remnants of a surface film visible. A very smooth surface visible in SEM. Grain boundaries corroded and clearly visible.

5 Discussion

The equilibrium time for the open circuit potential (corrosion potential) to reach a stable value has usually been between 20 to 30 hours. A potential value was considered stable when the variations were in the order of a few millivolts per hour. Waiting for a much longer time (>150 hours) in one case did not result in any large potential changes. The net change from the 24 hour value was -4 mV, and the total potential variation from the 24th hour and onwards was about 10 mV (Appendix C 2).

A complication in the measurement of the open circuit potential was when, in some cases (i.e. groundwaters with high HCO_3^- concentrations), a semiconducting and light sensitive surface film was formed. The corrosion potential of the sample was then affected by the spectrum and intensity of the light falling on the surface ("Daylight", Appendix C 2). To avoid any influence from photopotentials the polarisation measurements were consequently performed in darkness. No further investigation of the semiconducting and photoelectrochemical properties were made. The photoelectric effect is, however, a good indication of film formation on the surface.

The pH values and salt concentrations expected in groundwater at 500 m depth in crystalline bedrock (pH 8-10, >1000 ppm Cl^-) will most likely produce a chemical environment where the formation of a passive film on the copper surface to a large extent is inhibited. This can more clearly be seen when the polarisation behaviour is compared with copper in 20 mM NaOH without any salts added. In NaOH a large passive region (approx. 0.2-0.9 V_{SHE}) appears. Thus, general corrosion is the first concern in groundwater with high salt content, a conclusion which is in accordance with earlier discussions [4].

In most of the groundwater compositions tested here, the behaviour is similar and there is no or very little sign of passivity. The breakthrough potential is thus close to the corrosion potential and only a small anodic potential will give a large increase in the current. This is also seen in the SEM pictures where the whole or parts of the copper surface has no covering film. The influence of the high salt concentration is further established by the polarisation curve in a pure NaCl solution with the same ionic strength as the synthetic groundwater. The NaCl polarisation curve is very similar to the polarisation curves in most of the synthetic groundwater environments.

In some of the polarisation curves there is a slight hysteresis which is typically for cases with pitting corrosion. The hysteresis is usually small, but is more obvious when linear scales are used in the polarisation plots (Appendix C). In all cases but one, the hysteresis is limited to high anodic potentials, several hundreds of millivolts above the corrosion potential. Such high potentials are not very likely under the repository conditions. The one exception is an environment containing the hydrogen carbonate ion (HCO_3^-) at pH 8.5. With hydrogen carbonate there is a hysteresis going all the way back to the corrosion potential (Cu08, Appendix C). This may indicate an increased risk for pitting corrosion when HCO_3^- is present.

The HCO_3^- is sometimes said to inhibit corrosion and sometimes to promote corrosion. Also in this work is there differences between the cases where HCO_3^- is present. As the saturation concentration of this ion is strongly dependent on the pH of the water (HCO_3^- is in equilibrium with CO_3^{2-}, CO_2, H^+ and H_2O), it is not possible to say if the pH, the concentration or a combination of both causes the change of behaviour. There is a need for further investigations on this and on the effect of other species in the water.

Also without any clear film formation there may be pitting corrosion. As can be seen from the microscope pictures there are visible signs of pitting corrosion, also when the polarisation curves do not show any clear signs of pitting corrosion. But the applied anodic potential becomes rather high during the polarisation measurements, and it is uncertain to what extent conclusions can be drawn from the appearance of the electrode surface after the measurements.

The observed pitting is, however, an indication of the possibility to have non-uniform corrosion of the surface also under general corrosion conditions, due to variations in surface structure and transport phenomena. Deep surface defects such as cracks, pores and scratches could enhance this effect considerably.

Increasing the Cl^- concentration from the basic synthetic groundwater (~3000 ppm) to 1% or to 5% does not change the polarisation behaviour significantly. All three concentrations show the typical lack of passivity, with a breakthrough potential close to the corrosion potential. In SEM the highest concentration shows a film covering the surface and the surface is less corroded. The film is full of cracks and is evidently not passivating as the polarisation curve also indicates.

Changing the pH (between 7 and 10) of the groundwater gives only small changes in the polarisation behaviour. There is a slight tendency for a small region of passivity at pH 10, compared to pH 8,5 or pH 7. This could mean a small increase of the risk for pitting corrosion at the higher pH and a larger tendency to general corrosion at the lower pH. This also gets some support from the SEM pictures, but the differences are small.

Some small tendency towards passivity is seen in the polarisation curves in synthetic groundwater with added SO_4^{2-}, with added Cl^- at pH 10, and in synthetic groundwater alone after a very long resting time in the solution. The differences compared to the other polarisation curves are however too small to draw any firm conclusions.

The two copper materials with different grainsizes show no significant difference in their polarisation behaviour. A slight difference can be seen when comparing the SEM pictures. The larger grainsize material shows a little less tendency towards pitting. This could be due to corrosion taking place preferably at grain boundaries or on grains with a certain crystallographic orientation.

The groundwater with HS^- added gives a completely different polarisation behaviour, compared to the other tested environments. The decrease of the corrosion potential to very cathodic potentials is significant, and indicates an attack on the

surface by the HS^- ion already with no potential applied. A passivating, or at least partly passivating surface film is formed (partly passivating, since the anodic currents become higher then when true passivation takes place). This is in agreement with previous observations of differences between copper oxides and sulphides. The copper ion is more mobile in a sulphide matrix compounded with the oxide.

During the anodic scan there is growth of the surface film until "whiskers" are formed on the surface (Appendix F). When the breakthrough takes place it seems the whiskers, which are often formed at an attack in sulphide environments, detach (at least some of them) from the surface, and the corrosion potential is moved to a potential similar to what is found in other environments. This change is also seen during the cathodic scan that differs considerably from the anodic scan in the sulphide environment. The formation and growth of whiskers indicate a rapid transport of corrosion products from the copper surface through the whiskers to the growing tips of the whiskers. This again points to the high mobility of the copper ion in sulphide.

As the experiment was done with rather high concentrations of HS^- the question is how high the local HS^- concentration can become under real repository conditions and what will happen at that concentration over a long time. It is obvious that the formed surface layer (copper sulphide) has protected the copper surface to some extent during the polarisation measurements, and the surface is not much corroded. Still the very low corrosion potential must be a concern, as an eventual breakthrough of the surface layer will give a large potential difference between anodic and cathodic areas and thereby a large driving force for the local corrosion reactions. Furthermore, the formation of copper sulphide whiskers may increase the transport rate considerably.

What is needed to give corrosion in a sulphide environment is an electron acceptor to receive the electrons released from the copper when copper sulphide is formed. Possible species that can function as electron acceptors are Fe^{3+} and polysulphide ions.

6. Conclusions

The groundwater 500 m down in the Swedish rock will most likely have a rather high salt content. In waters with a high salt content the passivation of copper is inhibited and the general corrosion dominates. The amount of general corrosion will be determined by the possible cathodic reactions (such as the reduction of oxygen) that can drive the corrosion current. Pitting corrosion is not a problem in such a case.

If the environment promotes the formation of a passive film on the surface, the general corrosion will be inhibited. But, if there are spots where the surface is not passivated, these spots can be places of local attack. Although most of the surface is protected from corrosion there is an increased risk for pitting corrosion at the spots without a passive film. But as in the case of general corrosion there is a need for an cathodic reaction to drive the corrosion current. None of the tested environments have a clear formation of a passive layer, but in a few there are signs of film formation on the surface. The same is also seen in the polarisation curves; no clear passivation or pitting but small tendencies in a few environments.

An exception is the HCO_3^- ion at pH 8.5, that show an extended region of hysteresis in the polarisation curve. This indicates that pitting corrosion may occur in the presence of the HCO_3^- ion. Further studies are needed to establish under what conditions the HCO_3^- ion will give pitting corrosion.

A special case observed is when HS^- ions are present in the groundwater. This ion reacts willingly with the copper surface while lowering the surface potential. Higher concentrations of this ion at the surface will result in the formation of a surface film and a considerable lowering of the potential. Although the film is at least partly passivating, there is an increased danger of pitting corrosion due to the low potential at the film. A hole in the film with the copper surface exposed could experience severe pitting, driven by the large potential difference between bare copper surfaces and the film formed by HS^-. There may also be an increased risk with HS^- through formation of whiskers that enhance the transportation of HS^- to the surface, although it still is unclear what are the necessary conditions for the formation of whiskers. Also the HS^- needs further studies to establish the effect it has on the pitting corrosion of copper under repository conditions.

In several of the tested environments there are signs of pitting corrosion on the copper surfaces after the polarisation tests, but it is unclear to what extent this is an effect of high potentials and large currents during the tests. Thus no certain conclusions can be drawn from the surface appearance alone.

7. Recommendations

Based on the results of this study the following recommendations for further studies are given:

The critical concentration of Cl^- above which there is no formation of a passive film on copper should be determined.

The possibility for localised corrosion in connection with whisker formation in HS^- containing groundwaters should be further studied. It is important to find out more in detail what factors are necessary for whisker formation, such as HS^- concentration, pH of the water, species for the cathodic reaction etc.

The possibility of pitting corrosion taking place in HS^- containing waters when no whiskers are formed must also be considered. As with whiskers formation it is necessary to find the environmental factors that will give pitting of the copper surface.

Pitting corrosion in waters containing bicarbonate ions (HCO_3^-) also needs further investigation. The results reported in the literature and the results in this work give a somewhat contradicting picture on the pitting corrosion of copper in carbonate containing water. It is therefore necessary to establish more in detail under what circumstances pitting will take place.

Another important field of investigation is the role of the bentonite clay in pitting corrosion. The bentonite will have a great influence on the environment at the canister surface, and will affect many parameters such as pH value, redox potential, transport of water and ions, ion concentrations, etc. This may give local variations at the canister surface that are of large importance for the pitting behaviour.

To address the above mentioned areas, accelerated electrochemical testing similar to what has been done in this work could be used. However, the accelerated testing needs to be complemented with other methods, such as long term tests, to give a more complete and reliable picture.

References

1 ENGMAN, U. AND HERMANSSON, H-P.
Korrosion av kopparmaterial för inkapsling av radioaktivt avfall - en litteraturstudie.
Swedish Nuclear Power Inspectorate, 1994 (SKI Report 94:6)

2 HERMANSSON, H-P.
Some properties of copper and selected heavy metal sulfides - A limited literature review
Swedish Nuclear Power Inspectorate, 1995 (SKI Report 95:29)

3 ERIKSSON, S. AND PALMÉR, L.
Aqueous corrosion of copper alloys - a literature survey
Studsvik Material AB, 1995 (STUDSVIK/M-95/57)

4 HERMANSSON, H-P. OCH BEVERSKOG, B.
Gropfrätning på kopparkapseln
Swedish Nuclear Power Inspectorate, 1996 (SKI Rapport 96:25)

5 ERIKSSON, J.
Provtillverkning av kapslar för slutförvaring av använt kärnbränsle
SKB Projekt Inkapsling, Projektrapport 95-06, Stockholm 1995.

6 WAGNER, J. JR. AND YOUNG, W. T.
Corrosion in building water systems,
Materials Performance 29/10 (1990), s.40.

7 SHALABY, H. M., AL-KHARAFI, F. M. AND GOUDA, V. K.
A morphological study of pitting corrosion of copper in soft tap water,
Corrosion 45/7, (1989), s. 536.

8 COHEN, A. AND MYERS, J. R.
Water treatment to mitigate corrosion of copper plumbing systems,
Materials Performance 32/8, (1993), s.43.

9 COHEN, A.
Historical perspective - Corrosion by potable waters in building systems,
Materials Performance 32/8, (1993), s.56.

10 MYERS, J. R. AND COHEN, A.
Pitting corrosion of copper in cold potable water systems,
Materials performance 34/10 (1995), s.60-62.

11 ROYUELA, J. J. AND OTERO, E.
The assessment of short term data of pipe corrosion in drinking water - II. Copper,
Corrosion Science 34/10 (1993), s. 1595-1606.

12 EDWARDS, M., REHRING, J. AND MEYER, T.
Inorganic anions and copper pitting,
Corrosion 50/5 (1994), s. 366-372.

13 LAM, K. W.
Ontario Hydro studies on copper corrosion under waste disposal conditions, in: Corrosion of nuclear fuel waste containers - proceedings of a workshop, D. W. Shoesmith, Editor. AECL-10121 Atomic Energy of Canada Limited, Manitoba Canada 1990.

14 AALTONEN, P.
Corrosion of pure OFHC-copper in simulated repository conditions - part 2, Report YJT-90-07, 1990.

15 SRIDHAR, N. AND CRAGNOLINO, G. A.
Effects of environment on localized corrosion of copper-based, high-level waste container materials,
Corrosion 49/12, (1993), s. 967.

16 FARMER, J. C., GDOWSKI, G. E., McCRIGHT, R. D. AND AHLU-WAHLIA, H. S.
Corrosion models for performance assessment of high-level radioactive-waste containers,
Nuclear Engineering and Design 129 (1991), s. 57-88.

17 FARMER, J. C., von KONYNENBURG, R. A., McCRIGHT, R. D. AND GDOWSKI, G. E.,
Survey of degradation modes of candidate materials for high-level radioactive waste disposal containers, Vol. 5. Localized corrosion of copper-based alloys.
Lawrence Livermore Nat. Lab. UCID-21362 Vol. 5 (1988).

18 THOMPSON, N. G., BEAVERS, J.A. AND DURR, C. L.
Potentiodynamic polarization studies on candidate container alloys for the tuff repository,
NUREG/CR--5708 TI92 007821, 1992.

19 BEAVERS, J.A., THOMPSON, N. G. AND DURR, C. L.
Pitting, galvanic, and long term corrosion studies on candidate container alloys for the tuff repository,
NUREG/CR--5709 TI92 007822, 1992.

20 TAXÉN, C.
Pitting corrosion of copper with sulphide as the reaction of determining reactant,
SKB Arbetsrapport 91-40, December 1991.

21 TAXÉN, C.
Pitting of copper under moderately oxidizing conditions,
SKB Arbetsrapport 92-43, March 1992.

22 FISCHER, W. R., WAGNER, D. AND SIEDLAREK, H.
Microbiologically influenced corrosion in potable water installations -
An engineering approach to developing countermeasures,
Materials performance 34/10 (1995), s.50-54.

23 MAIYA, P. S.
A review of degradation behavior of container materials for disposal of high-level nuclear waste in tuff and alternative repository environments,
Argonne National Laboratory report, ANL-89/14, s. 44-58.

24 SEQUEIRA, C. A. C.
Inorganic, physiochemical, and microbial aspects of copper corrosion: literature survey,
British Corrosion Journal 30/2 (1995), s. 137-153.

25 ADELOJU, S. B. AND DUAN, Y. Y.
Influence of bicarbonate ions on stability of copper oxides and copper pitting corrosion,
British Corrosion Journal 29/4 (1994), s. 315-320.

26 ADELOJU, S. B. AND DUAN, Y. Y.
Corrosion resistance of Cu_2O and CuO on copper surfaces in aqueous media,
British Corrosion Journal 29/4 (1994), s. 309-314.

27 WERME, L., SELLIN, P. AND KJELLBERT, N.,
Copper canisters for nuclear high level waste disposal. Corrosion aspects.
SKB Technical report 92-26, October 1992.

28 BURKE, L. D., AHERN, M. J. G. AND RYAN, T. G.
An investigation of the anodic behavior of copper and its anodically produced oxides in aqueous solutions of high pH,
J. Electrochem. Soc. 137/2 (1990), s. 553.

29 CHONG-HONG PYUN AND SU-MOON PARK
In situ spectroelectrochemical studies on anodic oxidation of copper in alkaline solution,
J. Electrochem. Soc. 133/10 (1986), s. 2024.

Explanations to used electrochemical terminology

Corrosion potential = the potential a freely corroding metal sample surface spontaneously attains. This potential can also be taken from a polarisation curve as the potential where the current changes sign and no net current flows through the metal surface (see picture below). A better value is usually obtained by curve fitting around the corrosion potential.

Corrosion current = the residual current at the corrosion potential that can be calculated by extrapolation (see picture below).

Breakthrough potential = the potential during an anodic polarisation scan where there is a breakthrough in the passive layer shown by a rapid increase in the anodic current. When the breakthrough means initiation of pitting corrosion the potential may be called *pitting potential*. Usually a threshold current is given above which a breakthrough is said to occur (see picture below).

Repassivation potential = the potential during a cathodic polarisation scan where the passive layer recovers and the anodic current therefore drops rapidly below the given threshold value (see picture below).

Critical pitting potential = the potential at which pitting will initiate if given infinite time (related to, but not the same as breakthrough potential). Below this potential pitting is not expected.

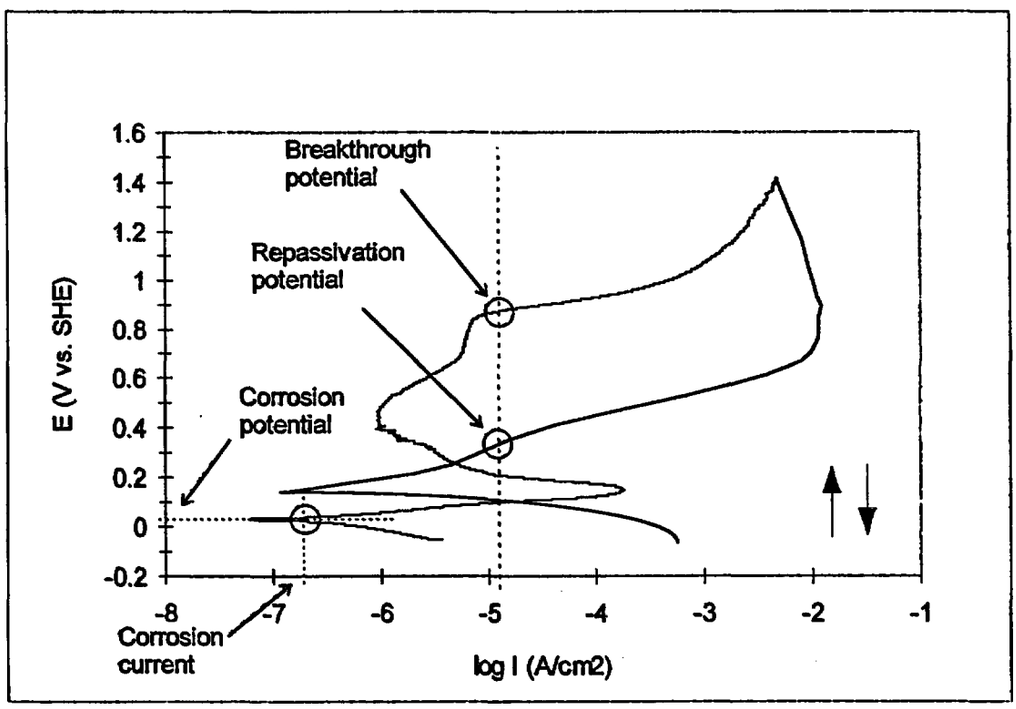

Photoelectrochemistry

When the oxide formed on a copper surface is non-stochiometric (for instance with oxygen vacancies), the oxide may show semiconducting properties. One semiconducting property is the ability to generate electric charge carriers (holes and electrons) when illuminated with light of short enough wavelength (with energy larger then the bandgap). If the conditions are right, the charge carriers are separated and the charge may appear as a potential across the illuminated surface oxide. Such conditions may be present when the surface oxide is in contact with an electrolyte. The copper surface then shows *photoelectrochemical sensitivity* and a potential can be measured between the copper electrode and an auxiliary electrode in the electrolyte. This potential will be superimposed on the corrosion potential of the copper surface in the electrolyte.

Optical microscope pictures of grains

Pictures of the copper materials used in the polarisation tests (the surfaces seen in the pictures are polished and etched to display the grains and grain boundaries).

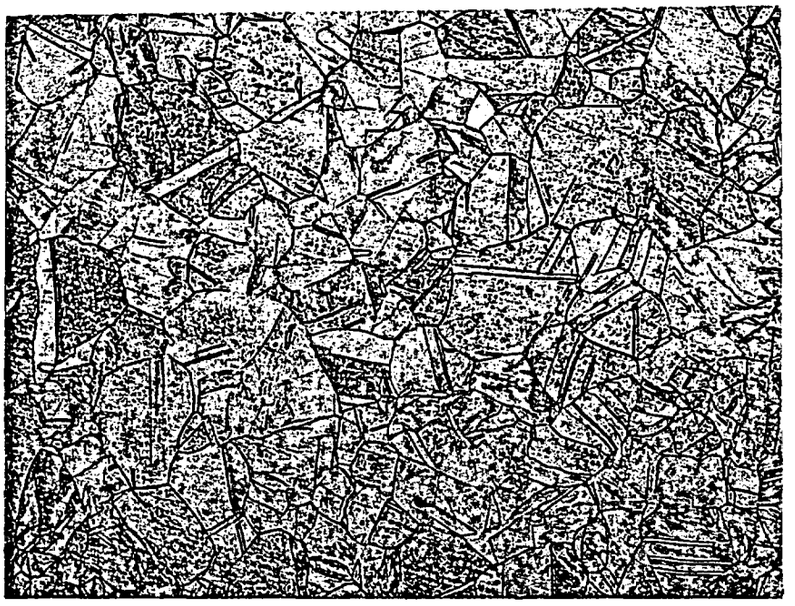

This is a sample the material supplied by Outokumpu Copper OY. The material was used for most of the polarisation tests. The grains are typically between 100-200 μm in size. 100 × magnification.

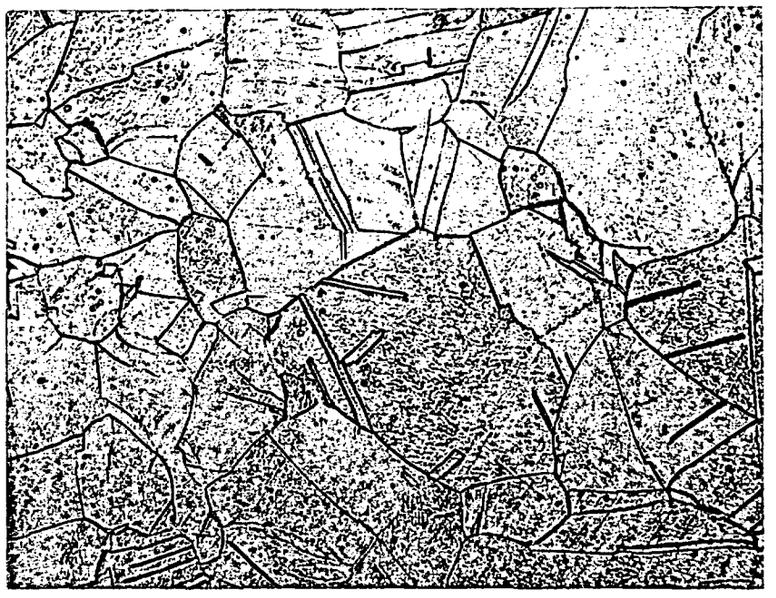

The same material as above in 200 × magnification.

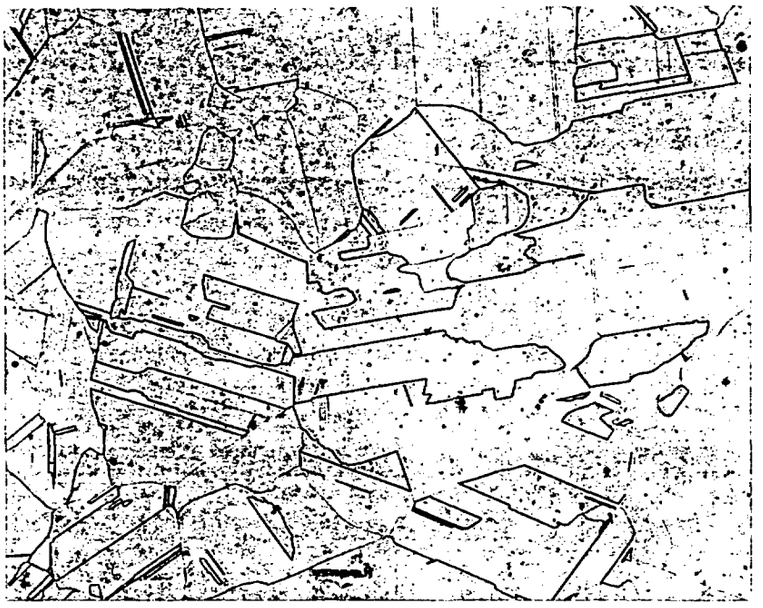

This is the material that was cut out from a test-manufactured copper canister. The grains are typically between 300-800 μm in size. 50 × magnification.

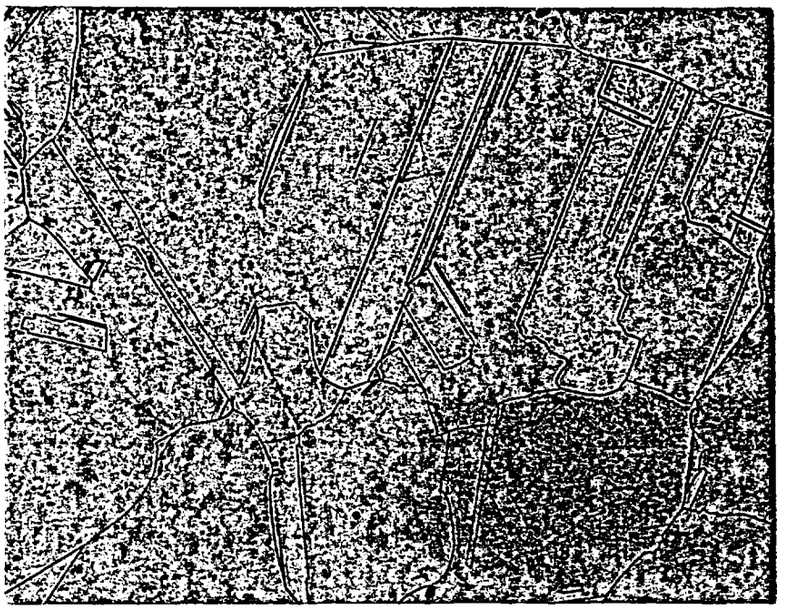

The same material as above in 100 × magnification.

Ecorr vs. time - curves

The corrosion potential (at open circuit) as a function of time at the start of the polarisation measurements:

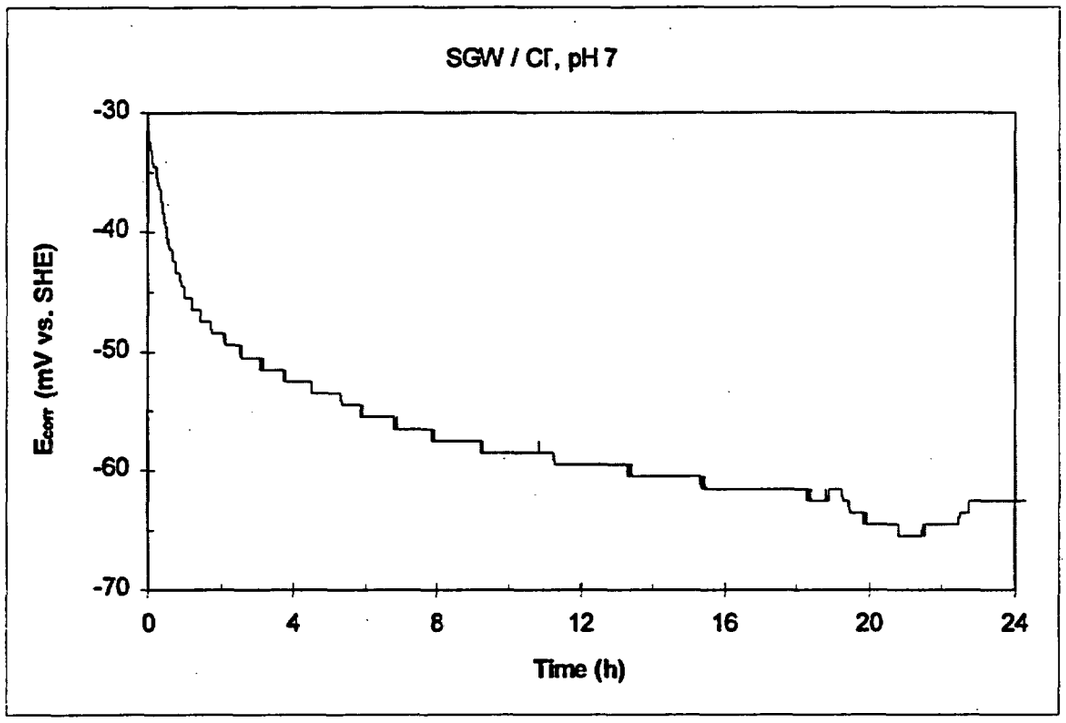

Cu106: A typical E_{corr} vs. time -curve for copper in synthetic groundwater. The large changes usually take place during the first 24 hours.

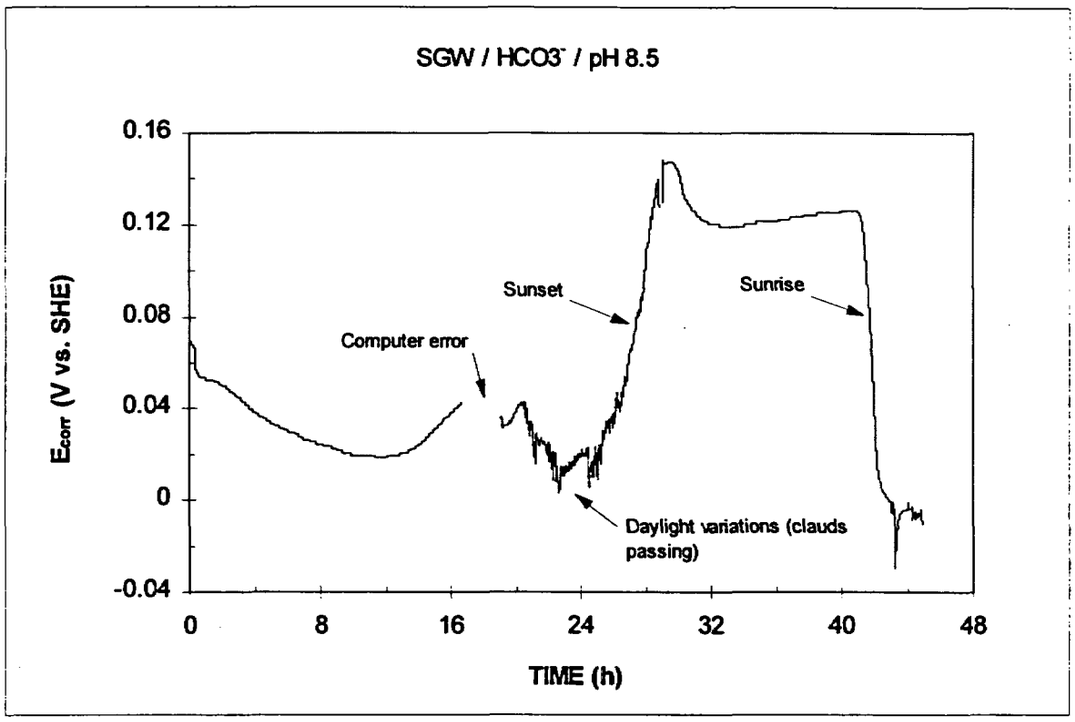

Cu8: The photoelectrochemical effect may be large in copper oxides and sulphides. Here shown in an oxide formed in SGW/HCO_3^- at pH 8.5.

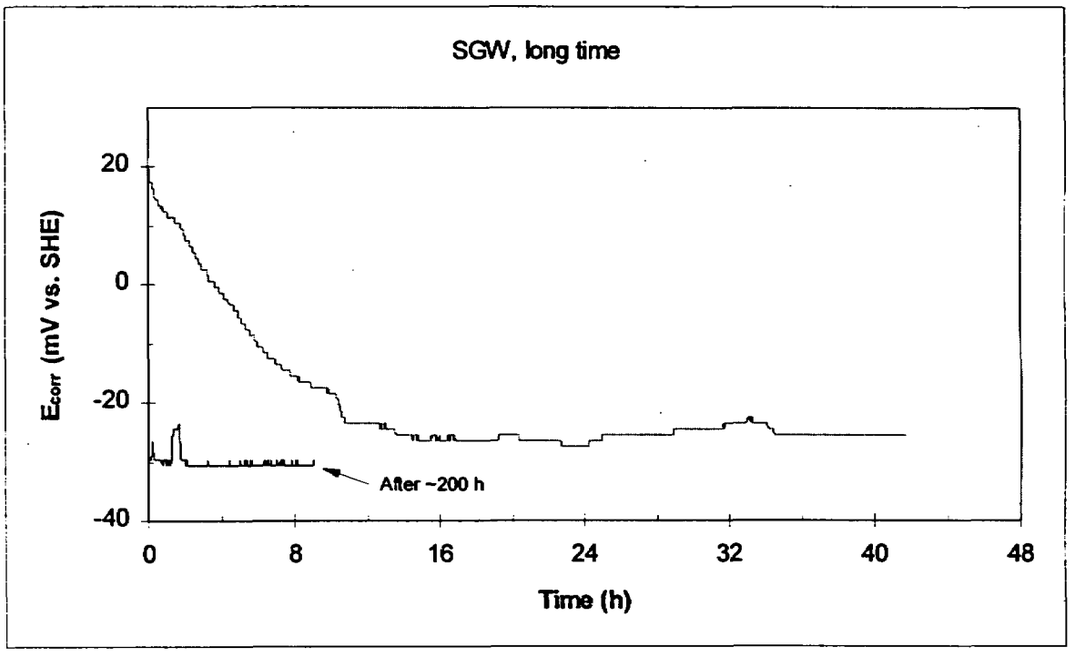

Cu101: The corrosion potential is rather stable over long time periods. The net change between 36 and 200 hours is about 4 mV.

Polarisation curves

Polarisation curves of the copper materials in different environments (SGW = Synthetic Ground Water, see text).

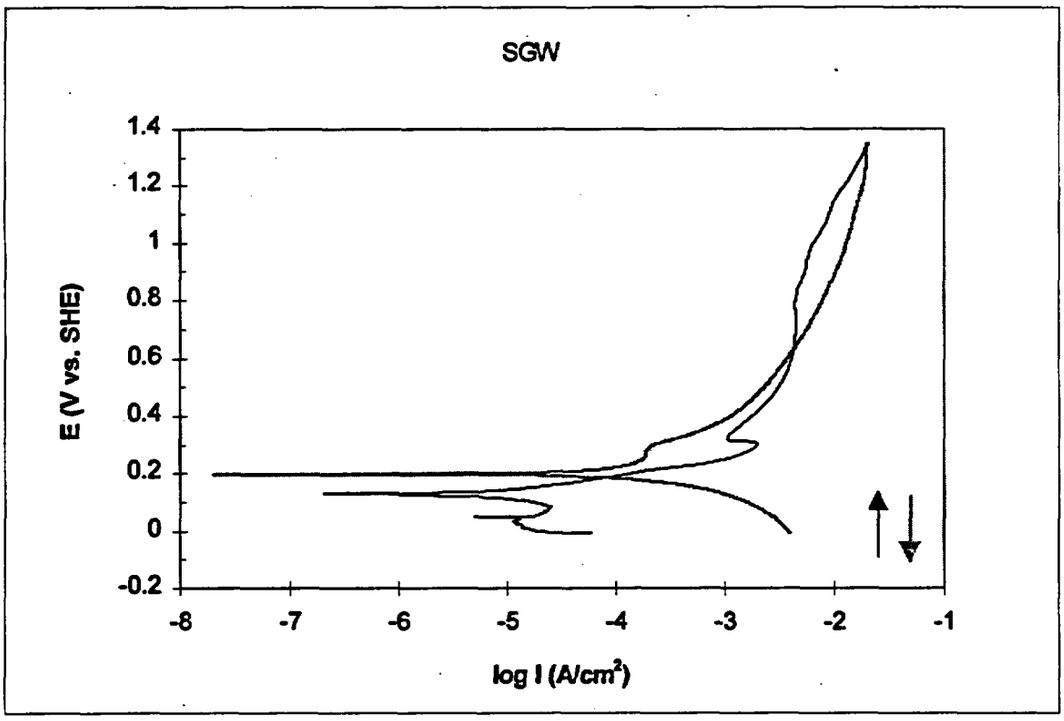

Sample: Cu02

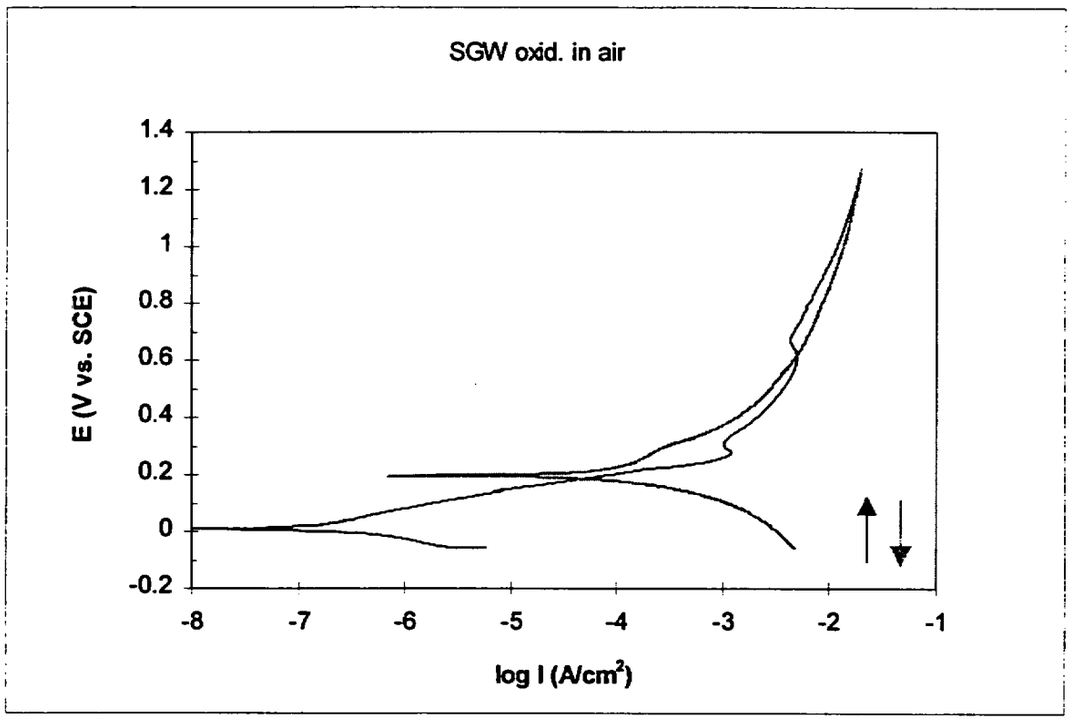

Sample: Cu03

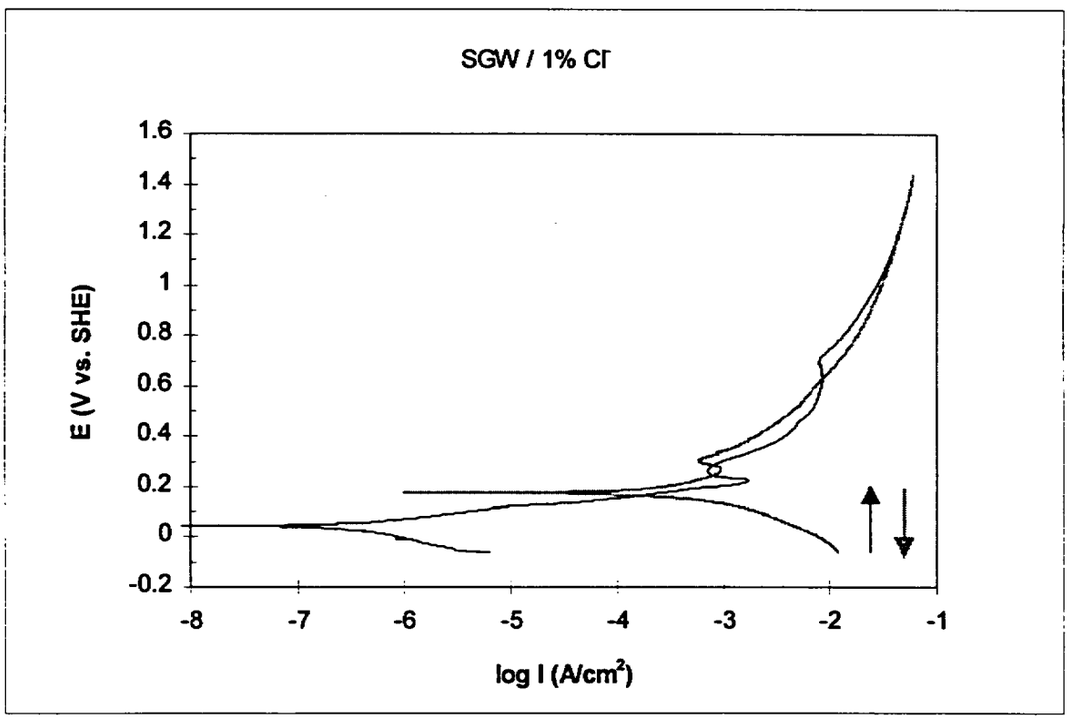

Sample: Cu04

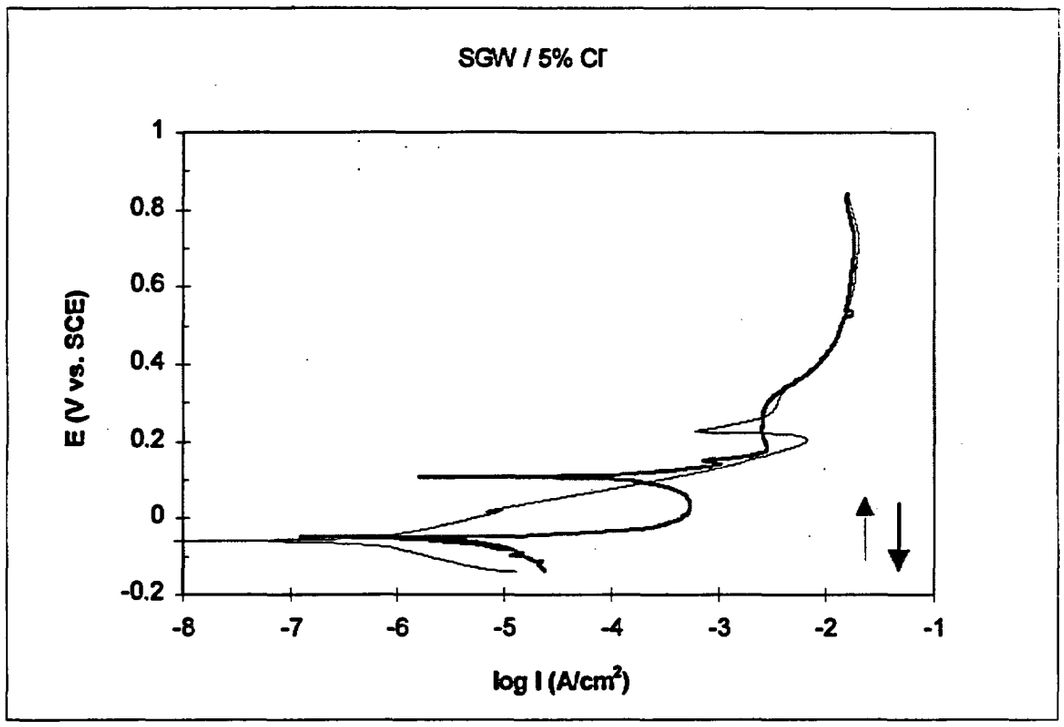

Sample: Cu05

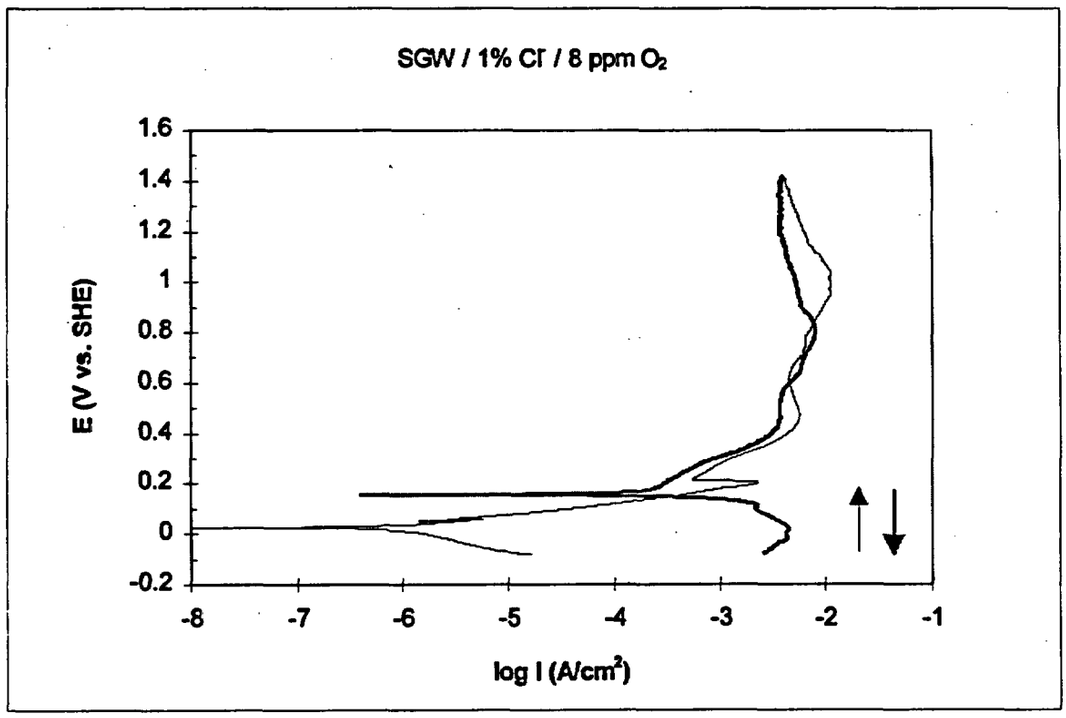

Sample: Cu06

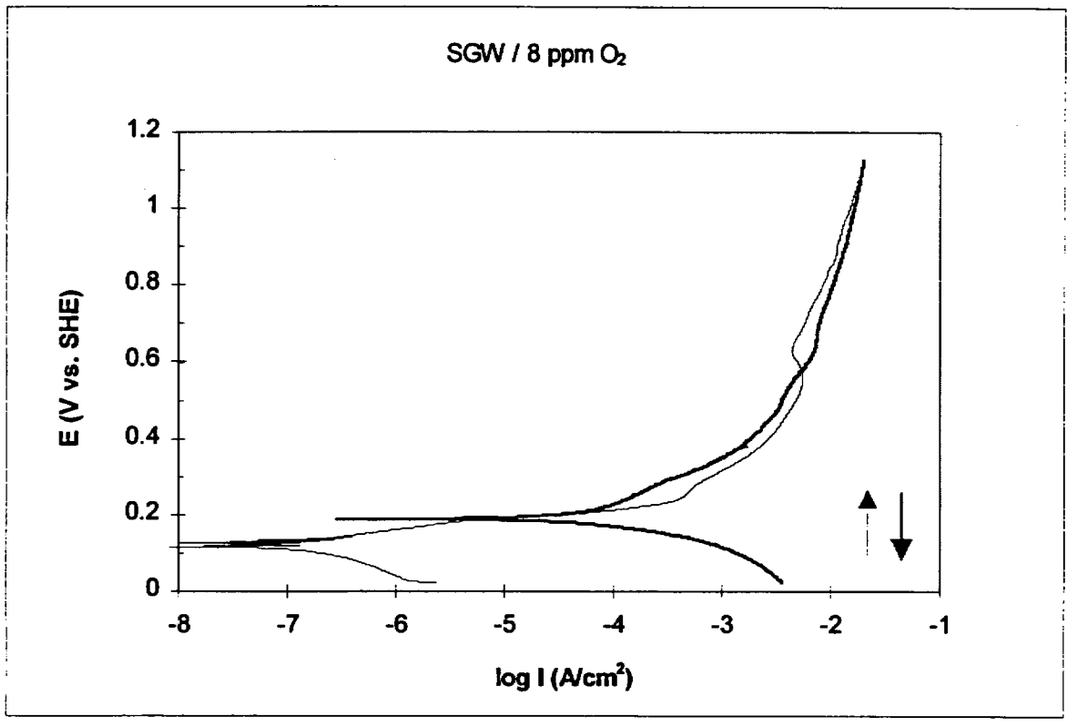

Sample: Cu07

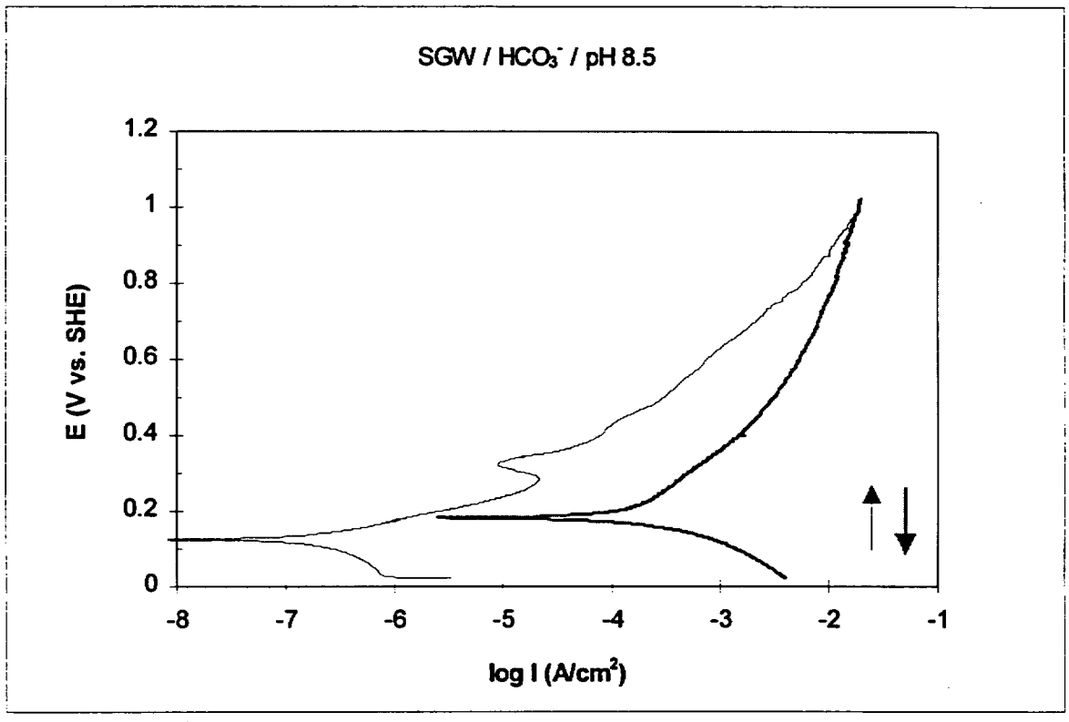

Sample: Cu08

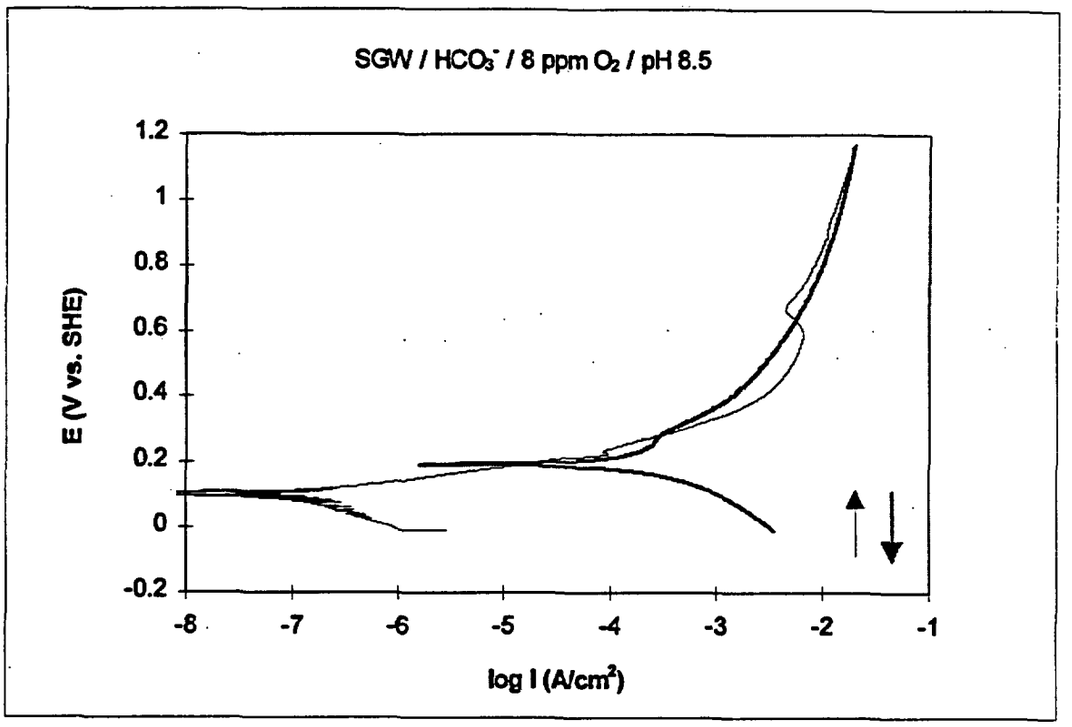

Sample: Cu09

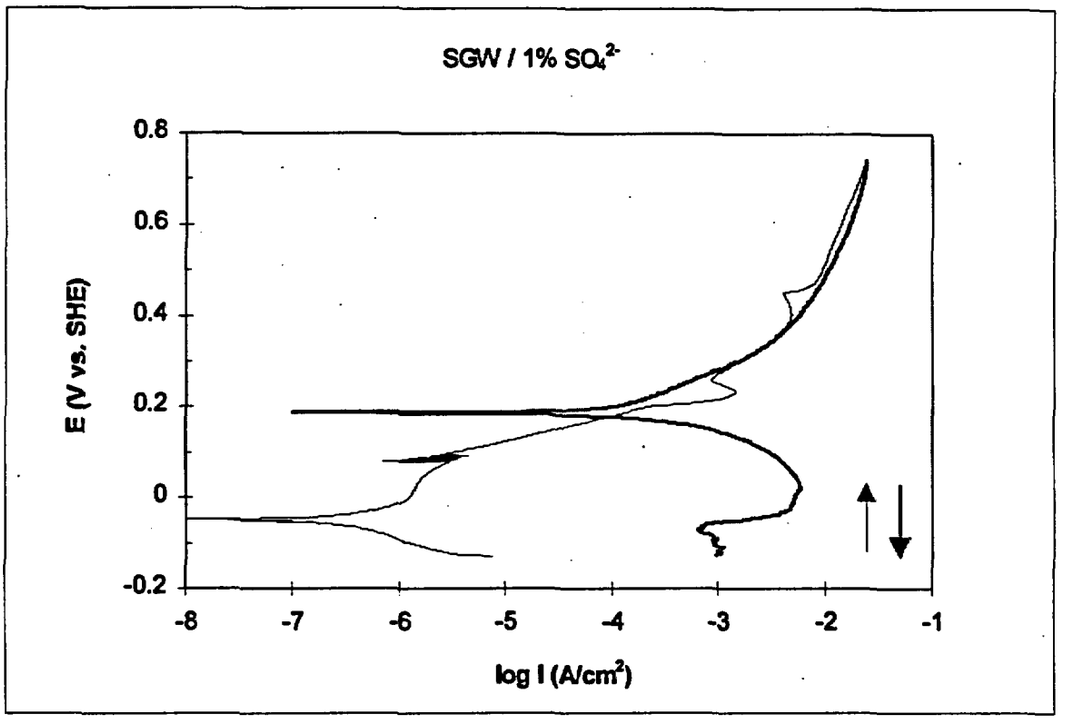

Sample: Cu10

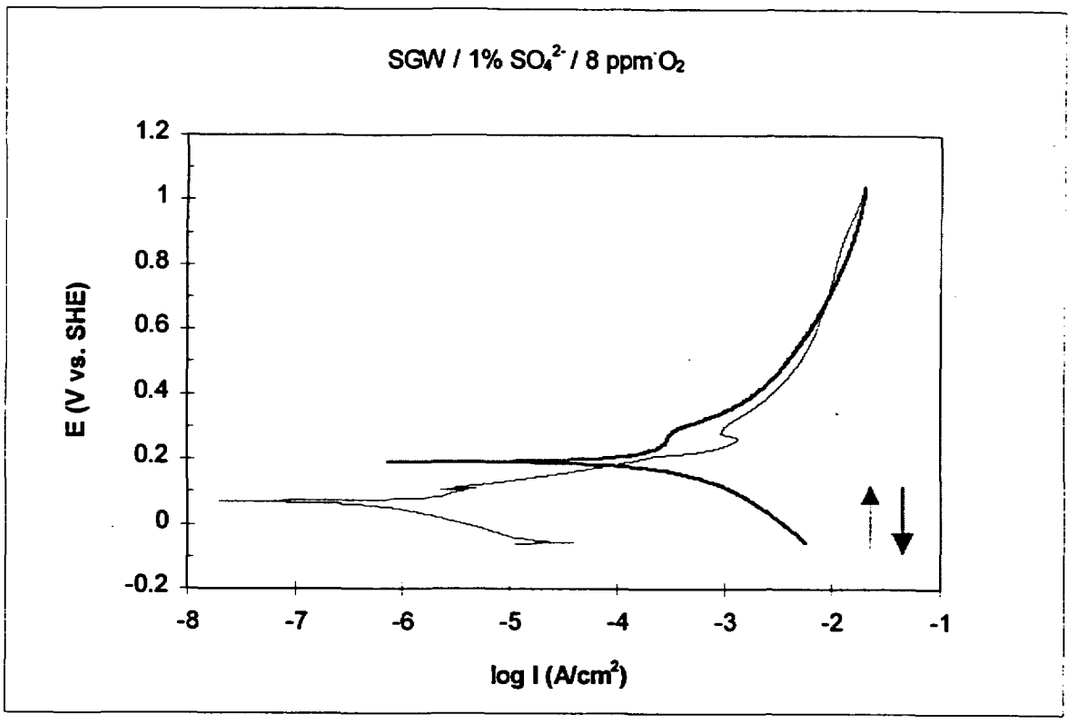

Sample: Cu11

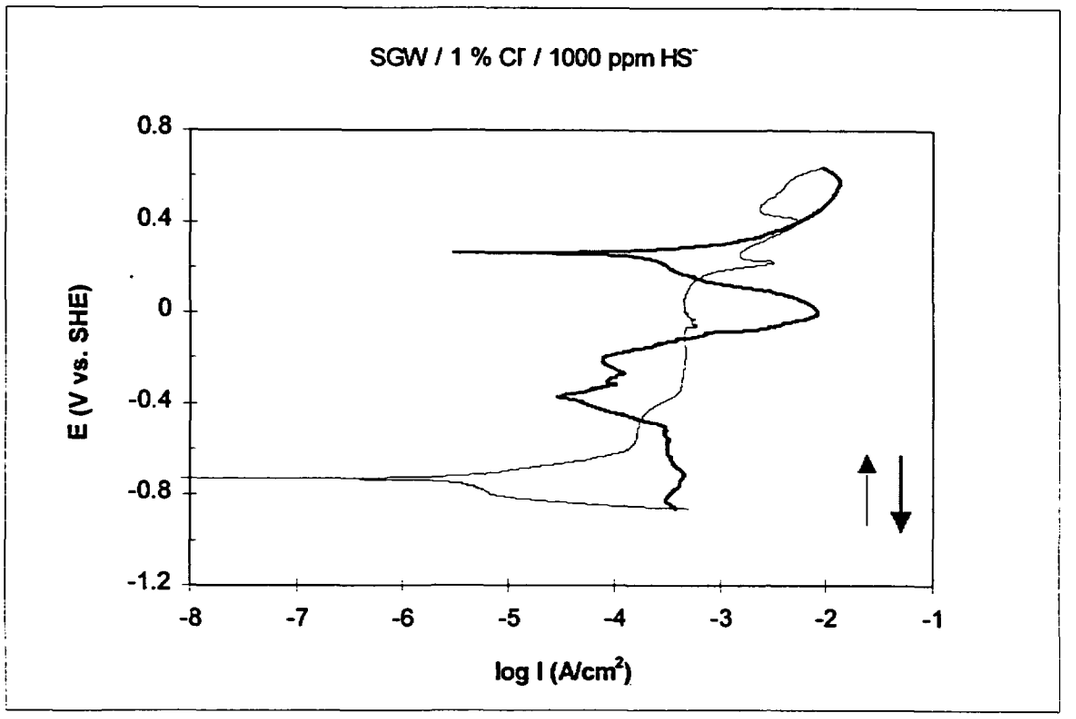

Sample: Cu12

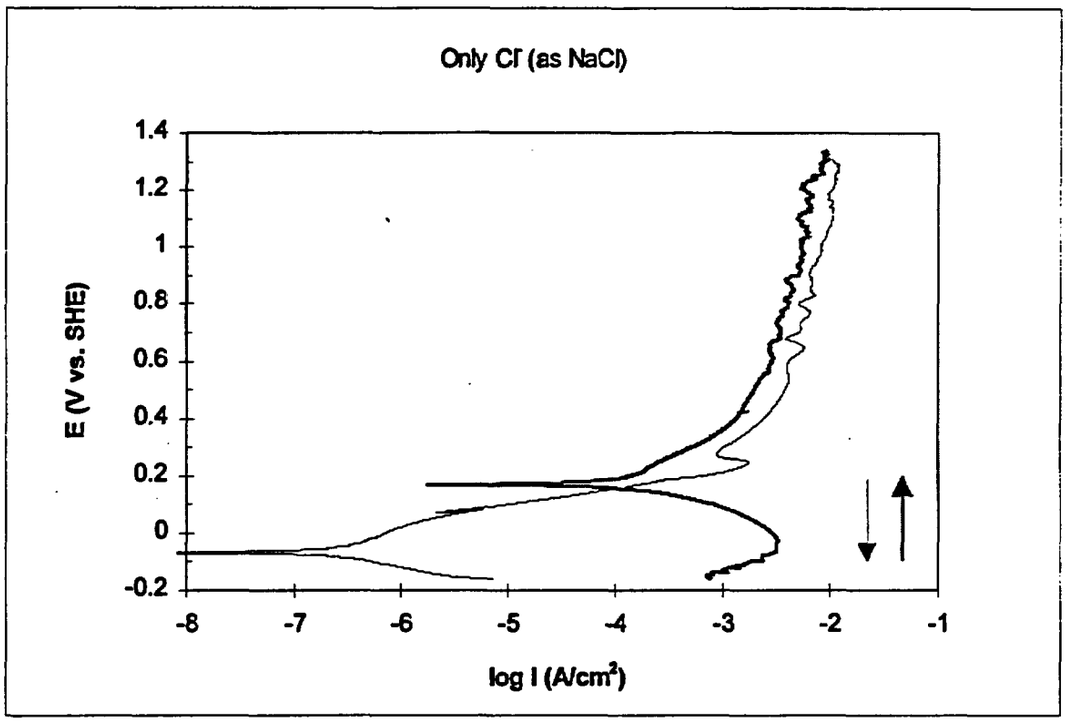

Sample: Cu14

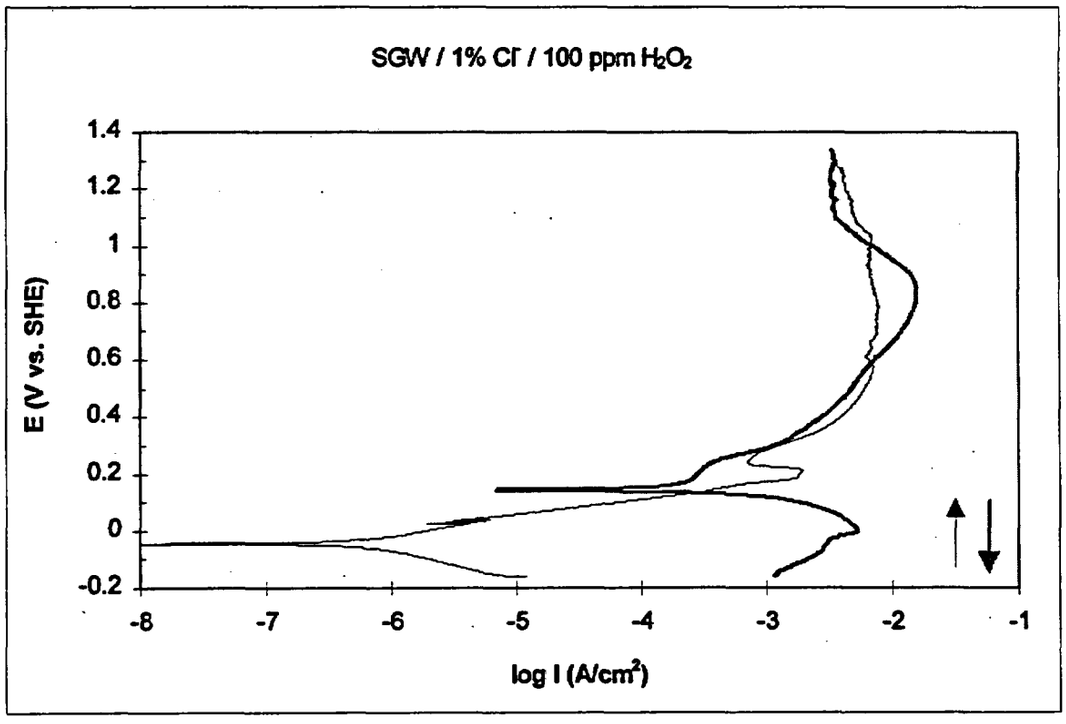

Sample: Cu15

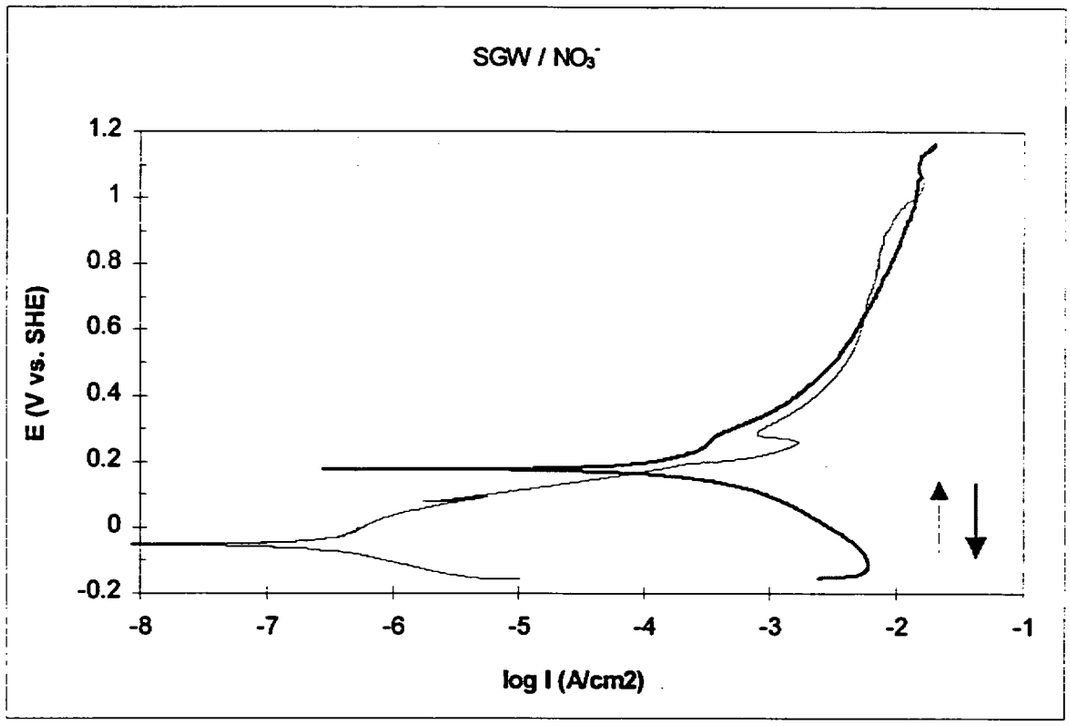

Sample: Cu16

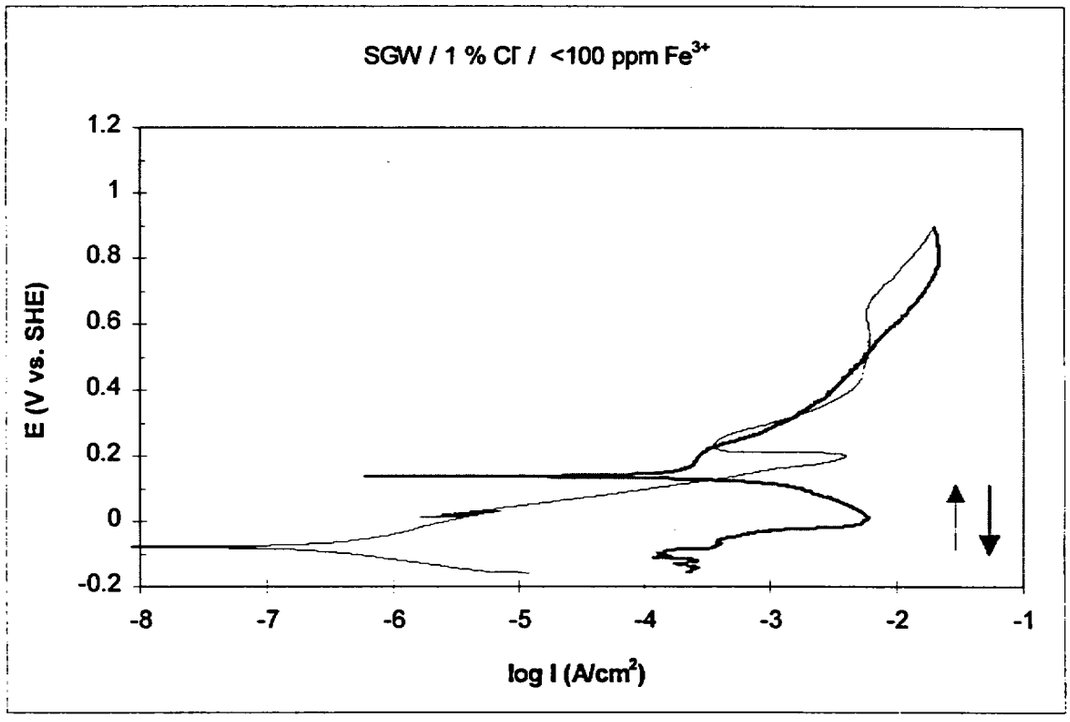

Sample: Cu17

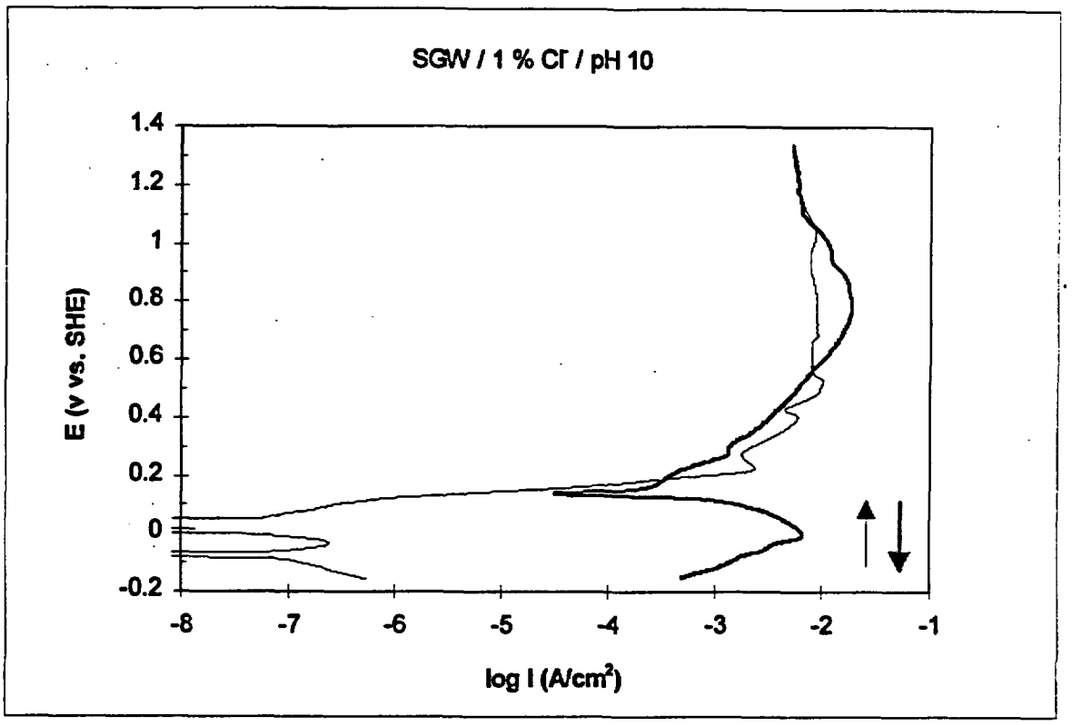

Sample: Cu18 (Anodic curve noise-filtered)

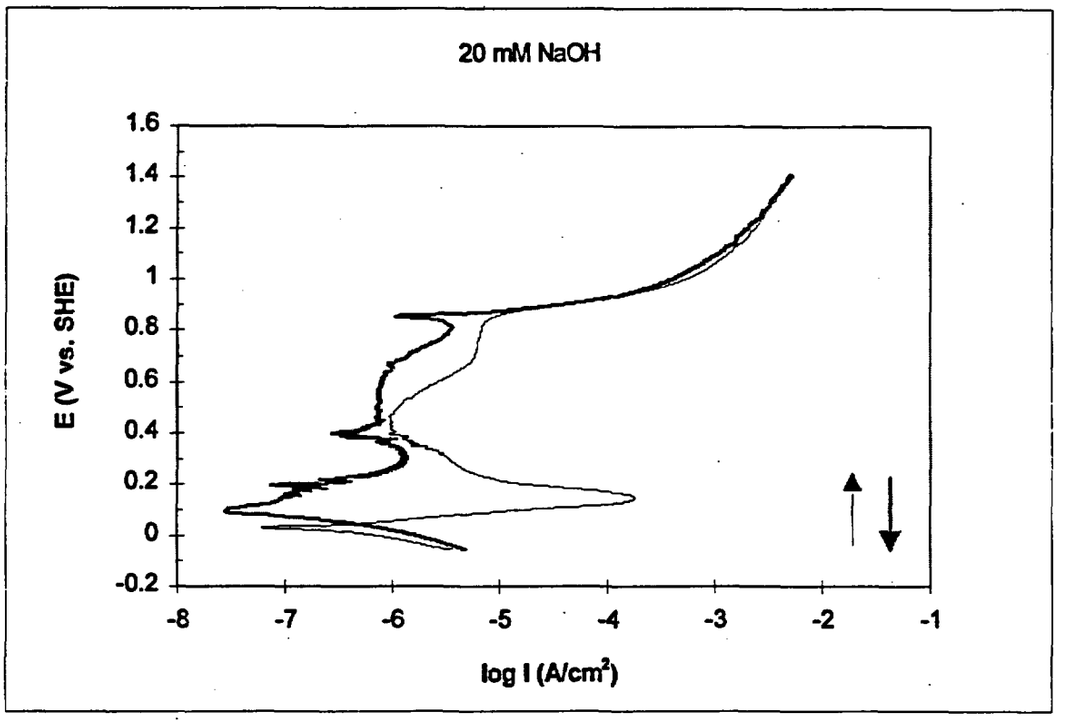

Sample: CuX1 (Curve noise-filtered)

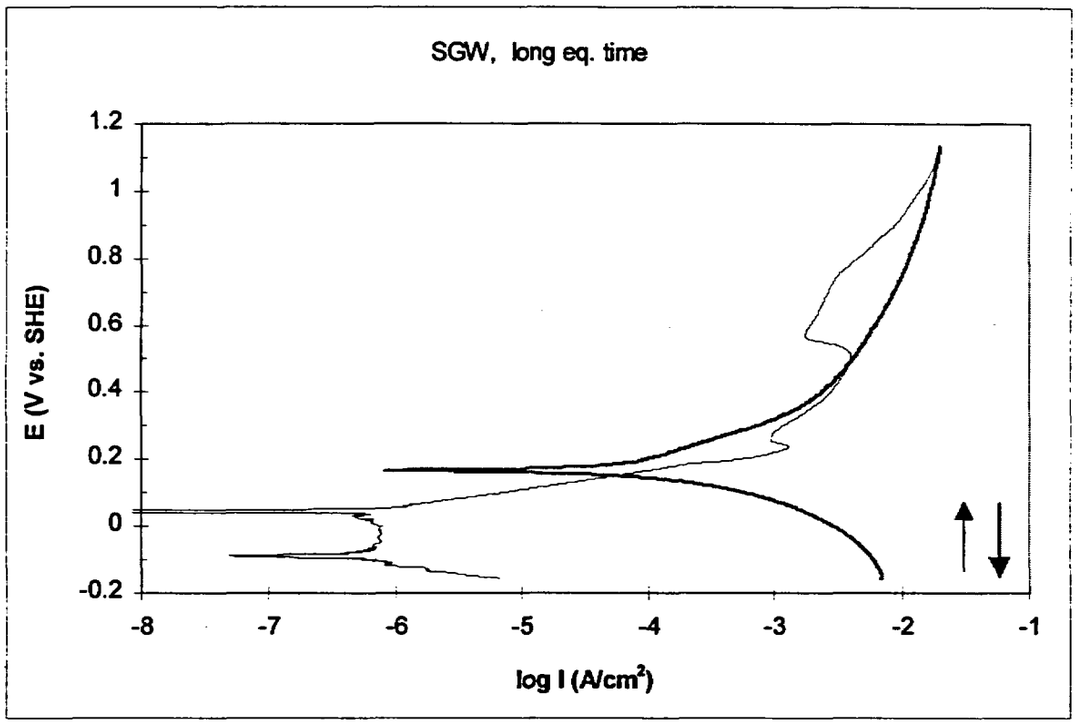

Sample: Cu101 (Anodic curve noise-filtered)

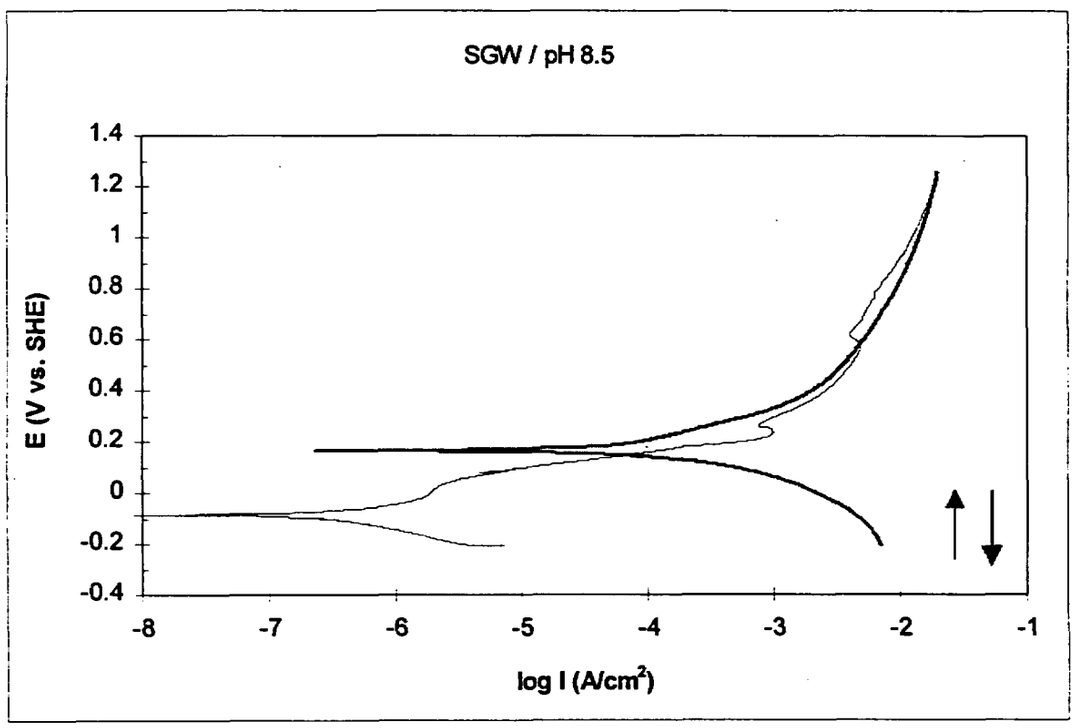

Sample: Cu102

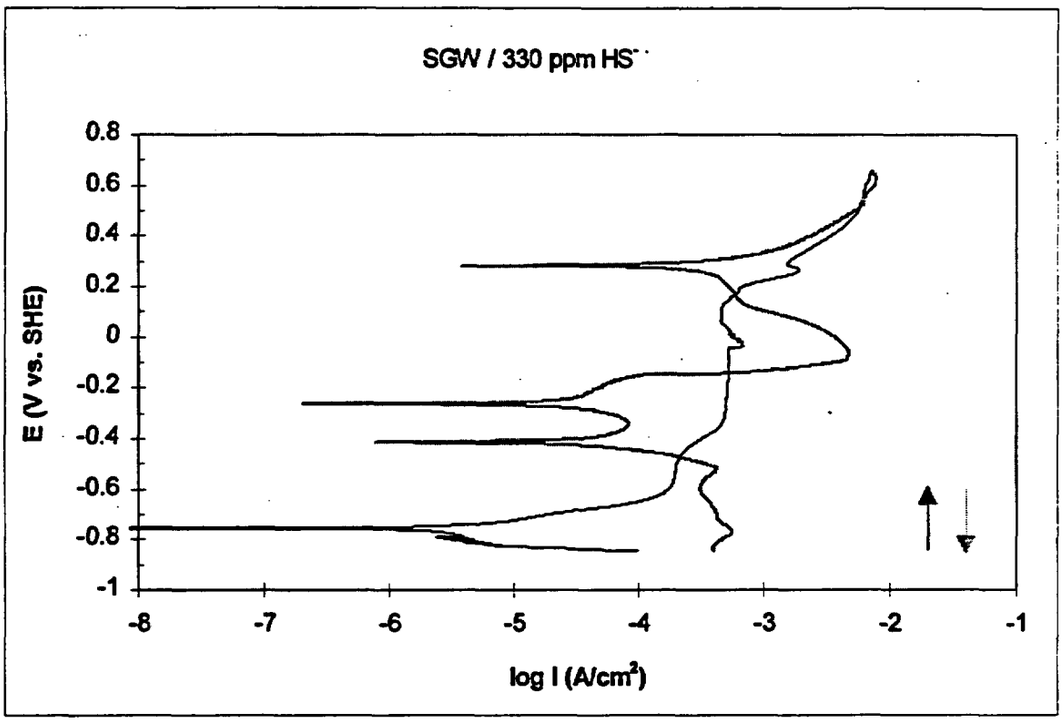

Sample: Cu103

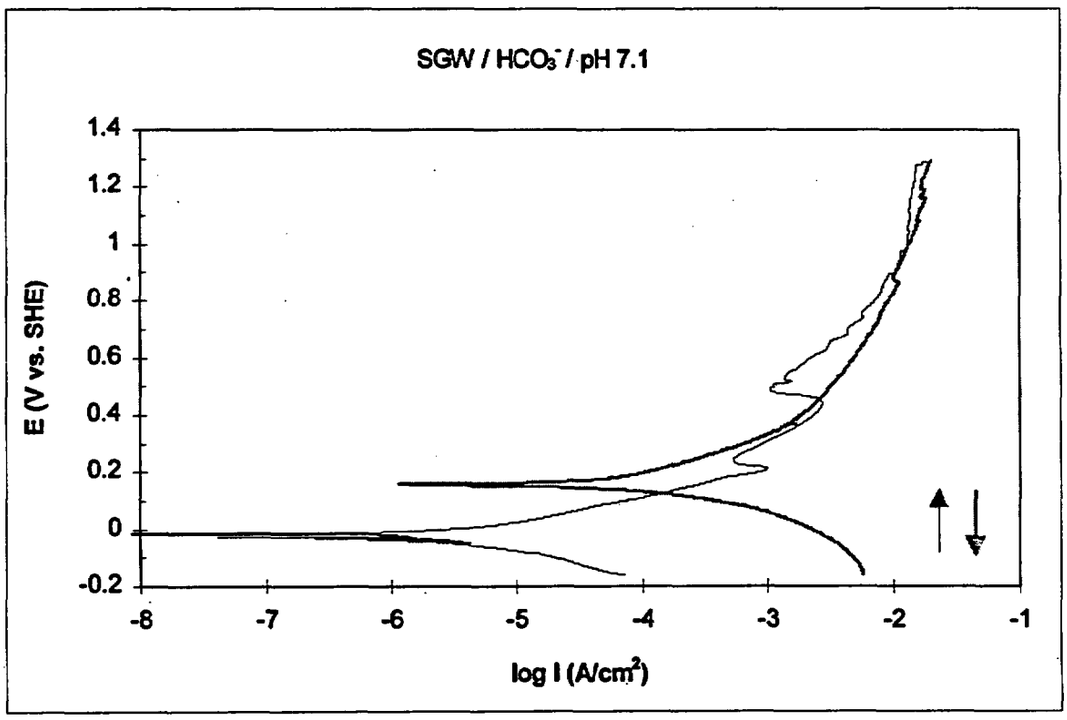

Sample: Cu104

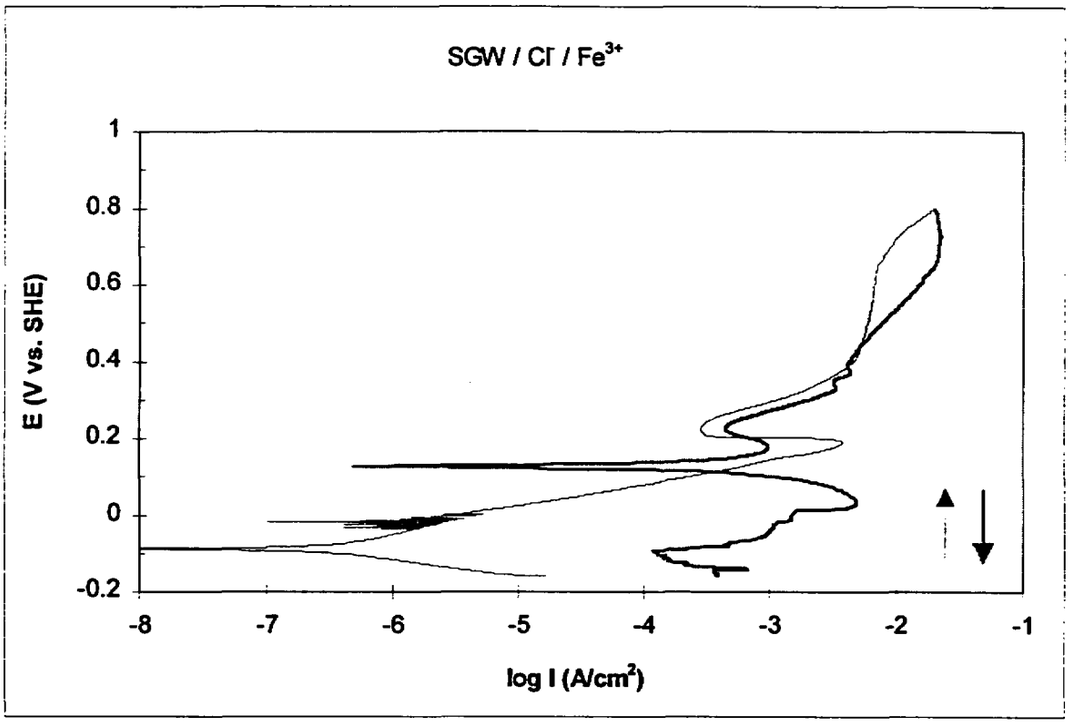

Sample: Cu105

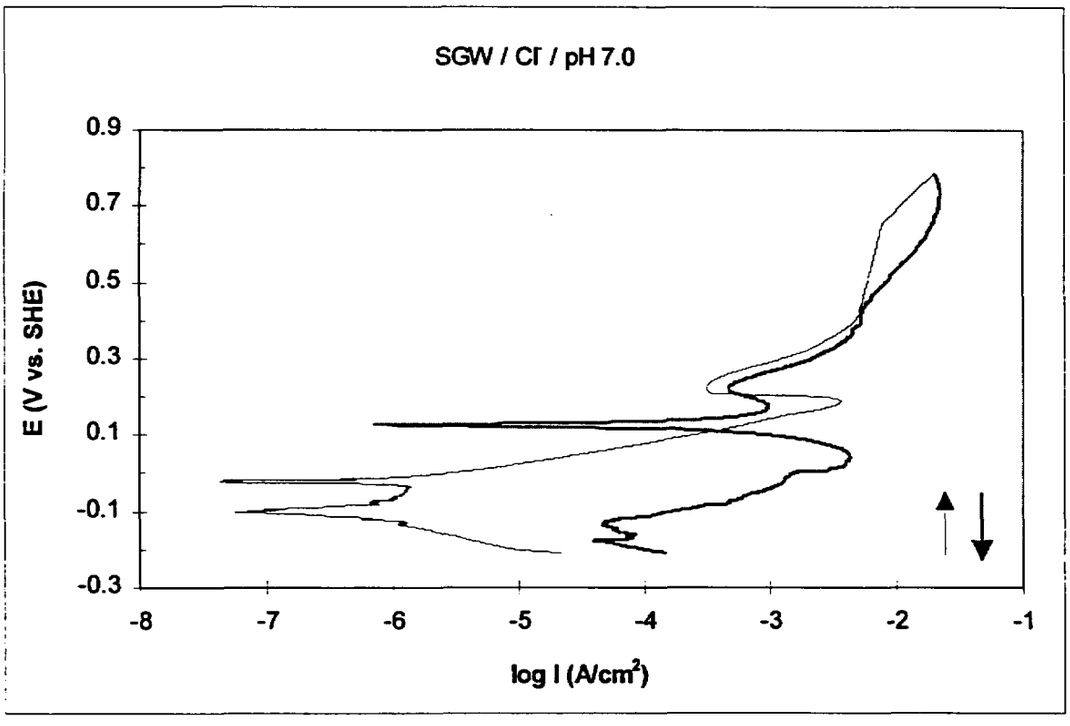

Sample: Cu106 (Anodic curve noise-filtered)

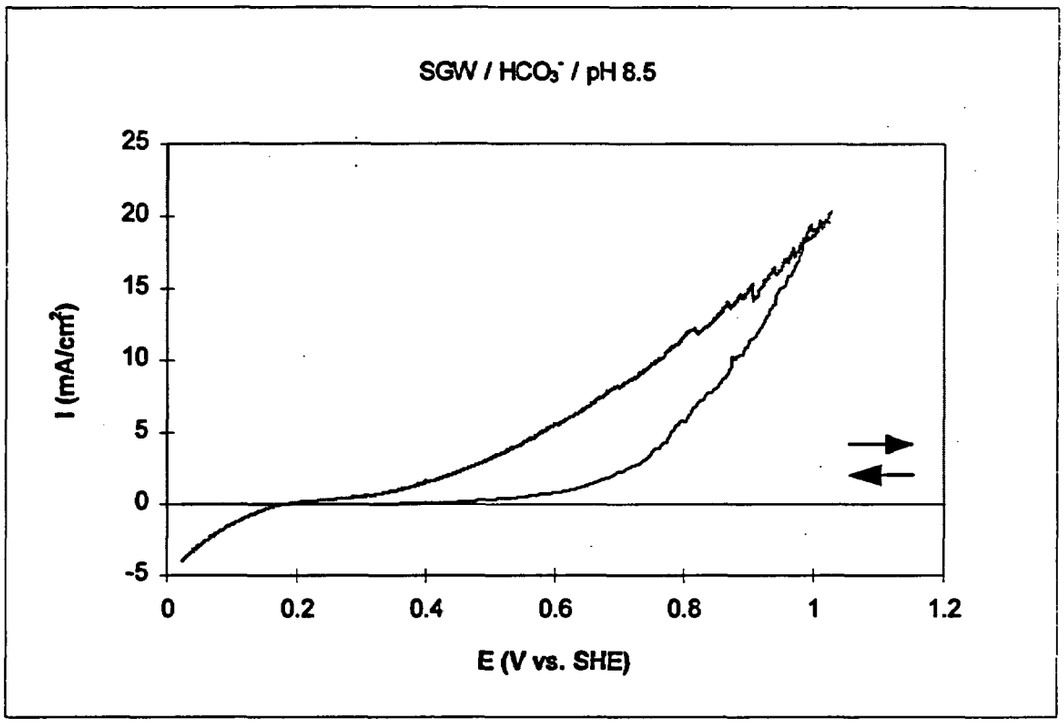

Sample: Cu08, linear curve showing hysteresis at high anodic potentials.

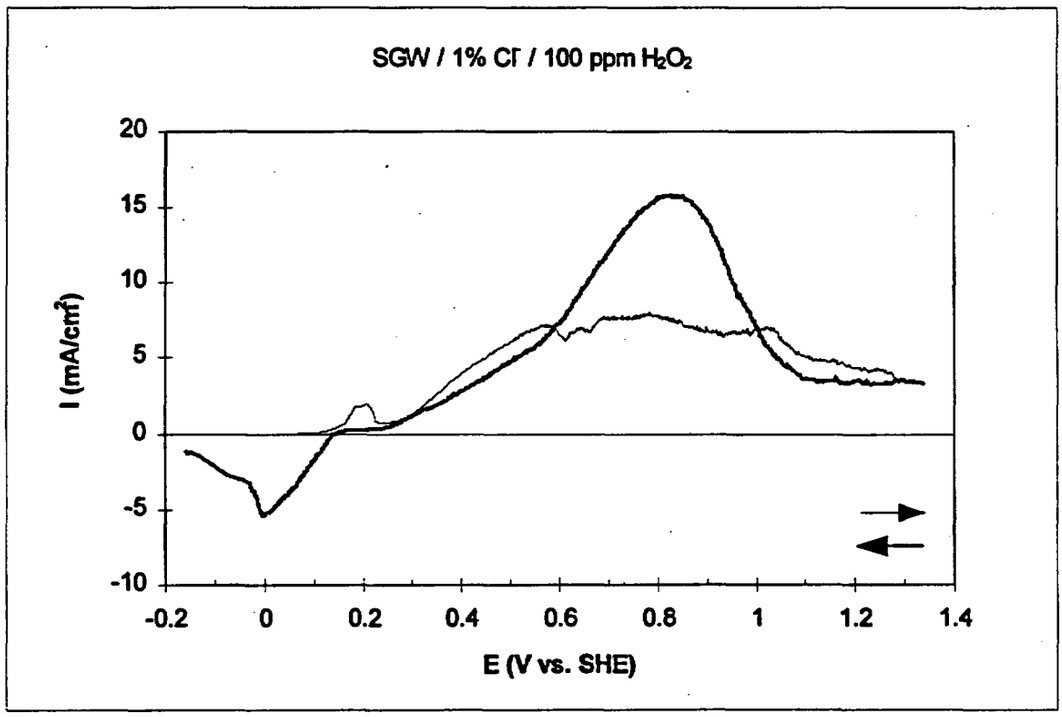

Sample: Cu15, linear curve showing hysteresis at high anodic potentials.

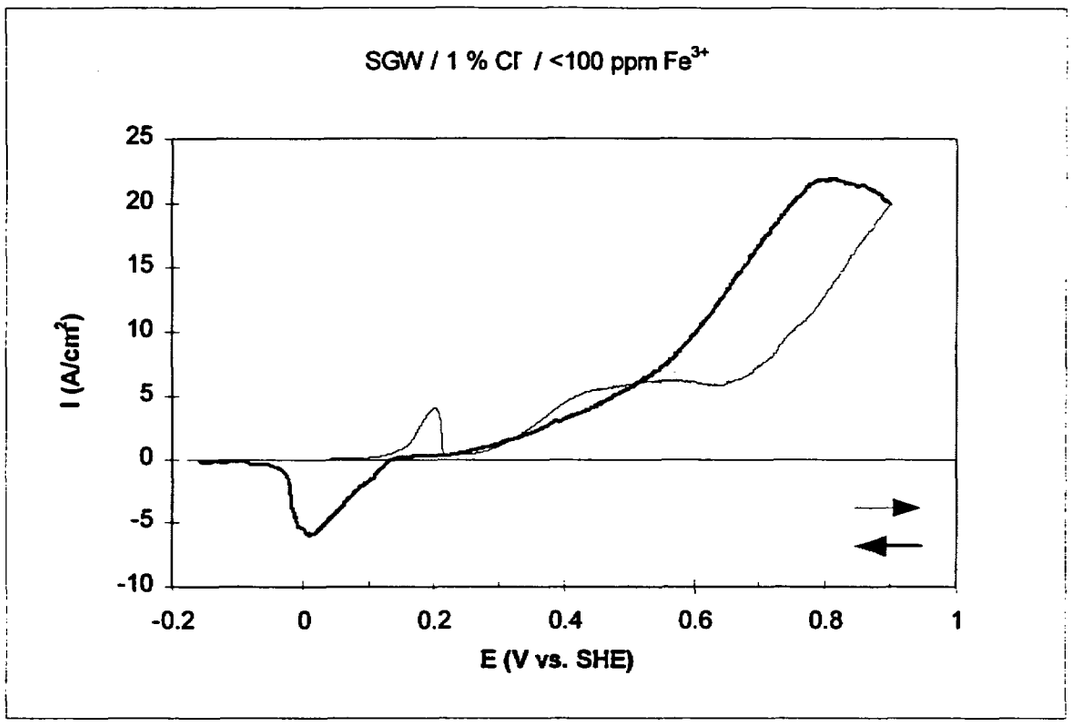

Sample: Cu17, linear curve showing hysteresis at high anodic potentials.

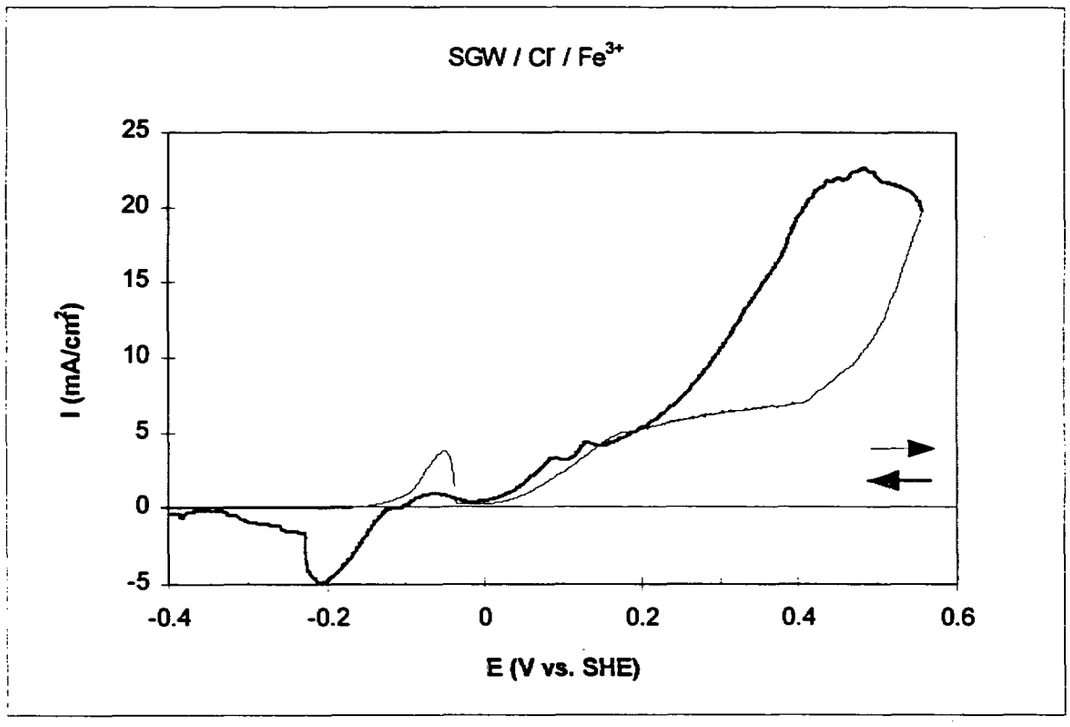

Sample: Cu105, linear curve showing hysteresis at high anodic potentials.

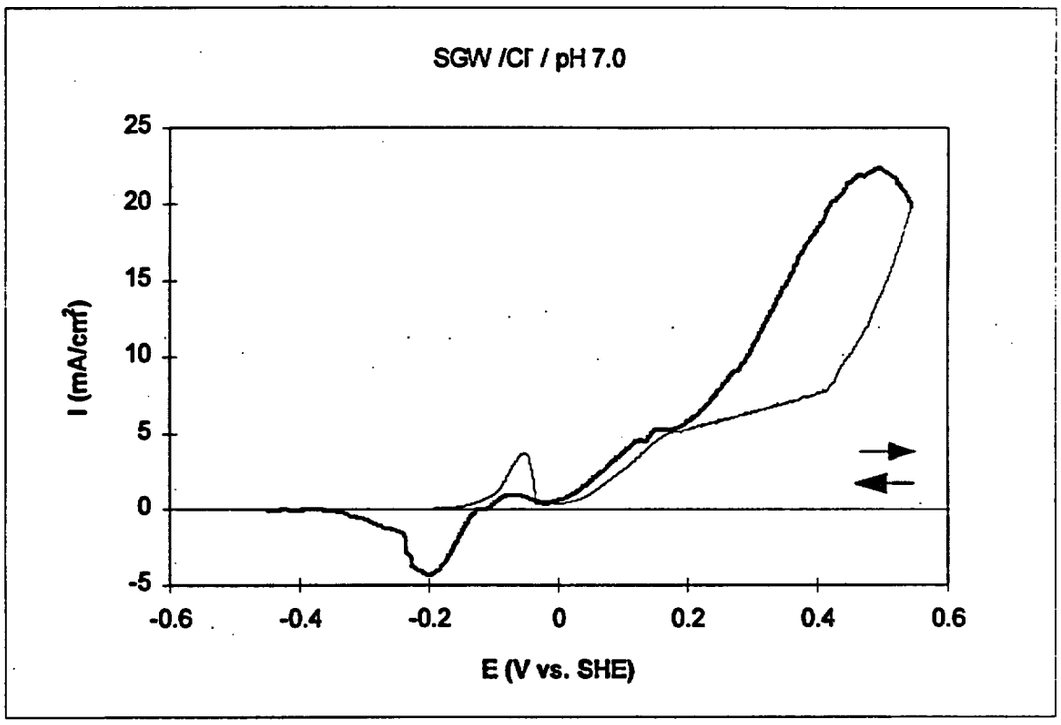

Sample: Cu106, linear curve showing hysteresis at high anodic potentials.

SEM pictures

SEM pictures of the sample copper surfaces taken after completion of the polarisation measurements.

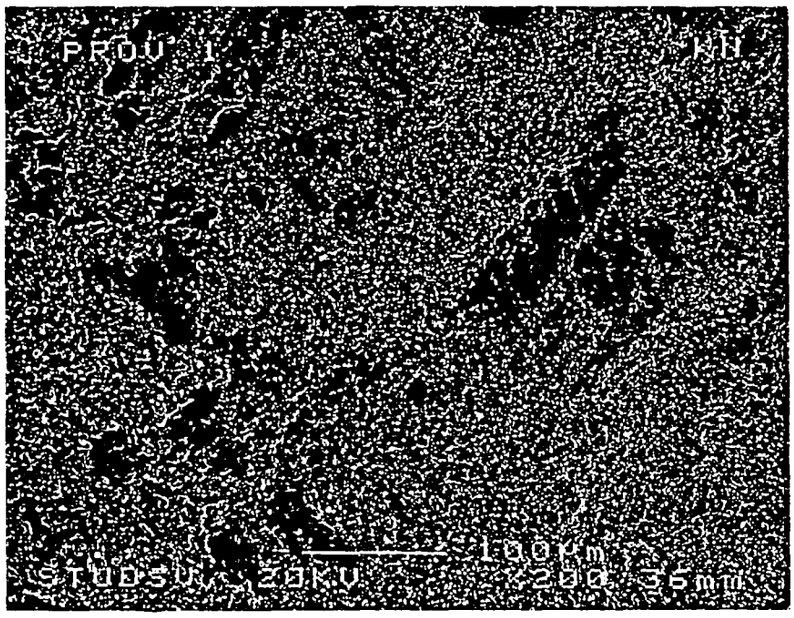

Sample Cu01 at ×200 magnification

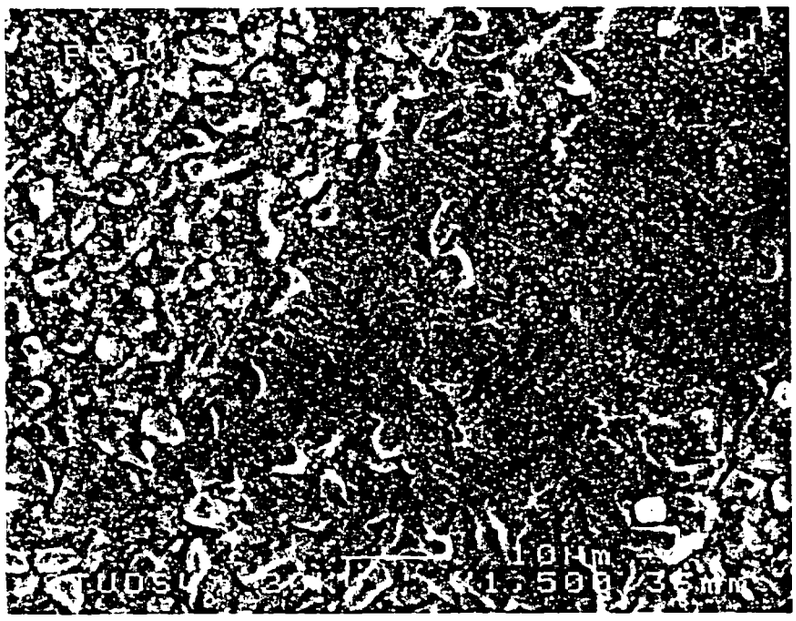

Sample Cu01 at ×1500 magnification

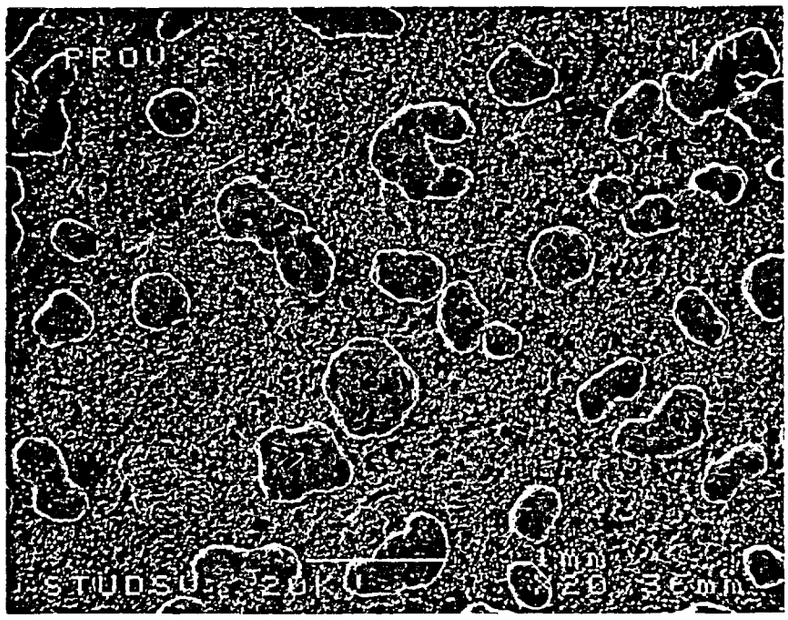

Sample Cu02 at ×20 magnification

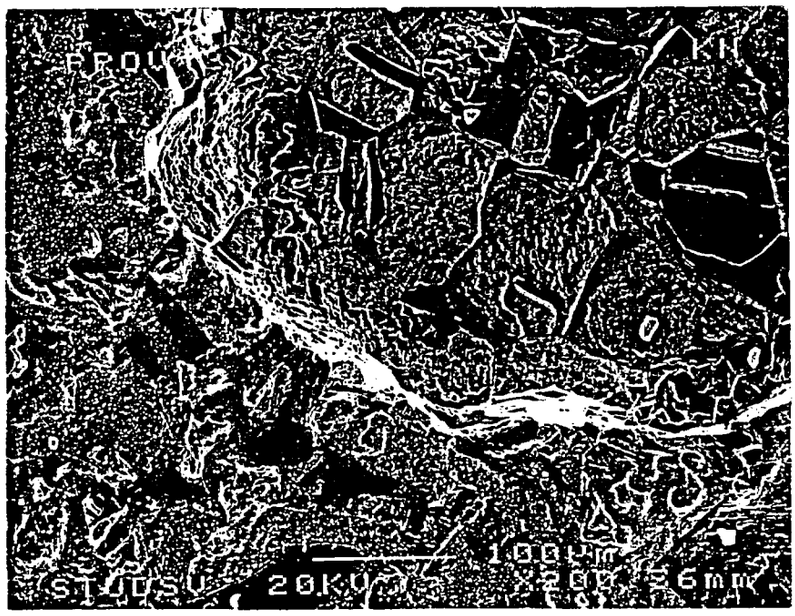

Sample Cu02 at ×200 magnification

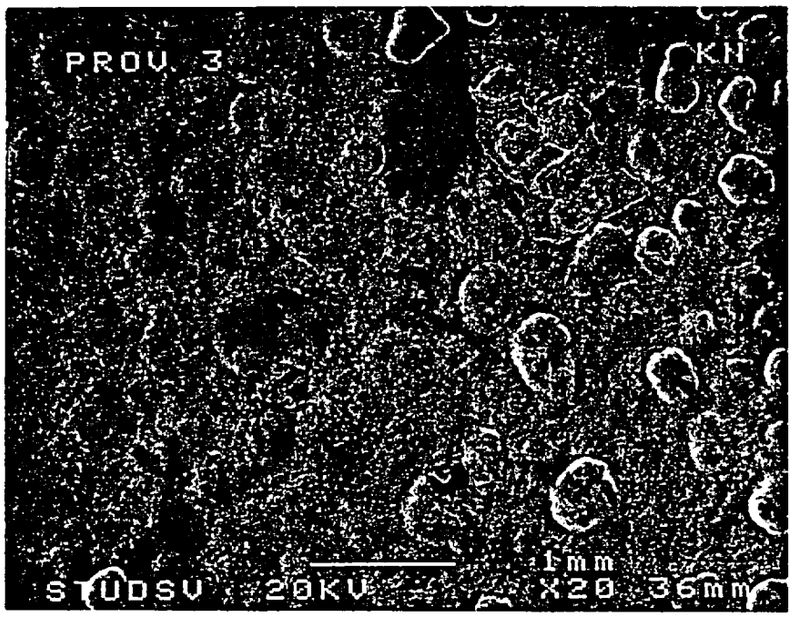

Sample Cu03 at ×20 magnification

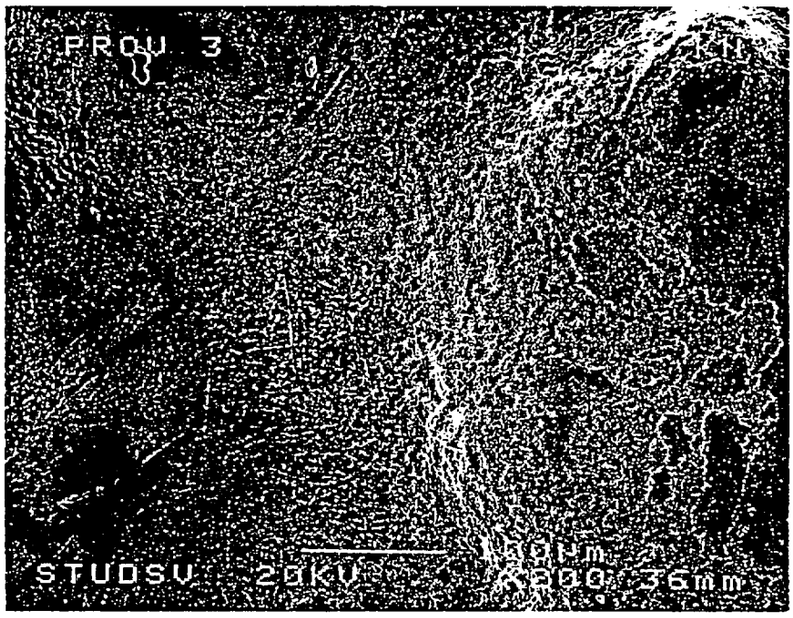

Sample Cu03 at ×200 magnification

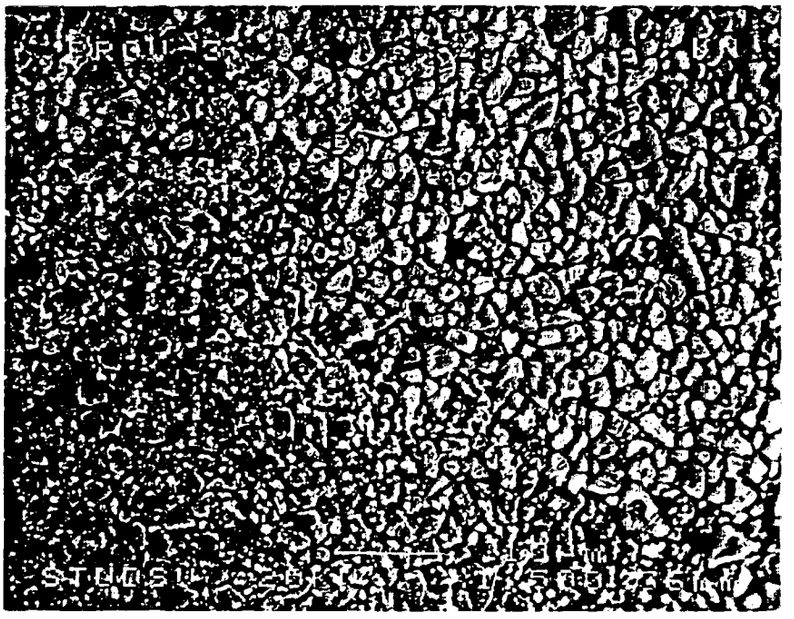

Sample Cu03 at ×1500 magnification

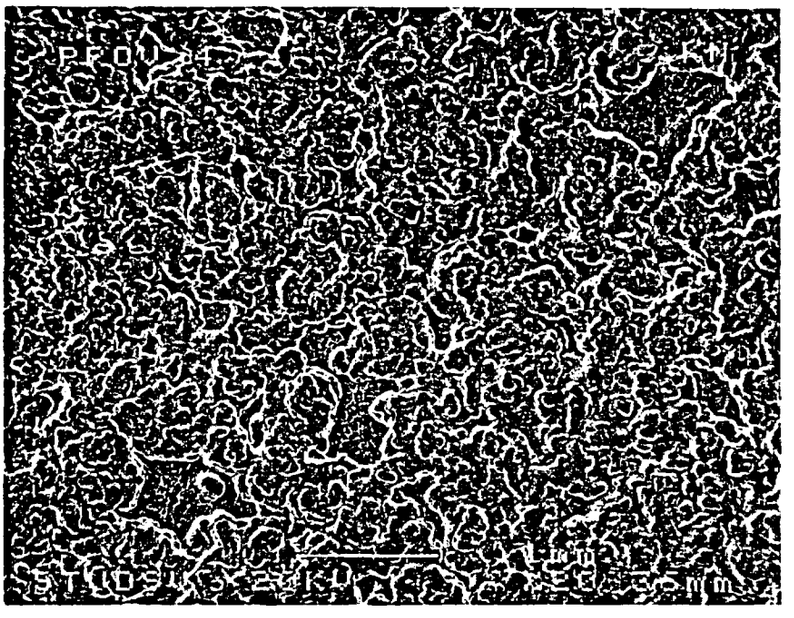

Sample Cu04 at ×20 magnification

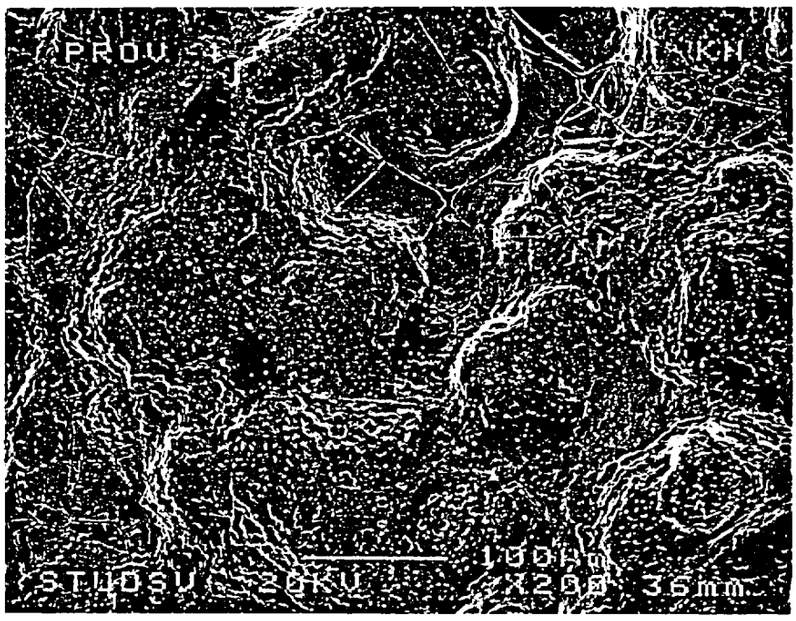

Sample Cu04 at ×200 magnification

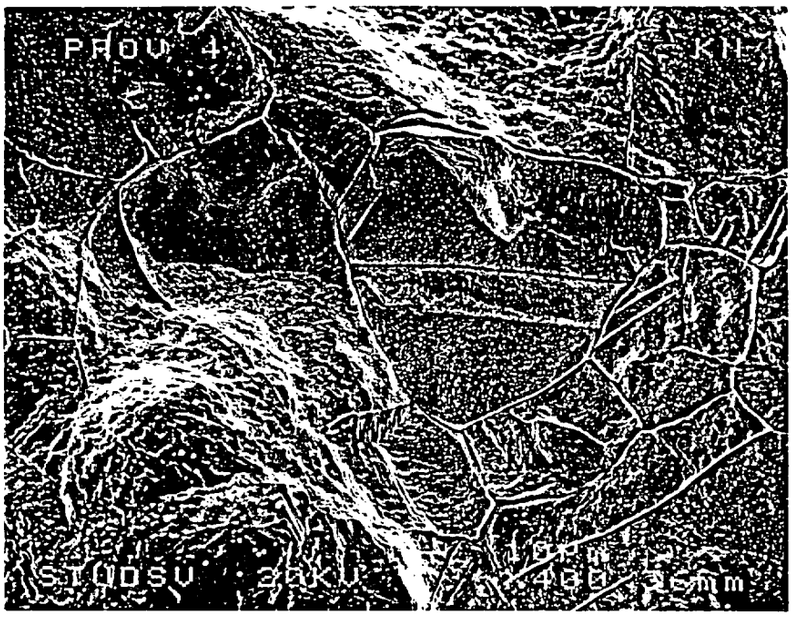

Sample Cu04 at ×400 magnification (from a frequently appearing feature on the surface)

Sample Cu04 at ×1500 magnification

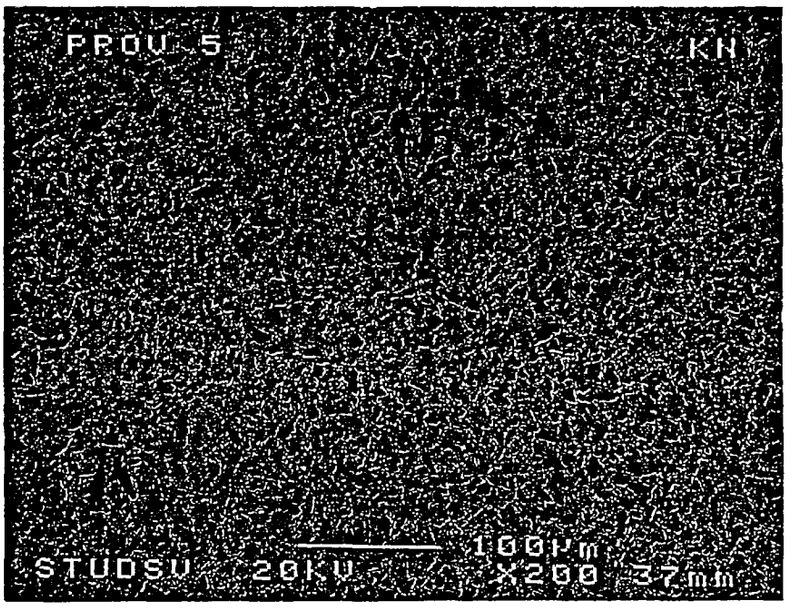

Sample Cu05 at ×200 magnification

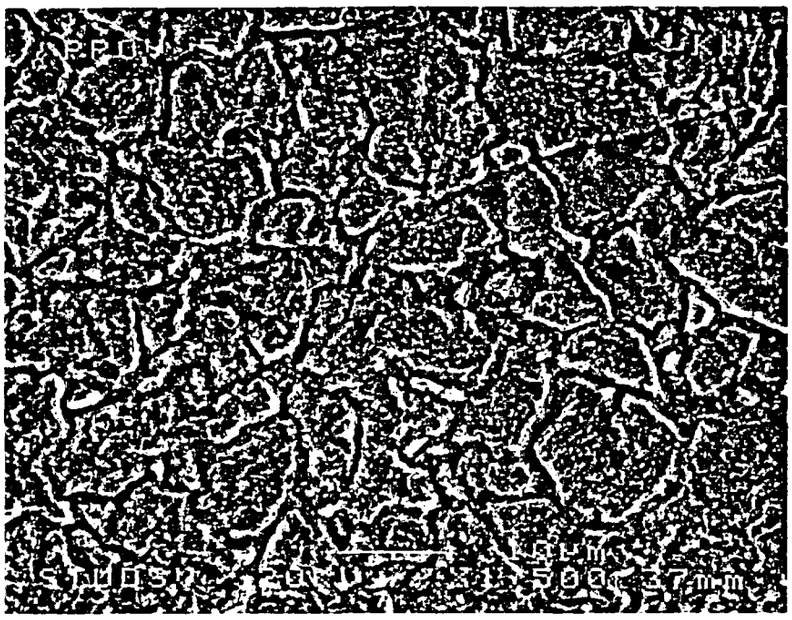

Sample Cu05 at ×1500 magnification

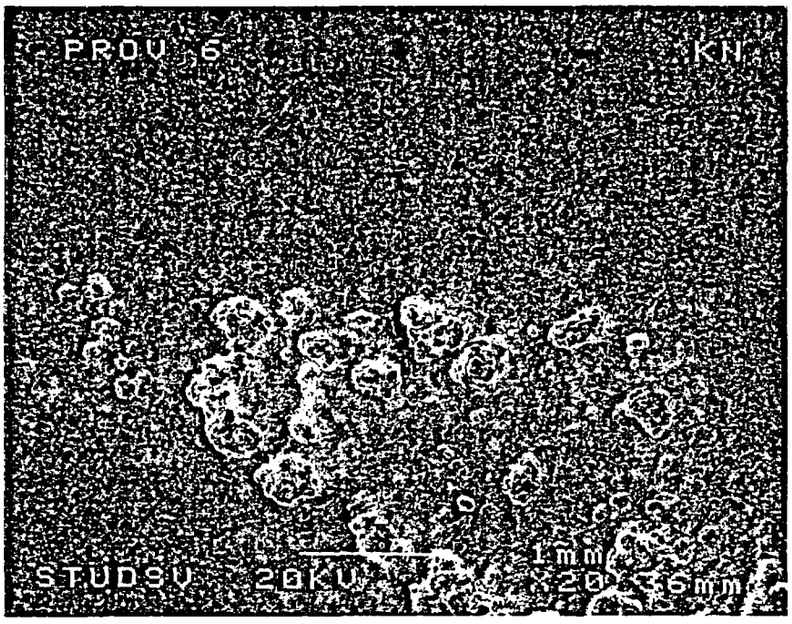

Sample Cu06 at ×20 magnification

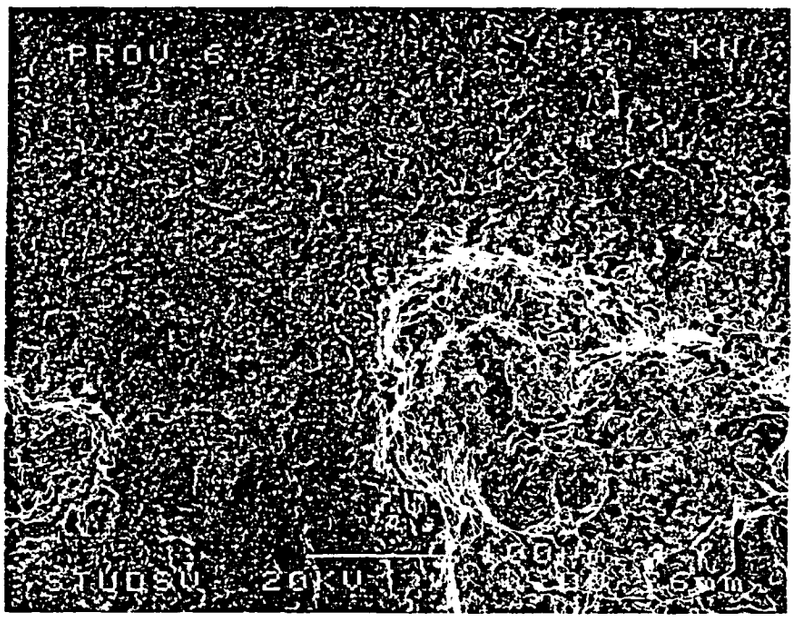

Sample Cu06 at ×200 magnification

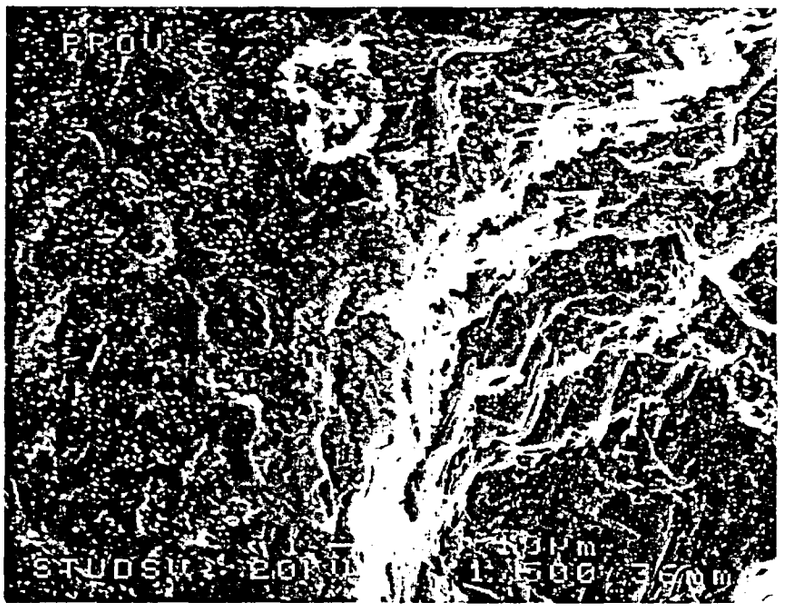

Sample Cu06 at ×1500 magnification

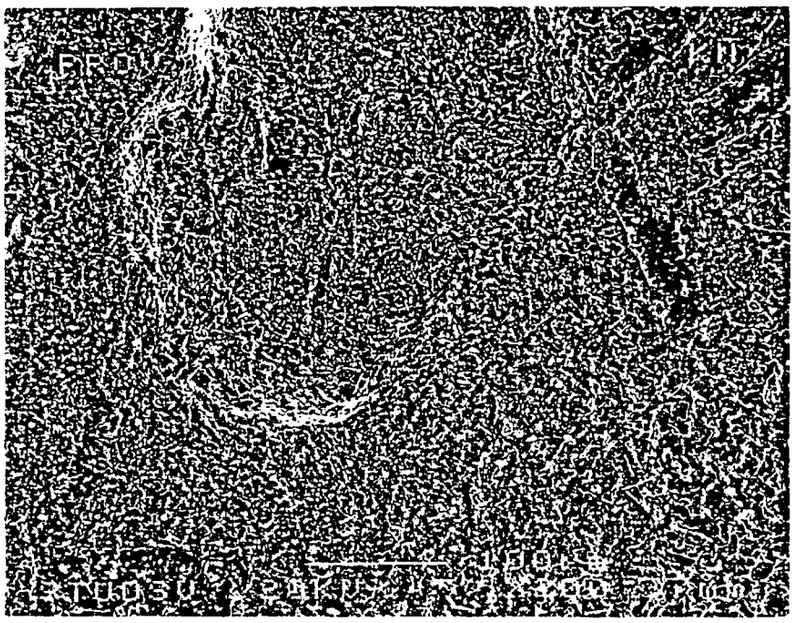

Sample Cu07 at ×200 magnification

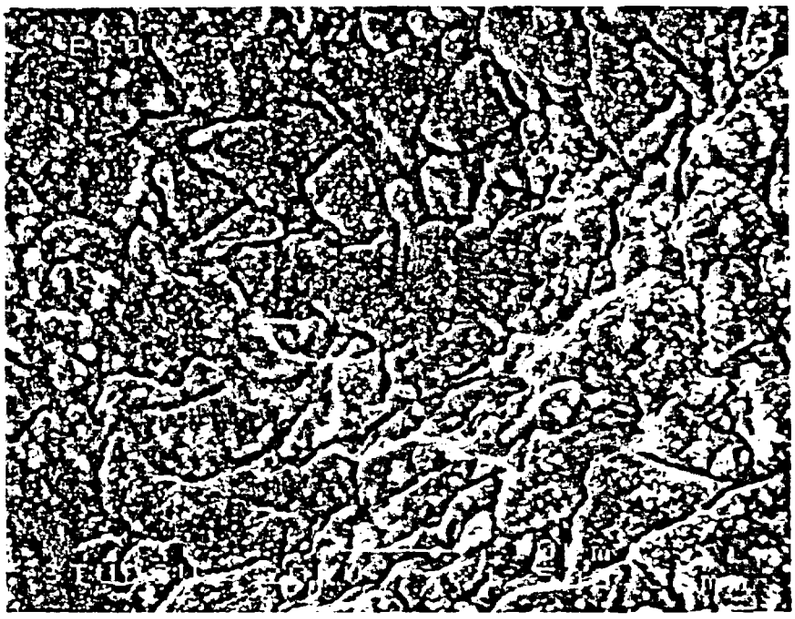

Sample Cu07 at ×1500 magnification

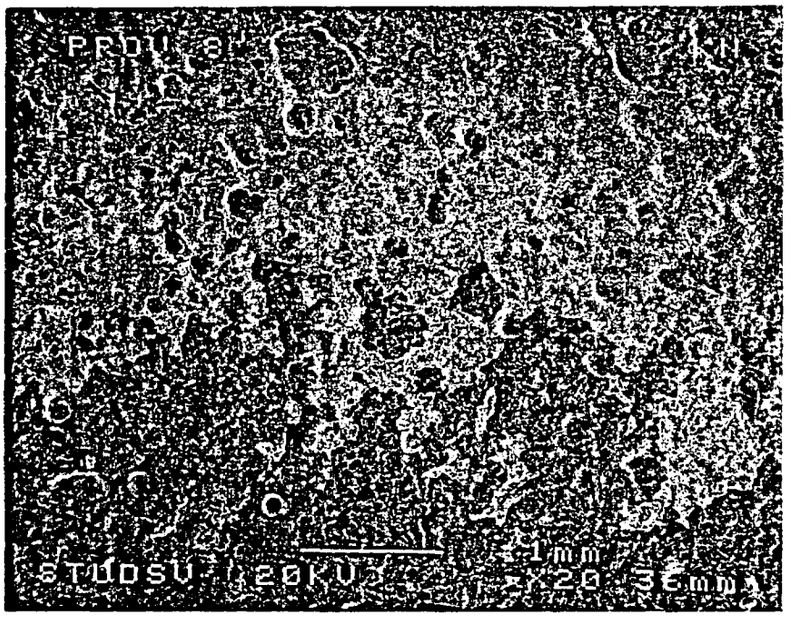

Sample Cu08 at ×20 magnification

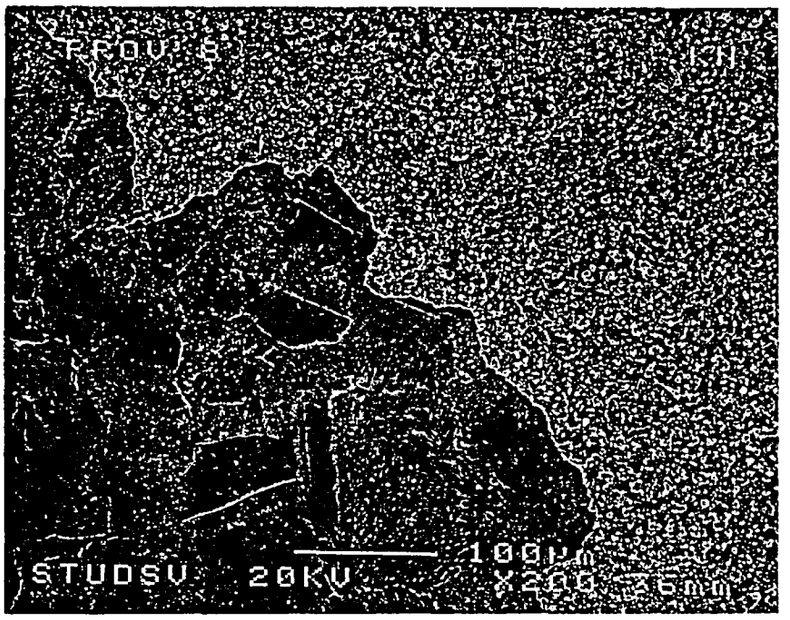

Sample Cu08 at ×200 magnification

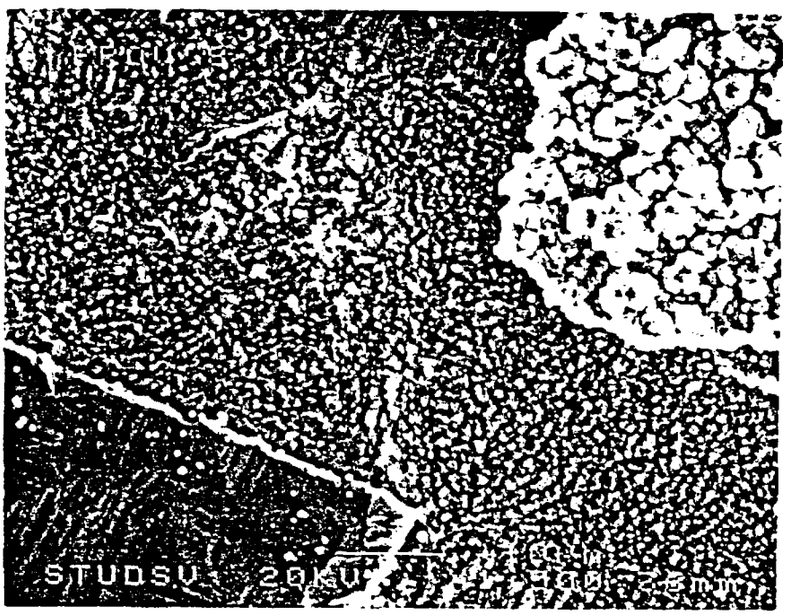

Sample Cu08 at ×1500 magnification

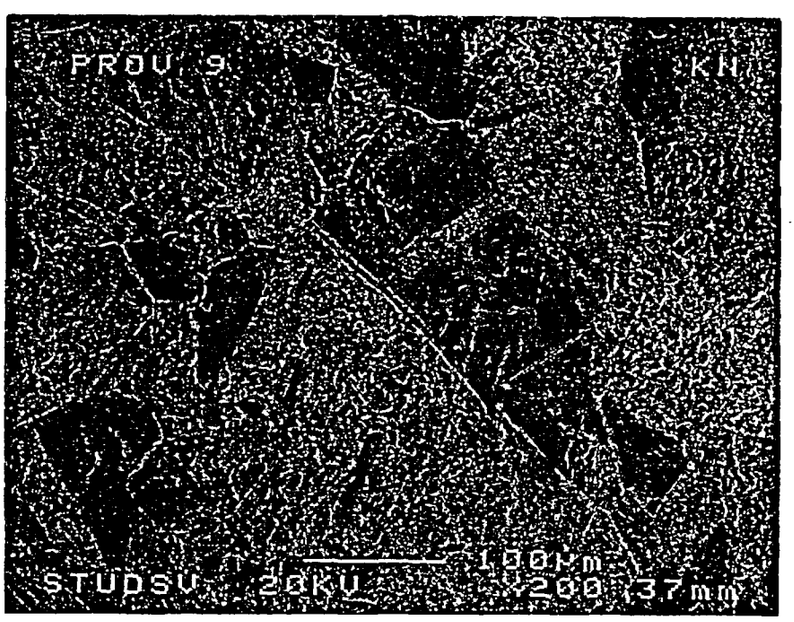

Sample Cu09 at ×200 magnification

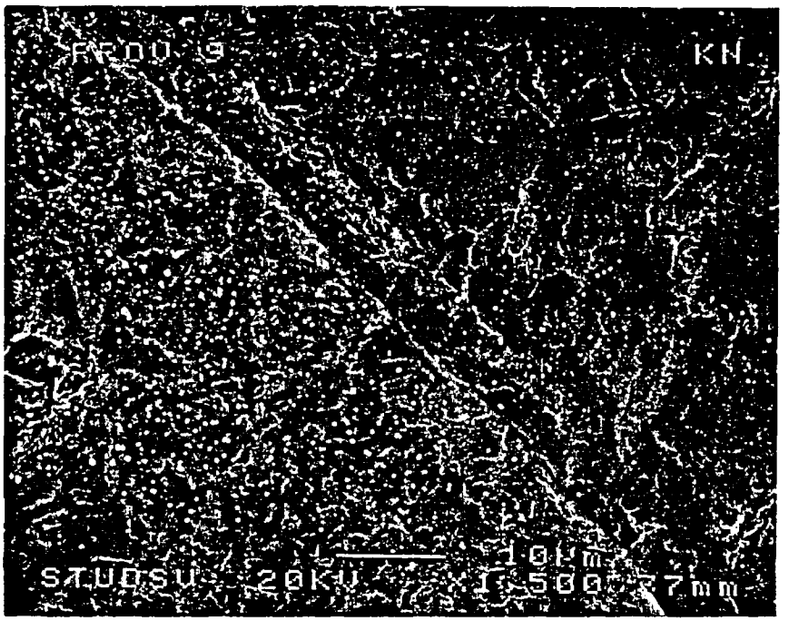

Sample Cu09 at ×1500 magnification

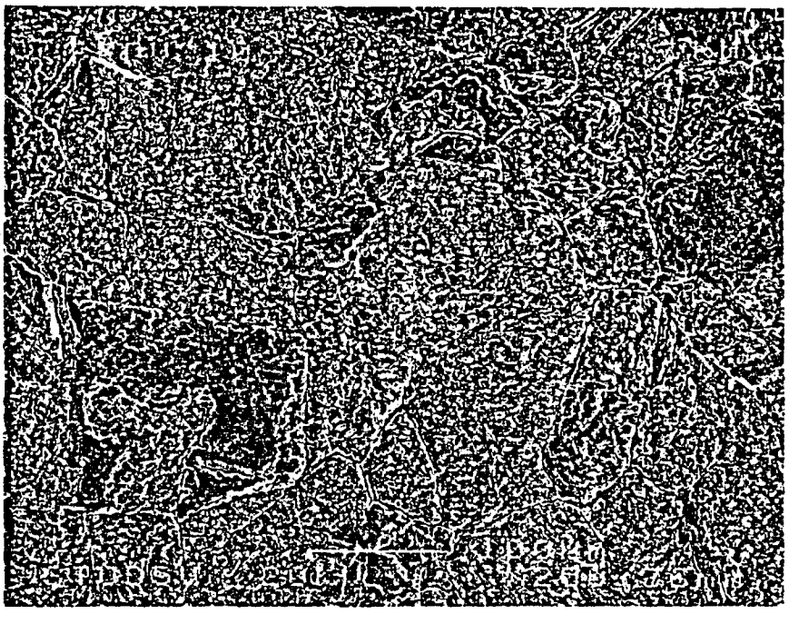

Sample Cu10 at ×200 magnification

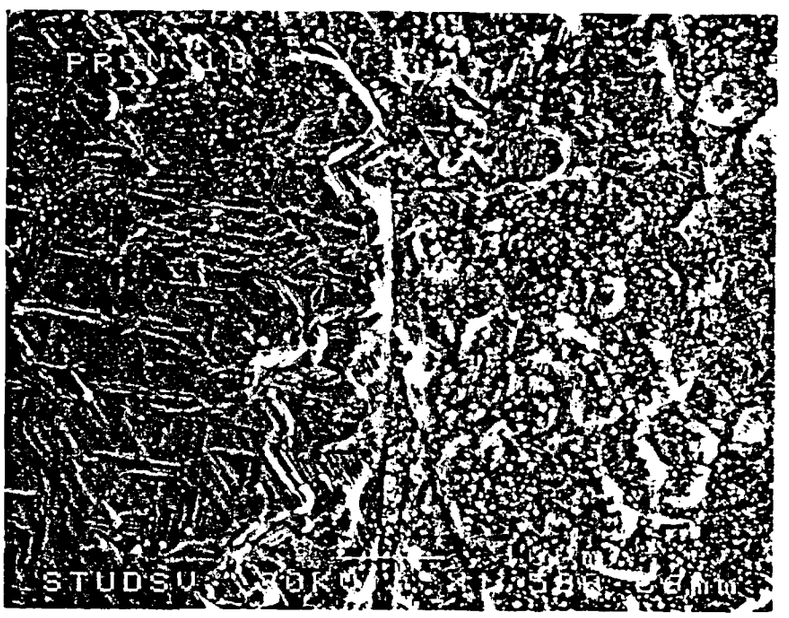

Sample Cu10 at ×1500 magnification

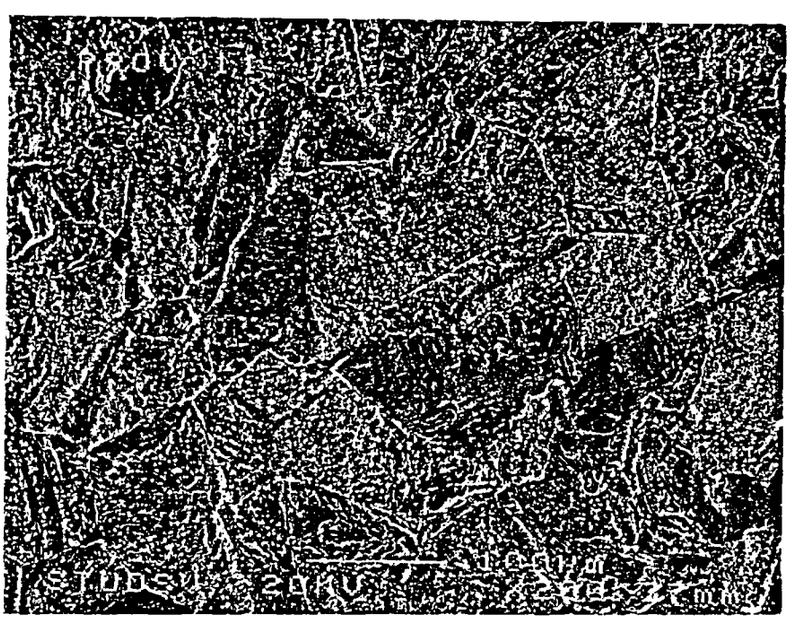

Sample Cu11 at ×200 magnification

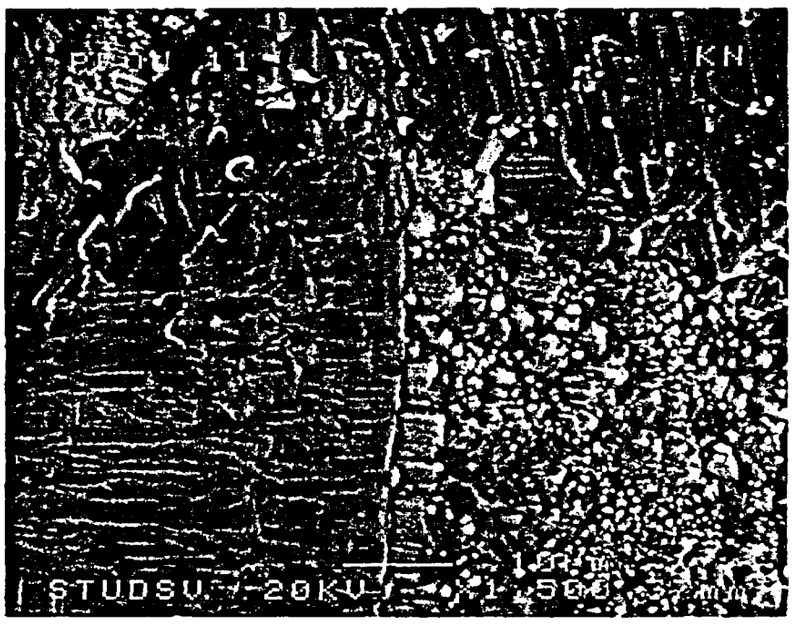

Sample Cu11 at ×1500 magnification

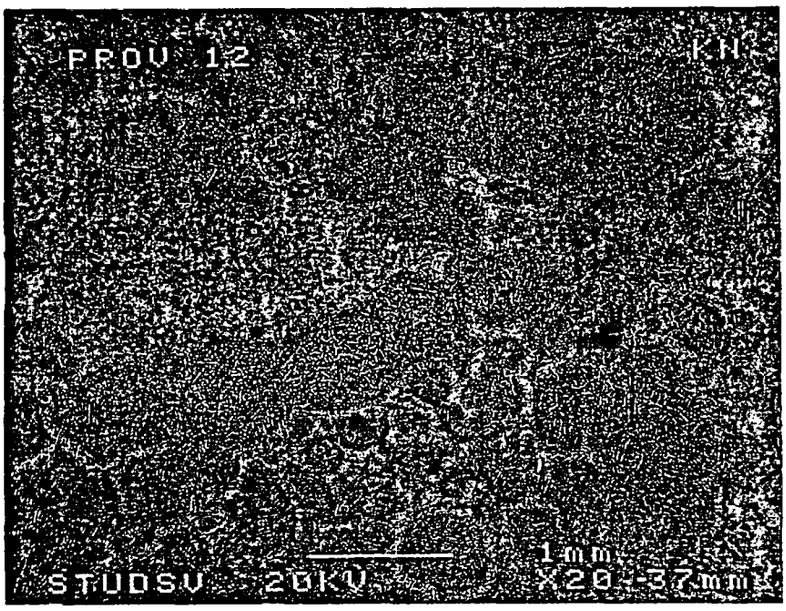

Sample Cu12 at ×20 magnification

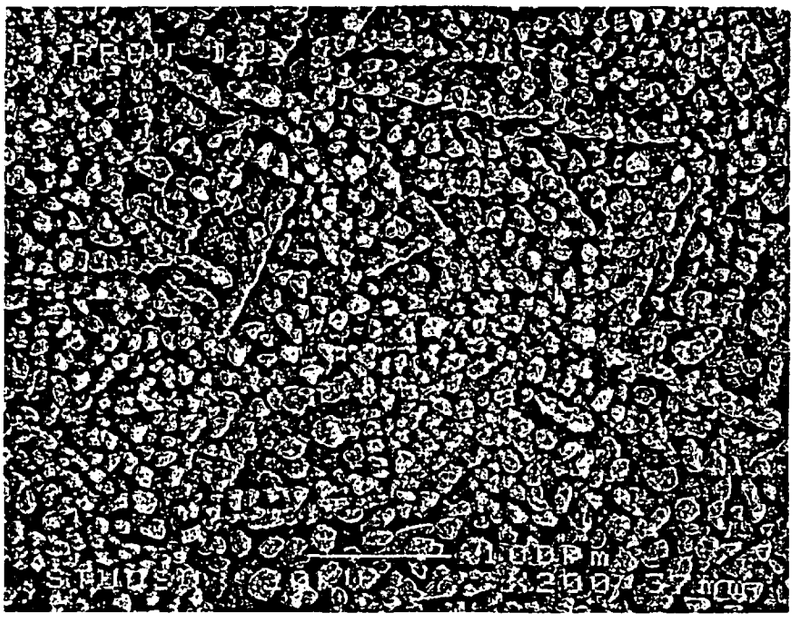

Sample Cu12 at ×200 magnification

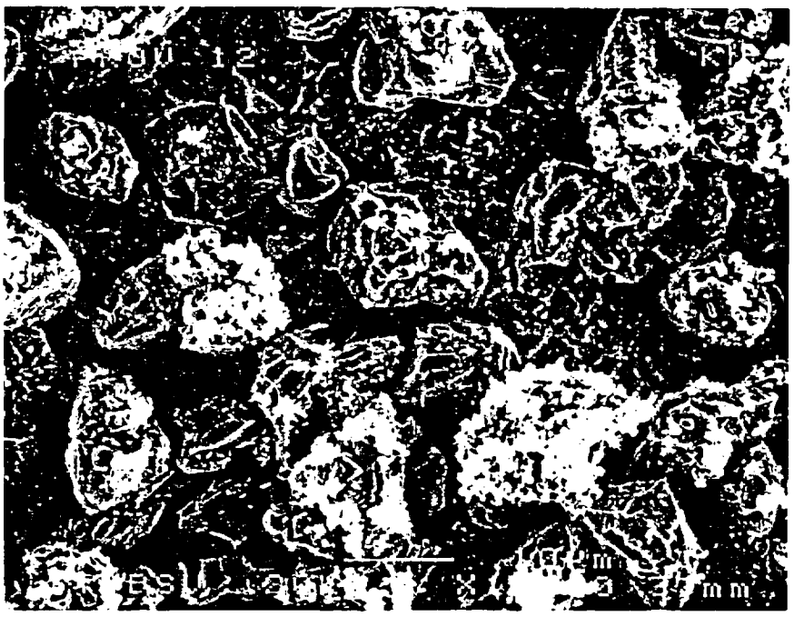

Sample Cu12 at ×1500 magnification

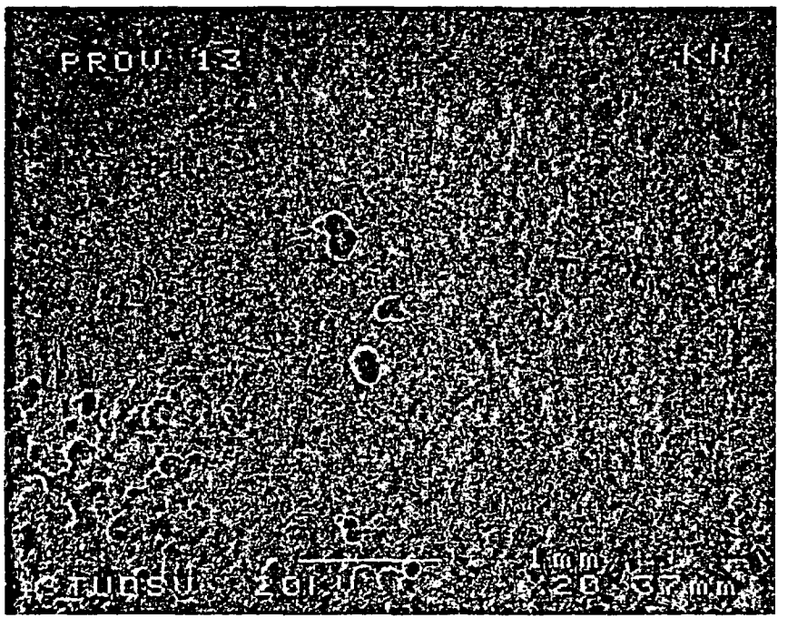

Sample Cu13 at ×20 magnification

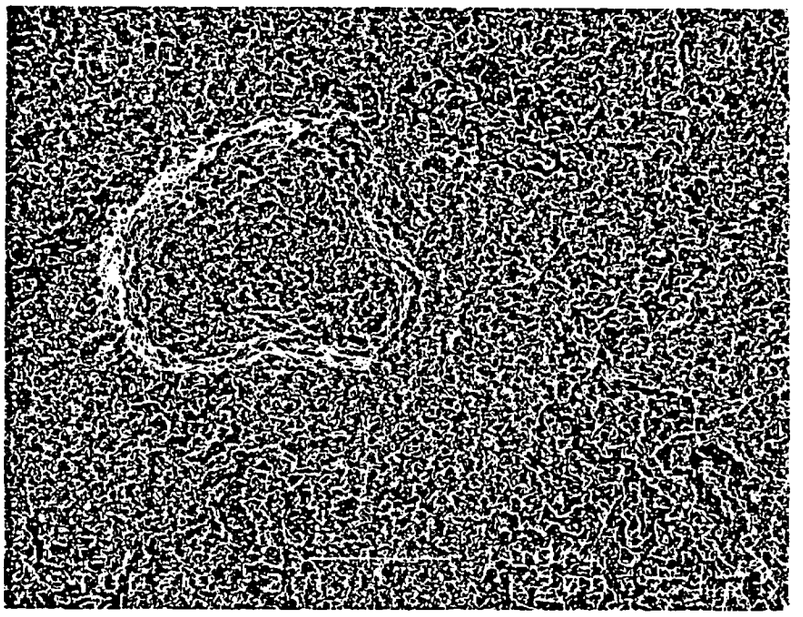

Sample Cu13 at ×200 magnification

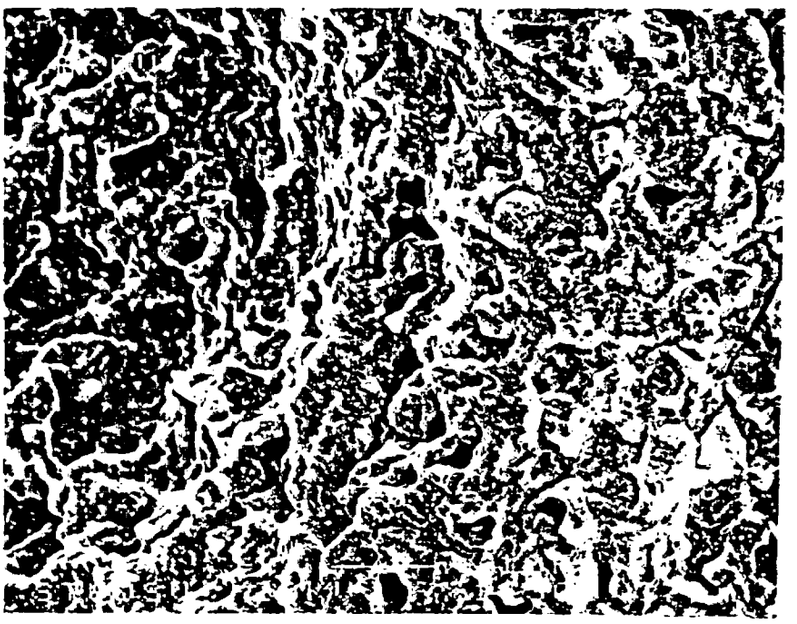

Sample Cu13 at ×1500 magnification

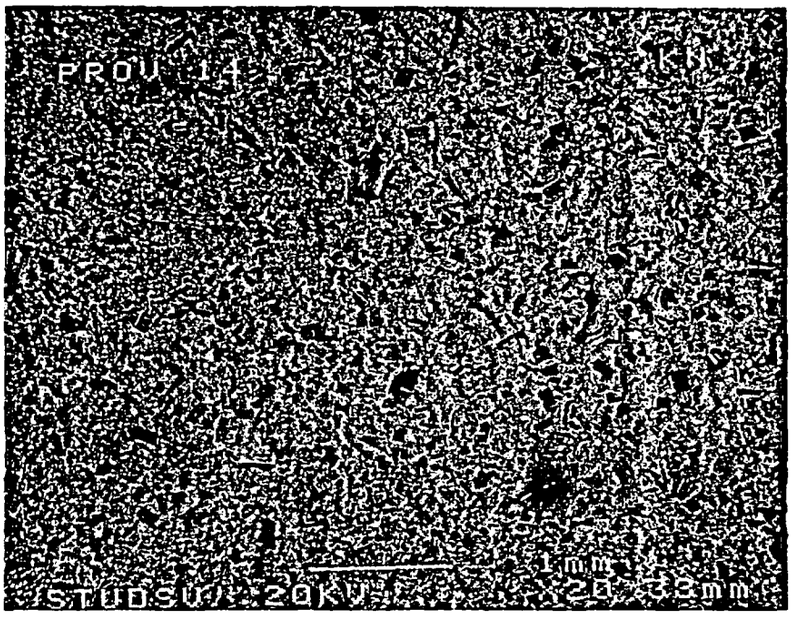

Sample Cu14 at ×20 magnification

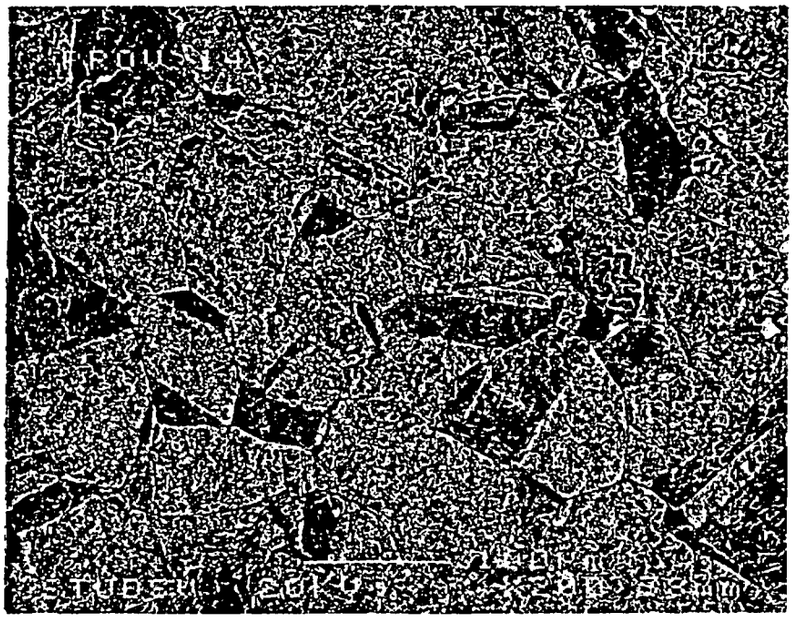

Sample Cu14 at ×200 magnification

Sample Cu14 at ×1500 magnification

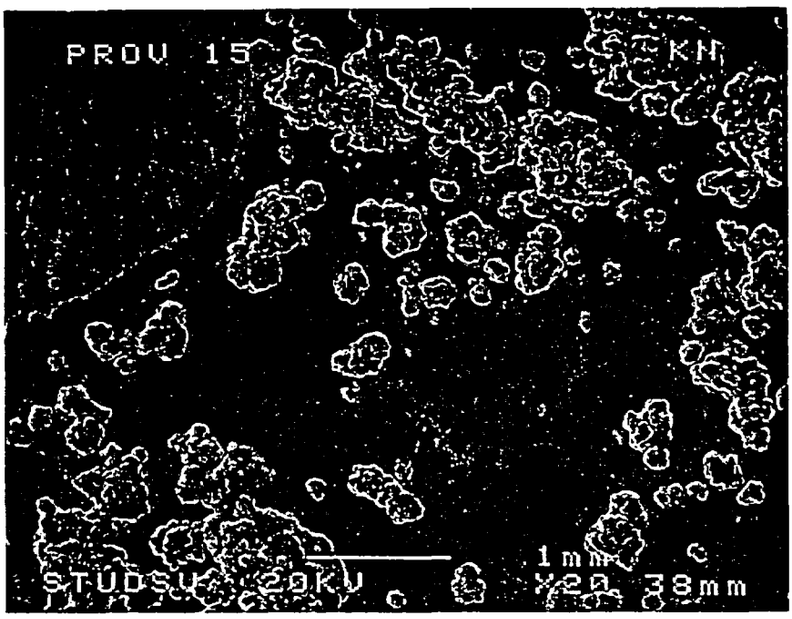

Sample Cu15 at ×20 magnification

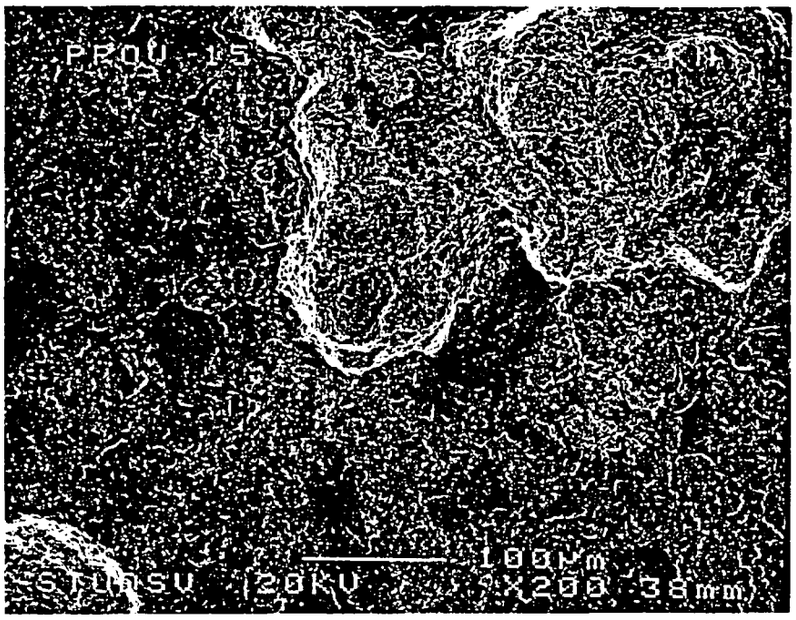

Sample Cu15 at ×200 magnification

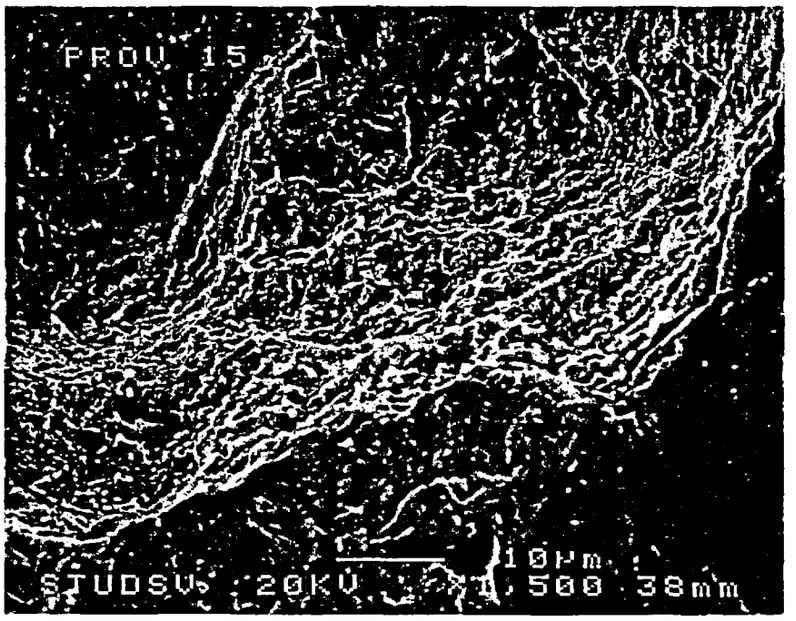

Sample Cu15 at ×1500 magnification

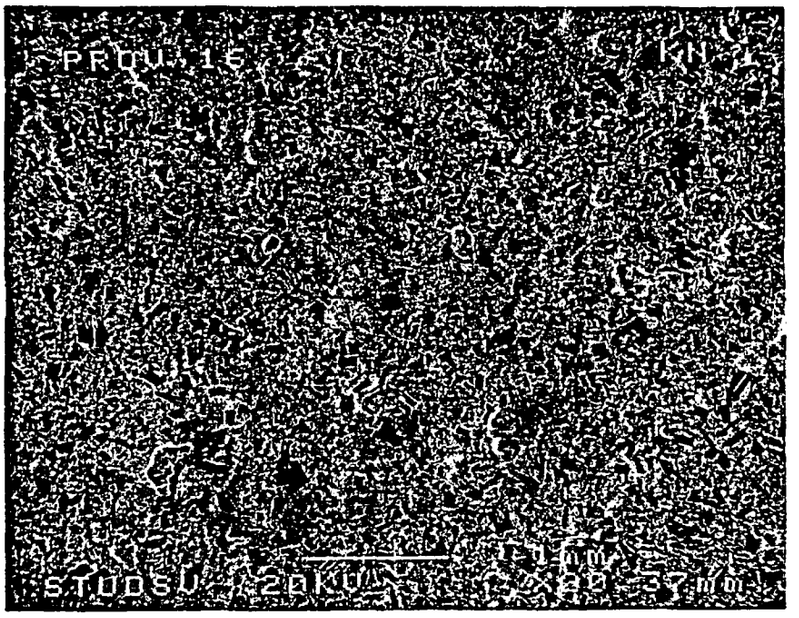

Sample Cu16 at ×20 magnification

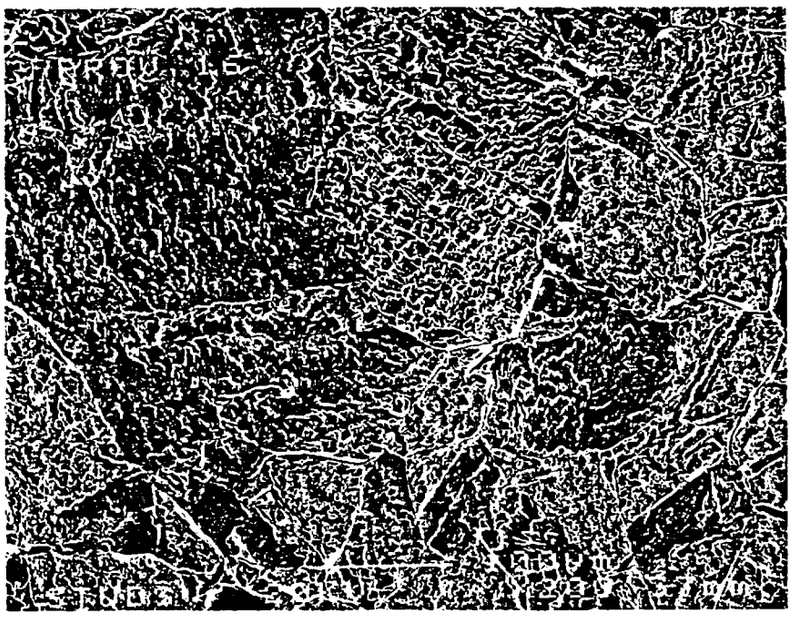

Sample Cu16 at ×200 magnification

Sample Cu16 at ×1500 magnification

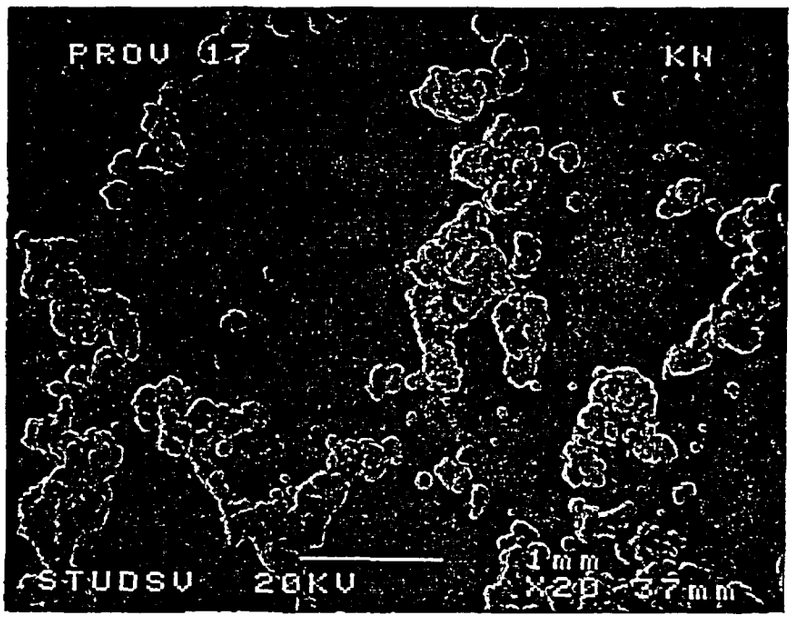

Sample Cu17 at ×20 magnification

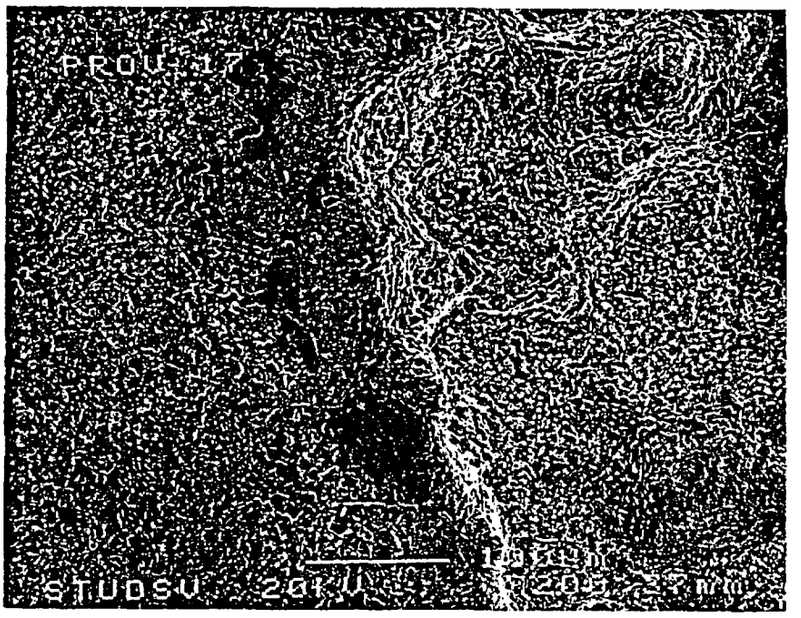

Sample Cu17 at ×200 magnification

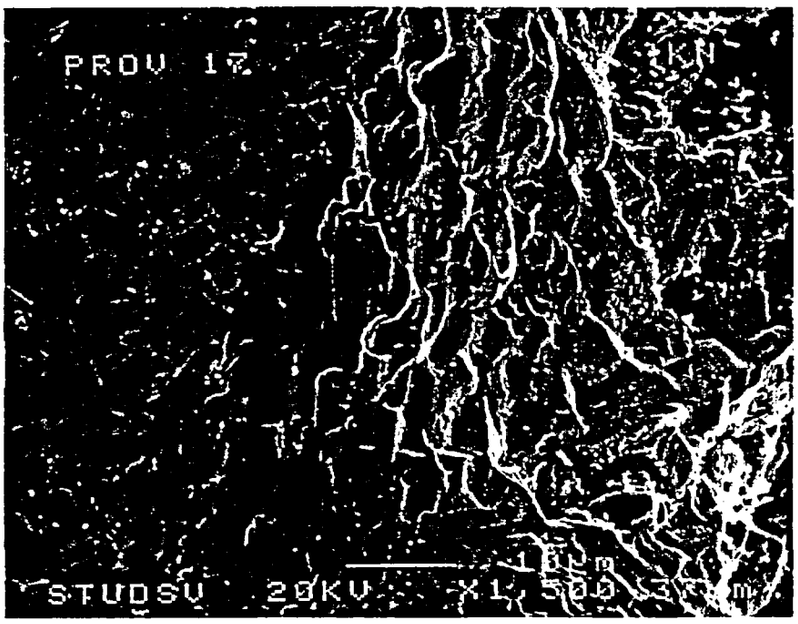

Sample Cu17 at ×1500 magnification

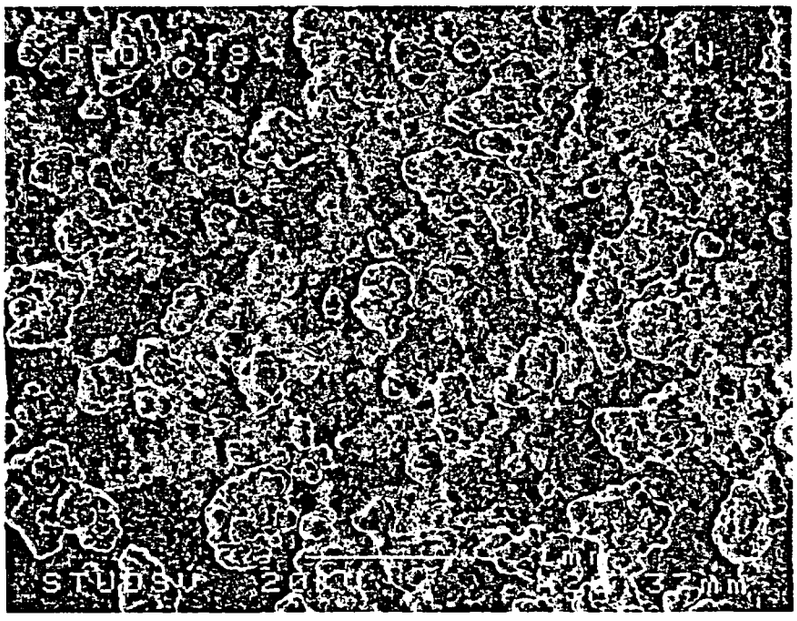

Sample Cu18 at ×20 magnification

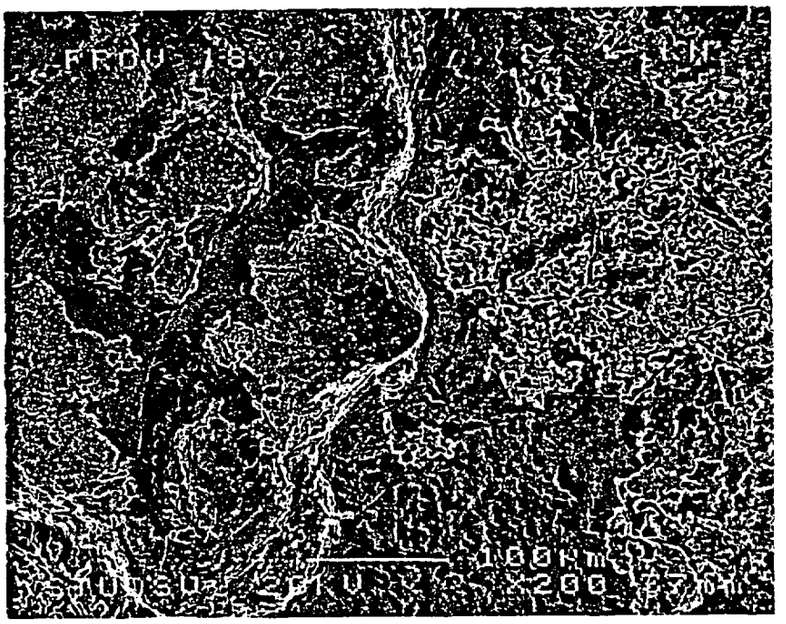

Sample Cu18 at ×200 magnification

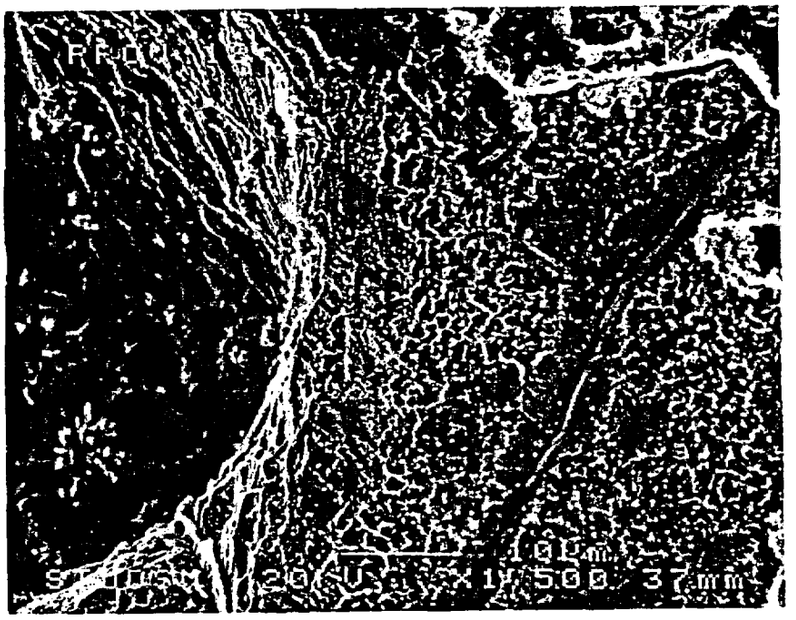

Sample Cu18 at ×1500 magnification

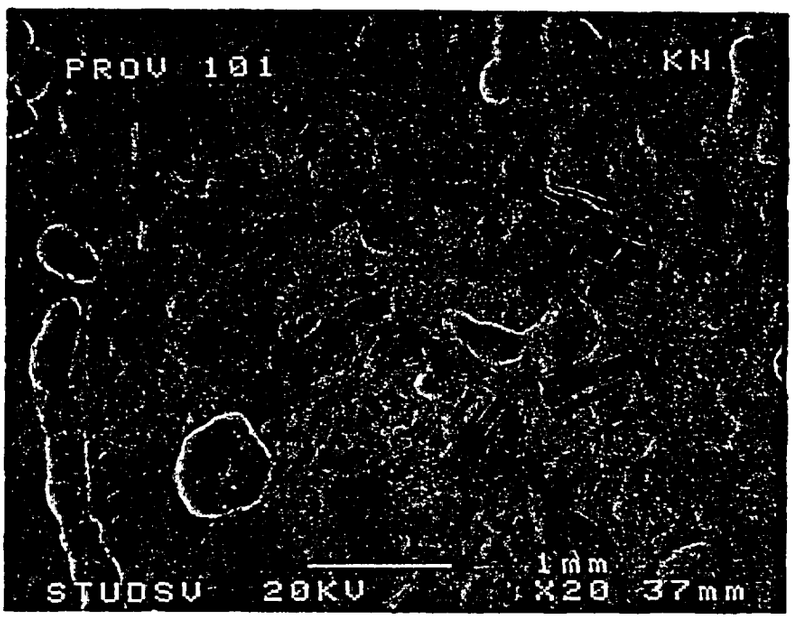

Sample Cu101 at ×20 magnification

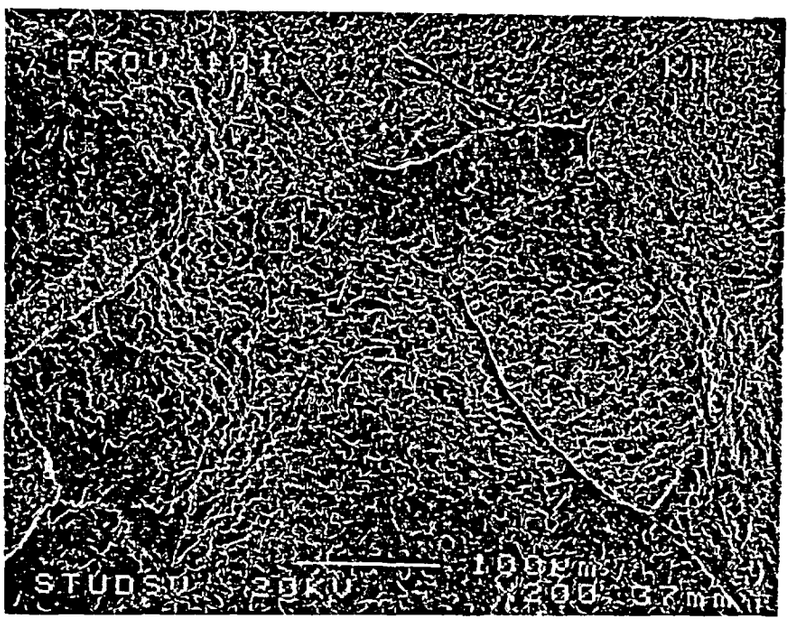

Sample Cu101 at ×200 magnification

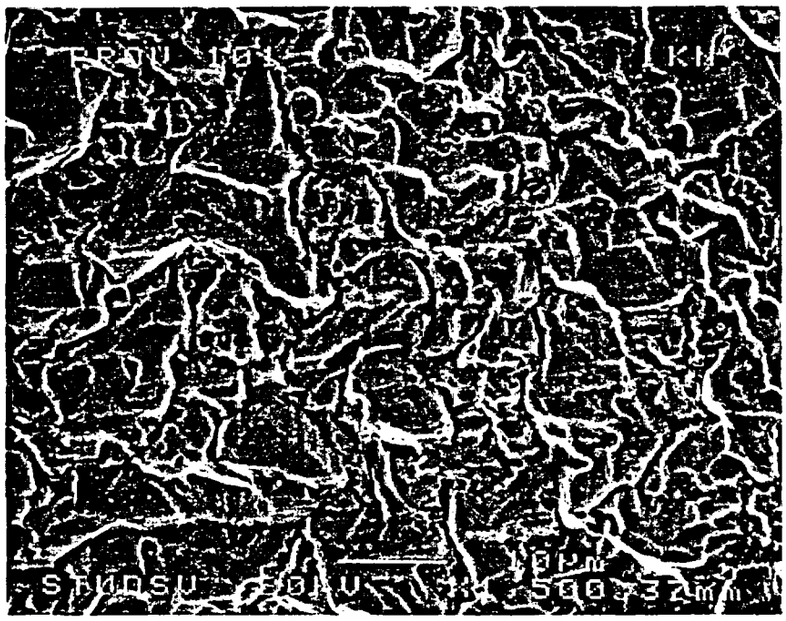

Sample Cu101 at ×1500 magnification

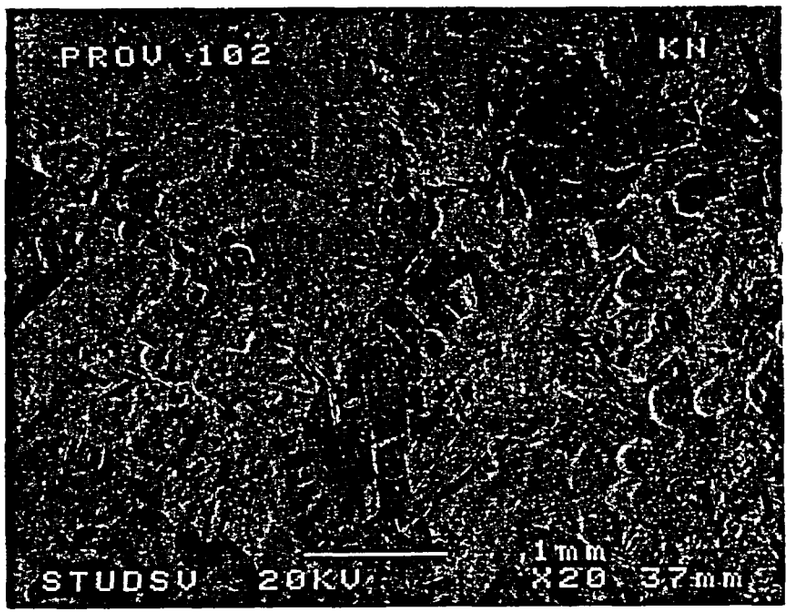

Sample Cu102 at ×20 magnification

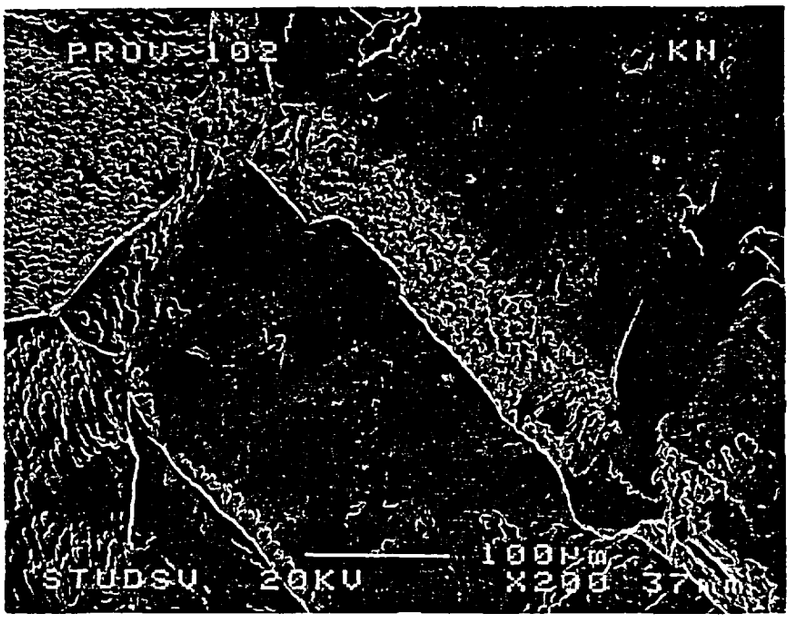

Sample Cu102 at ×200 magnification

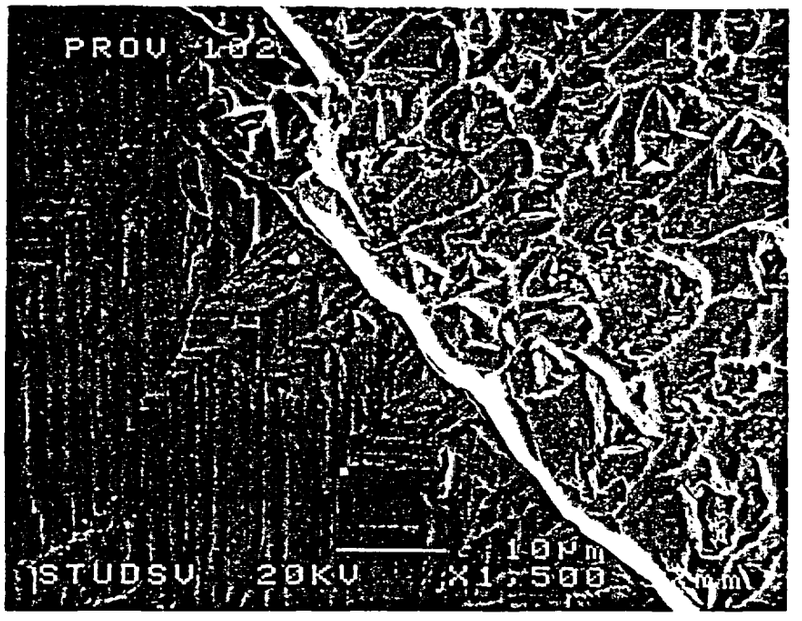

Sample Cu102 at ×1500 magnification

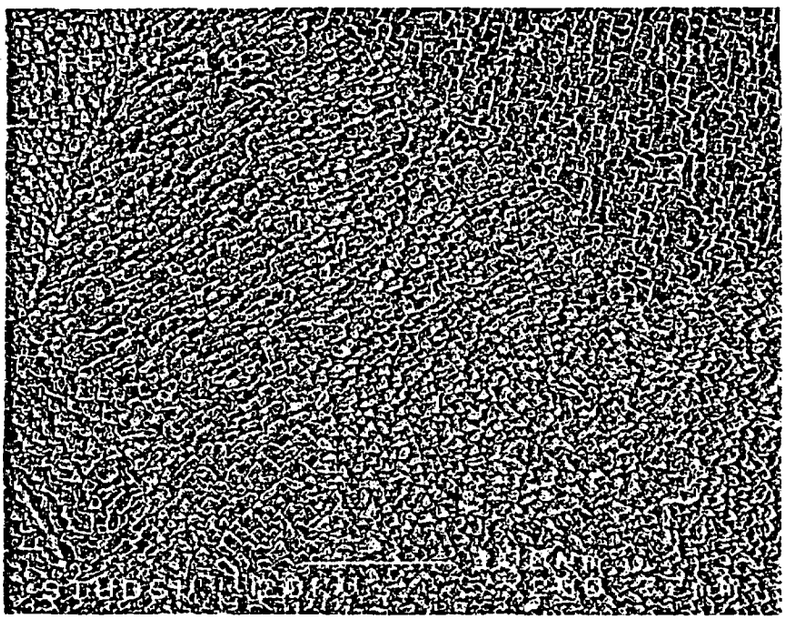

Sample Cu103 at ×200 magnification

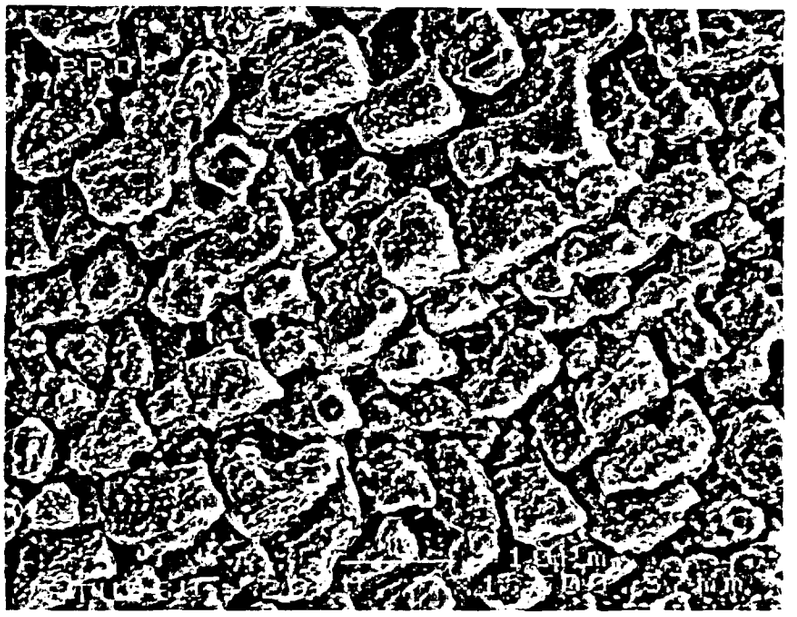

Sample Cu103 at ×1500 magnification

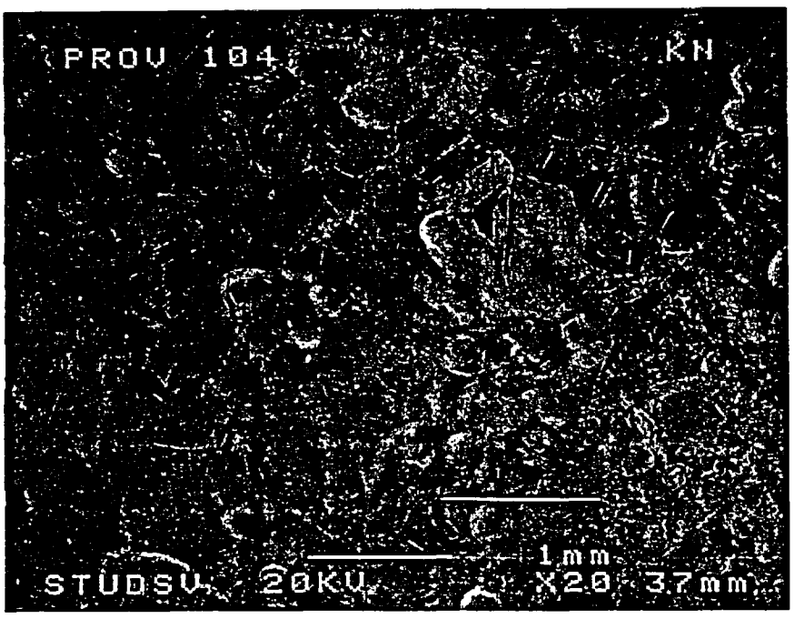

Sample Cu104 at ×20 magnification

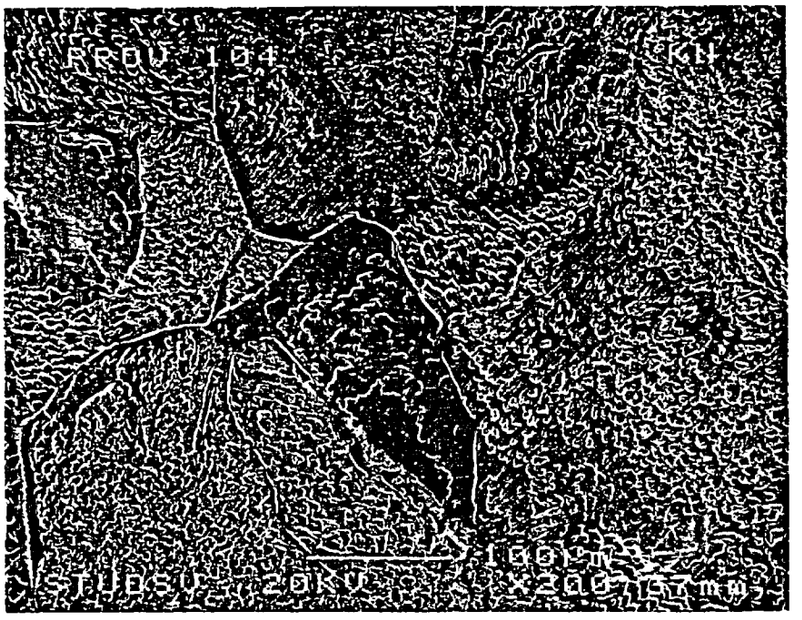

Sample Cu104 at ×200 magnification

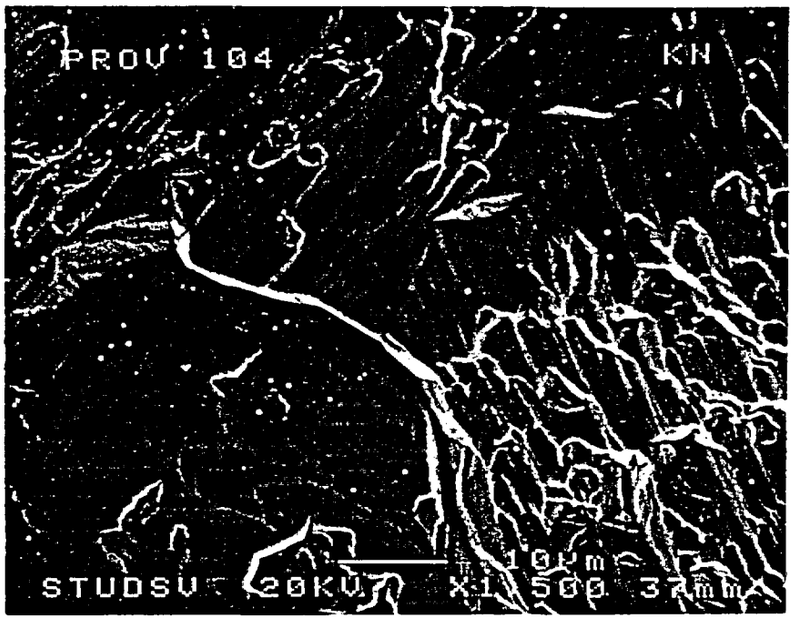

Sample Cu104 at ×1500 magnification

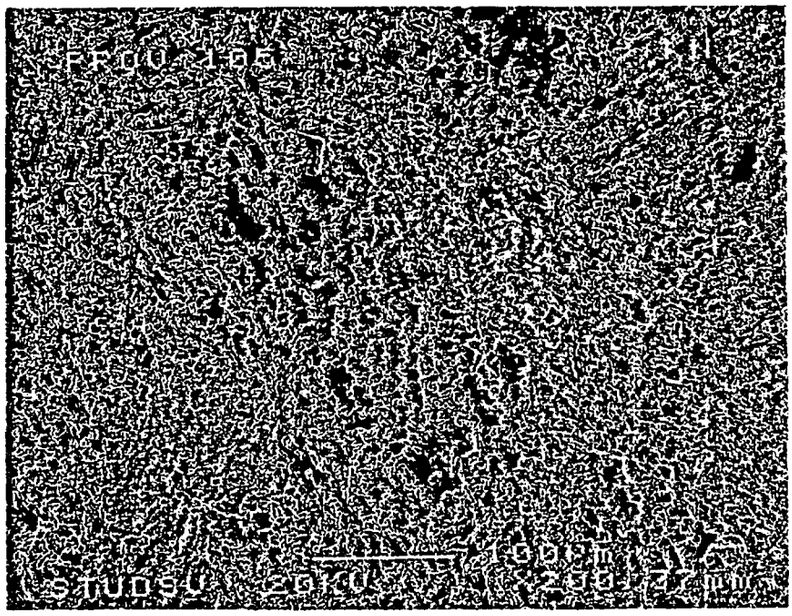

Sample Cu105 at ×200 magnification

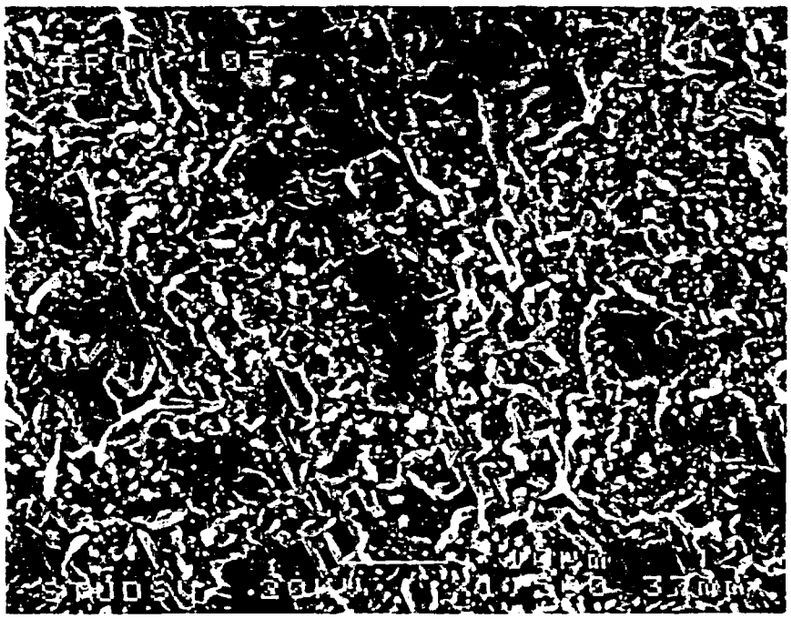

Sample Cu105 at ×1500 magnification

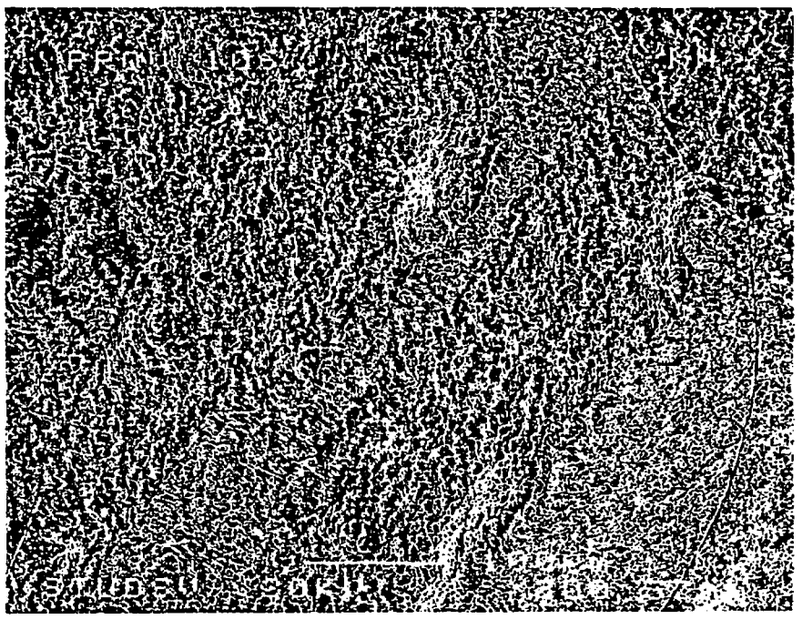

Sample Cu106 at ×200 magnification

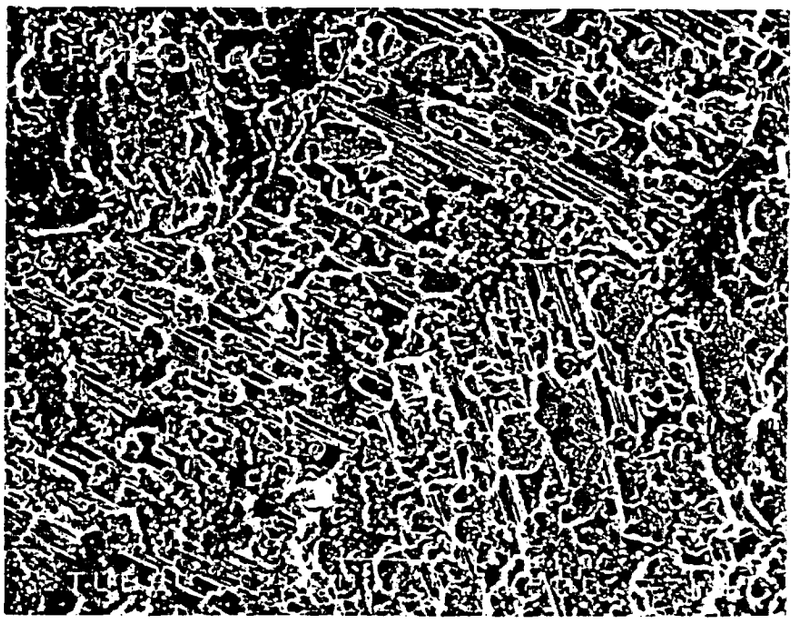

Sample Cu106 at ×1500 magnification

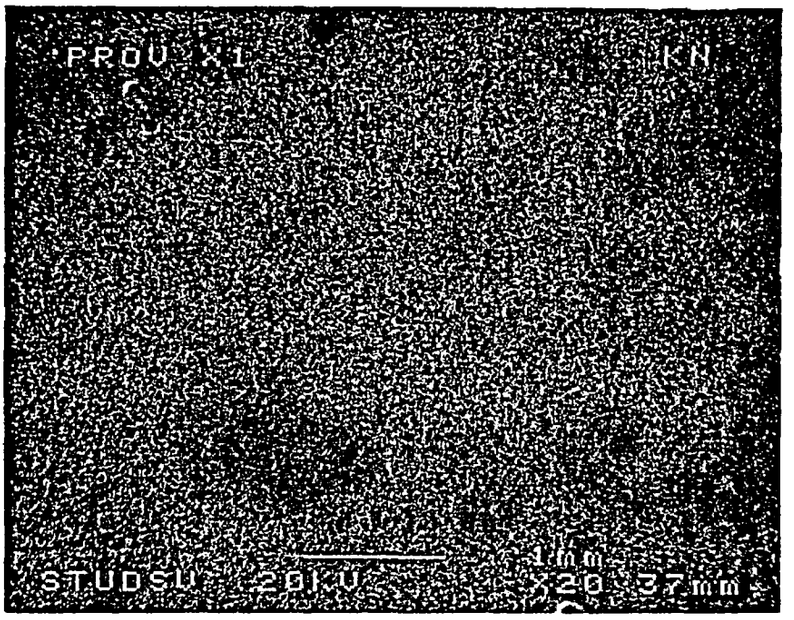

Sample CuX1 at ×20 magnification

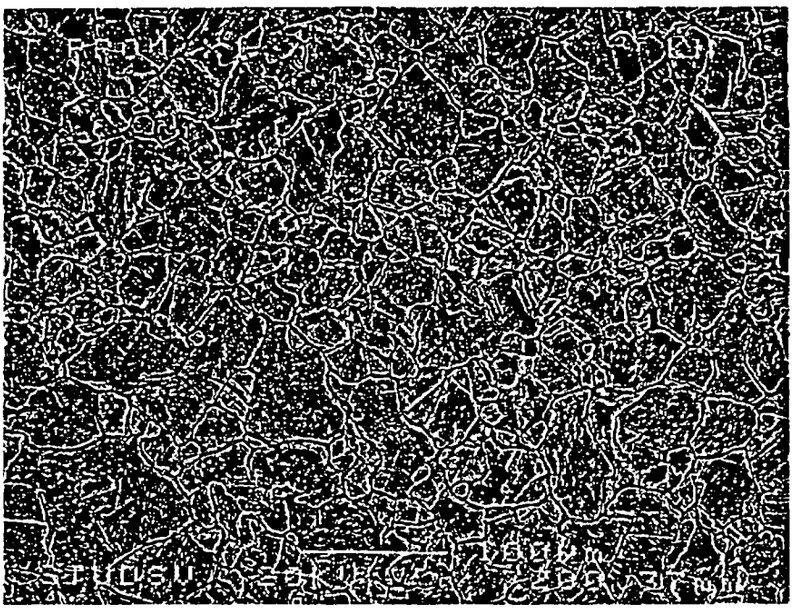

Sample CuX1 at ×200 magnification

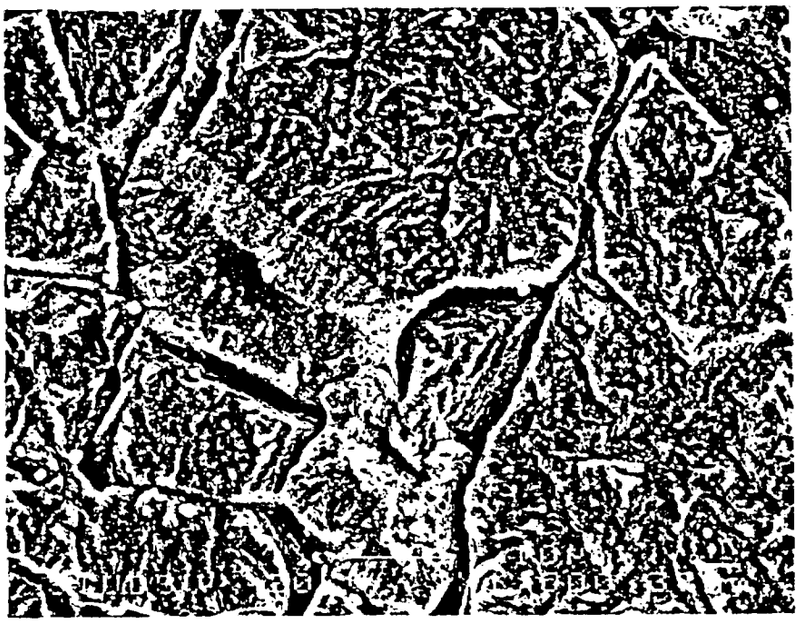

Sample CuX1 at ×1500 magnification

Photos of whiskers

Photos of whiskers formed on the copper electrode during polarisation measurements in HS^--containing water.

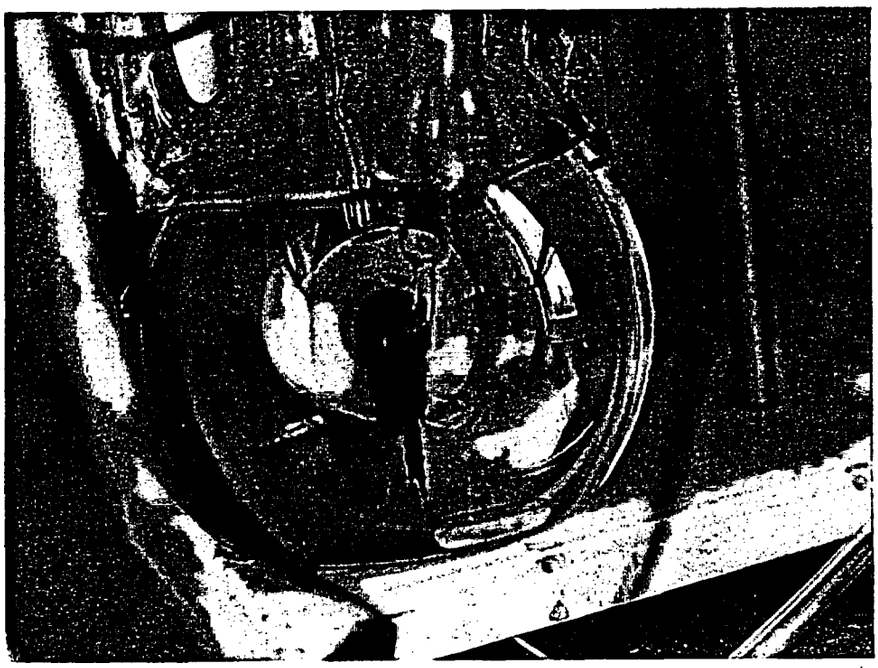

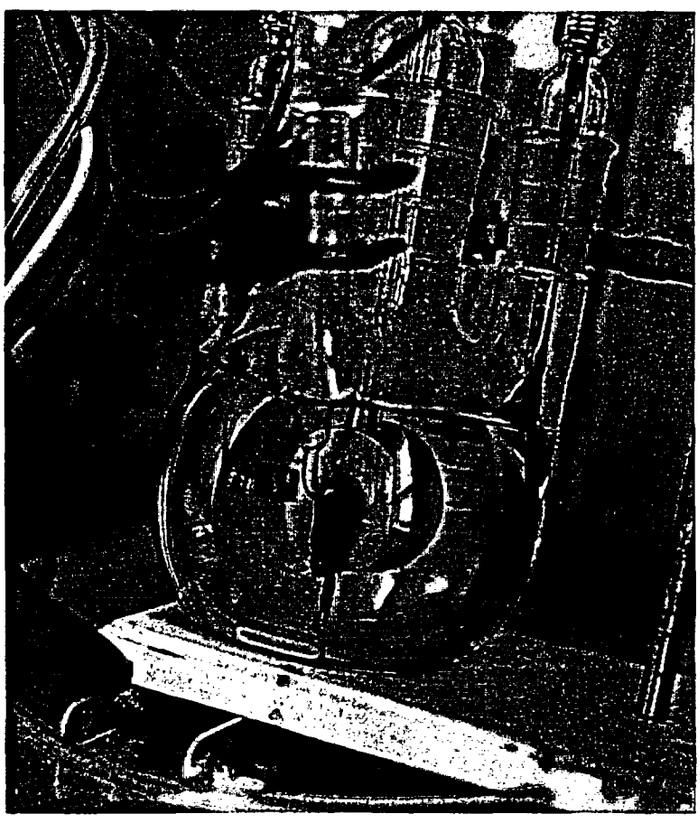

SKi

STATENS KÄRNKRAFTINSPEKTION
Swedish Nuclear Power Inspectorate

Postadress/Postal address	Telefon/Telephone	Telefax	Telex
SKI	Nat 08-698 84 00	Nat 08-661 90 86	11961 SWEATOM S
S-106 58 STOCKHOLM	Int +46 8 698 84 00	Int +46 8 661 90 86	